Geotechnical Engineering Research Laboratory
One University Avenue
Lowell, Massachusetts 01854
Tel: (978) 934-2277 Fax: (978) 934-3046
e-mail: Samuel_Paikowsky@uml.edu
web site: http://www.uml.edu/research_labs/Geotechnical_Engineering/
DEPARTMENT OF CIVIL AND
ENVIRONMENTAL ENGINEERING

Samuel G. Paikowsky, Sc.D
Professor

14.533 Advanced Foundation Engineering

SHORT & LONG TERM SETTLEMENT ANALYSIS OF SHALLOW FOUNDATIONS

S. G. Paikowsky

TABLE OF CONTENTS

SETTLEMENT OF SHALLOW FOUNDATIONS

(Das Sections 5.1 through 5.20, pp. 223 - 290)
(Bowles Ch.5, pp.284-340)

SETTLEMENT CRITERIA AND CONCEPT OF ANALYSIS

1. Tolerance Criteria of Settlement and Differential Settlement

- Settlement most often governs the design as allowable settlement is exceeded before B.C. becomes critical.

- Concerns of foundation settlement are subdivided into 3 levels of associated damage:

  - Architectural damage - cracks in walls, partitions, etc.
  - Structural damage - reduced strength in structural members
  - Functional damage - impairment of the structure functionality

  The last two refer to stress and serviceability limit states, respectively.

- In principle, two approaches exist to determine the allowable displacements.

  (a) Rational Approach to Design

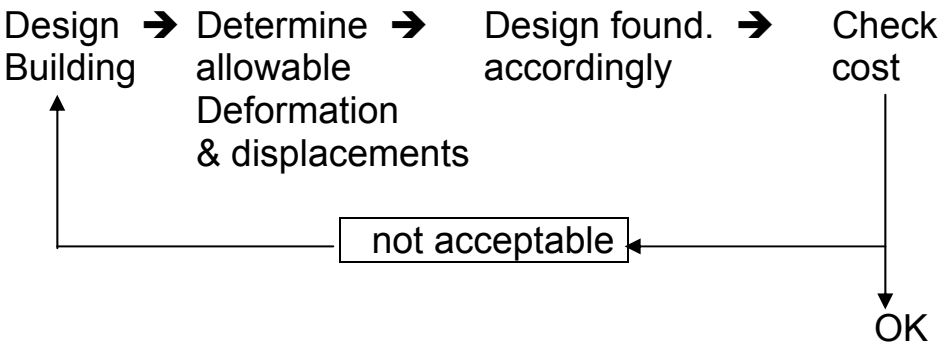

  Problems: - expensive analysis
  - limited accuracy in all predictions especially settlement & differential settlement

1. Empirical Approach (see text section 5.20, "Tolerable Settlement of Buildings", pp. 283-285)

   - based on performance of many structures, provide a guideline for maximum settlement and maximum rotation

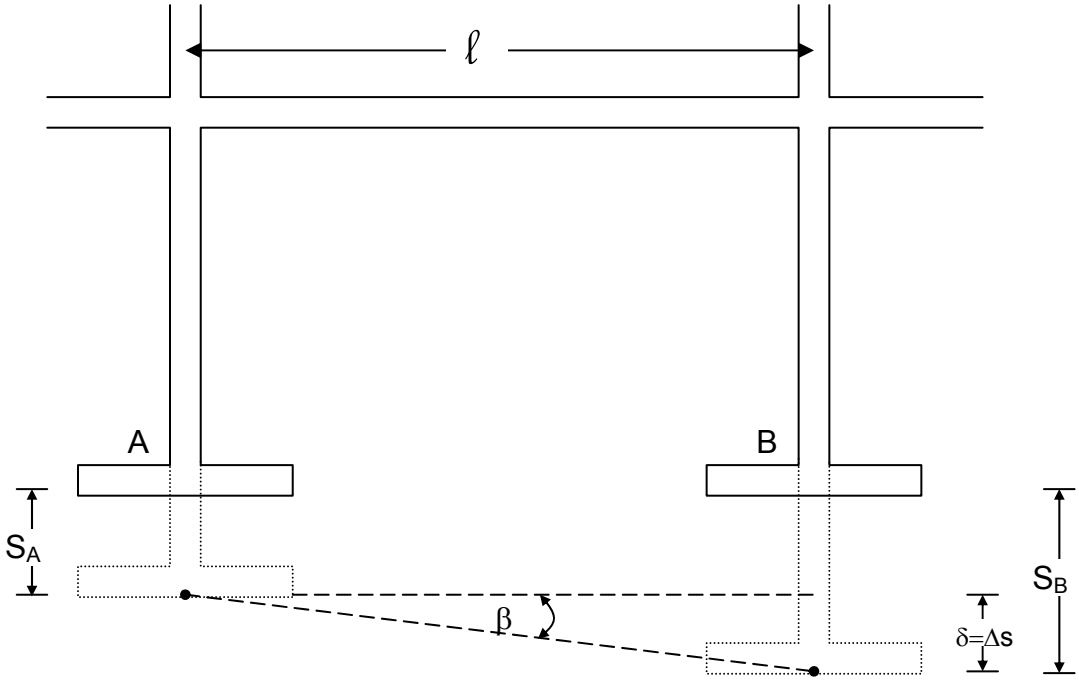

   - S_{max} = maximum settlement
   - $\delta = \Delta s$ = differential settlement (between any two points)
   - $(\frac{\delta}{\ell})_{max}$ = maximum rotation

Angular distortion = $\tan\beta = (\frac{\Delta s}{\ell})_{max} = \frac{\delta}{\ell} = \frac{S_A - S_B}{\ell}$

$(\frac{\delta}{\ell})_{max} \geq \frac{1}{300}$ architectural damage

$(\frac{\delta}{\ell})_{max} \geq \frac{1}{250}$ tilting of high structures become visible

$(\frac{\delta}{\ell})_{max} \geq \frac{1}{150}$ structural damage likely

maximum settlement (S_{max}) leading to differential settlement

- Masonry wall structure 1 - 2”
- Framed structures 2 - 4”
- Silos, mats 3 - 12”
- Lambe and Whitman “Soil Mechanics” provides in Table 14.1 and Figure 14.8 (see next page) the allowable maximum total settlement, tilting and differential movements as well as limiting angular distortions.

Correlation Between Maximum Settlement to Angular Distortion

Grant, Christian & Van marke (ASCE - 1974)
correlation between angular settlement to maximum settlement, based on 95 buildings of which 56 were damaged.

Type of Found	Type of Soil	$\frac{s_{max}\ (in)}{(\delta/\ell)_{max}}$	$\frac{\rho_{all}\ (in)}{(\delta/\ell)_{max} = 1/300}$
Isol. Footings	Clay	1200	4”
	Sand	600	2”
Mat	Clay	$\geq$ 138 ft	$\geq$ 0.044 B (ft)
	Sand	no relationship	

Limiting values of serviceability are typically s_{max} = 1” for isolated footing and s_{max} = 2” for a raft which is more conservative than the above limit based on architectural damage. Practically serviceability needs to be connected to the functionality of the building and the tolerable limit.

Table 14.1 Allowable Settlement

Type of Movement	Limiting Factor	Maximum Settlement
Total settlement	Drainage	6–12 in.
	Access	12–24 in.
	Probability of nonuniform settlement:	
	Masonry walled structure	1–2 in.
	Framed structures	2–4 in.
	Smokestacks, silos, mats	3–12 in.
Tilting	Stability against overturning	Depends on height and width
	Tilting of smokestacks, towers	0.004*l*
	Rolling of trucks, etc.	0.01*l*
	Stacking of goods	0.01*l*
	Machine operation-cotton loom	0.003*l*
	Machine operation-turbogenerator	0.0002*l*
	Crane rails	0.003*l*
	Drainage of floors	0.01–0.02*l*
Differential movement	High continuous brick walls	0.0005–0.001*l*
	One-story brick mill building, wall cracking	0.001–0.002*l*
	Plaster cracking (gypsum)	0.001*l*
	Reinforced-concrete building frame	0.0025–0.004*l*
	Reinforced-concrete building curtain walls	0.003*l*
	Steel frame, continuous	0.002*l*
	Simple steel frame	0.005*l*

From Sowers, 1962.
Note. l = distance between adjacent columns that settle different amounts, or between any two points that settle differently. Higher values are for regular settlements and more tolerant structures. Lower values are for irregular settlements and critical structures.

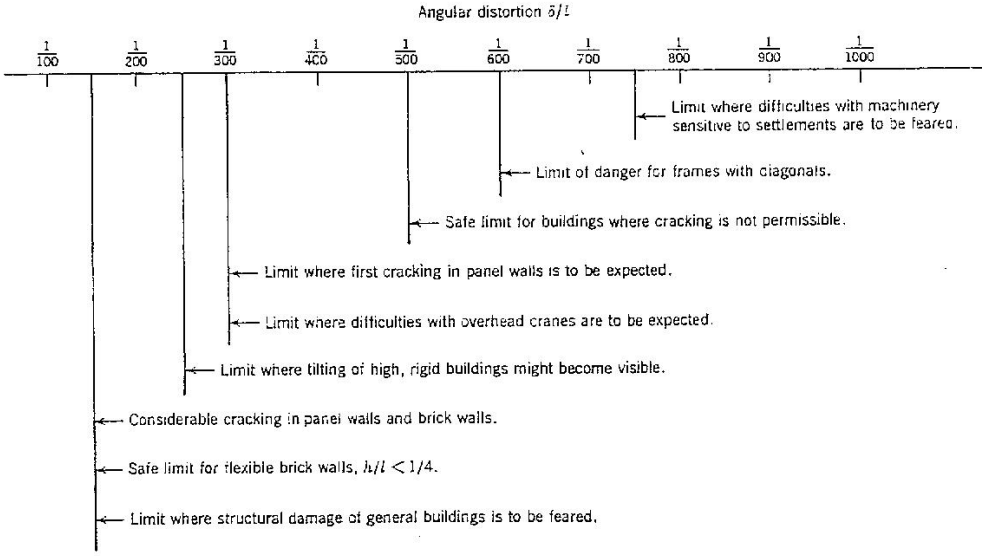

Fig. 14.8 Limiting angular distortions (From Bjerrum, 1963a).

(Lambe & Whitman, *Soil Mechanics*)

2. Types of Settlement and Methods of Analysis

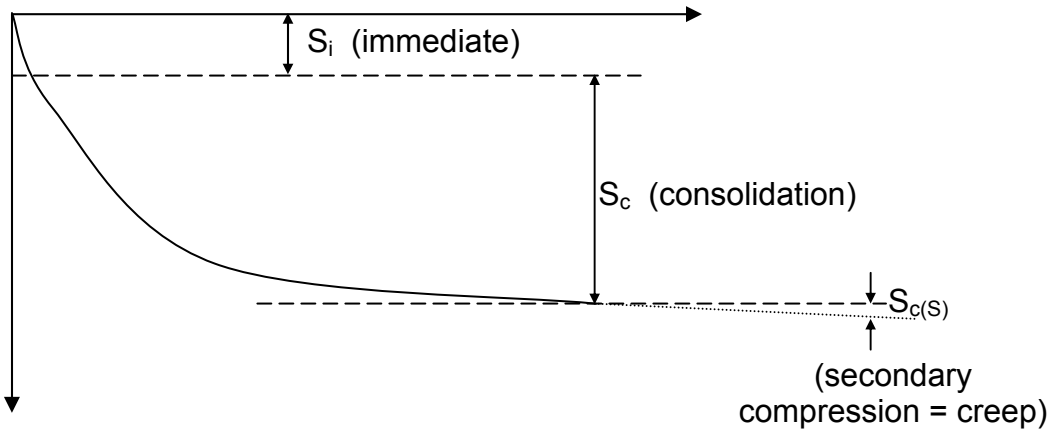

Si = Granular Soils → Elastic Theory

S_c, $S_{c(s)}$ - Cohesive Soils → Consolidation Theory; Empirical Correlations

In principle, both types of settlement; the immediate and the long term, utilize the compressibility of the soil, one however, is time dependent (consolidation and secondary compression).

3. General Concept of Settlement Analysis

Two controlling factors influencing settlements:

- Net applied stress - Δq
- Compressibility of soil - c = $(settlement/load)$

when dealing with clay c = f (t) as it changes with time

$$s = \Delta q \times c \times f(B)$$

where

s = settlement	[L]
Δq = net load	[F/L^2]
c = compressibility	[L/(F/L^2)]
f (B) = size effect	[dimensionless]

obtain c by $\rightarrow$ lab tests, plate L.T., SPT, CPT

c will be influenced by:

- width of footing = B
- depth of footing = D/B
- location of G.W. Table = d_w/B
- type of loading $\rightarrow$ static or repeated
- soil type & quality affecting the modulus

VERTICAL STRESS INCREASE IN THE SOIL DUE TO A FOUNDATION LOAD

(Das 7th ed., Sect. 5.2-5.8, pp.224-243)
(Bowles Sections 5.2 to 5.5, pp.286-302)

1. Principle

(a) Required: Vertical stress (pressure) increase under the footing in order to asses settlement.

(b) Solution: Theoretical solution based on theory of elasticity assuming load on ∞, homogeneous, isotropic, elastic half space.

- Homogeneous — Uniform throughout at every point we have the same qualities.
- Isotropic — Identical in all directions, invariant with respect to direction
- Orthotropic — (tend to grow or form along a vertical axis) different qualities in two planes
- Elastic — capable of recovering shape

(c) Why can we use the elastic solutions for that problem?

- Is the soil elastic?
  no, but…

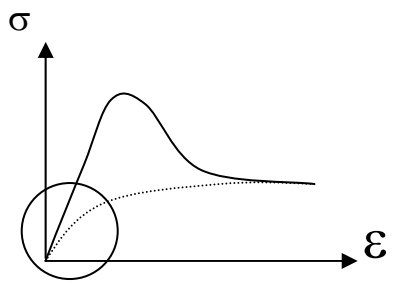

i. We are practically interested in the service loads which are approximately the dead load.
   - The ultimate load = design load x F.S.
   - Design load = (DL x F.S.) + (LL x F.S.)
   - Service load ≅ DL → within the elastic zone

ii. The only simple straight forward method we know

2. Stress due to Concentrated Load (Bowles p.287)

Boussinesq, 1885

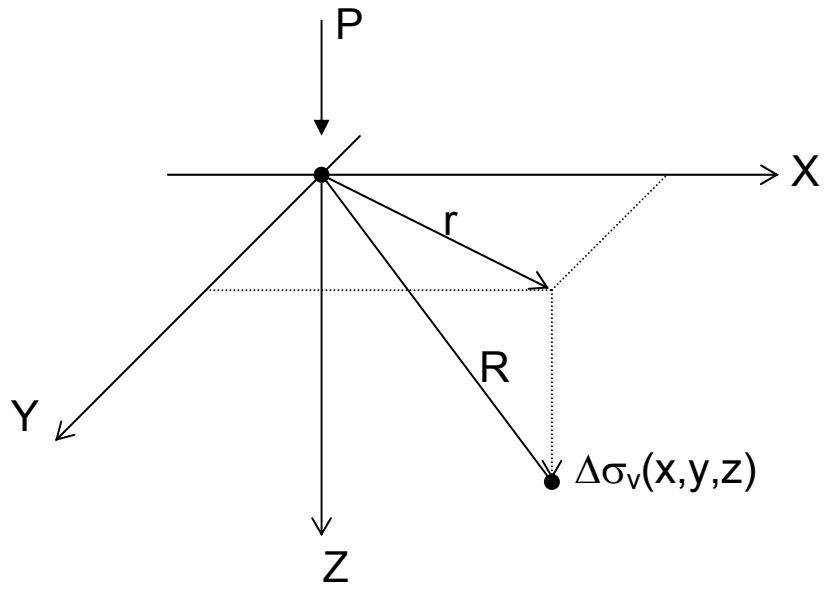

$$\Delta p = \Delta\sigma_v = \frac{3P}{2\pi z^2 \left[1 + \left(\frac{r}{z}\right)^2 \right]^{5/2}} \qquad r = \sqrt{x^2 + y^2}$$

(Das eq. 5.1)

(Bowles eq. 5.3)

3. Stress due to a Circularly Loaded Area

- referring to flexible areas as we assume uniform stress over the area. Uniform stress will develop only under a flexible footing.
- integration of the above load from a point to an area.
  - see Das Eqs. 5.2, 5.3 (text p.225) (Bowles Eq. 5.4, 5.5)

$$\Delta p = \Delta\sigma_v = q_o \left\{ 1 - \frac{1}{\left[1 + \left(\frac{B}{2z}\right)^2\right]^{3/2}} \right\}$$

vertical stress under the center

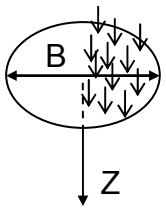

See Das Table 5.1 (p.226) for $\frac{\Delta\sigma_v}{q_0} = f\left(\frac{r}{(B/2)} \& \frac{z}{(B/2)} \right)$

4. Stress below a Rectangular Area

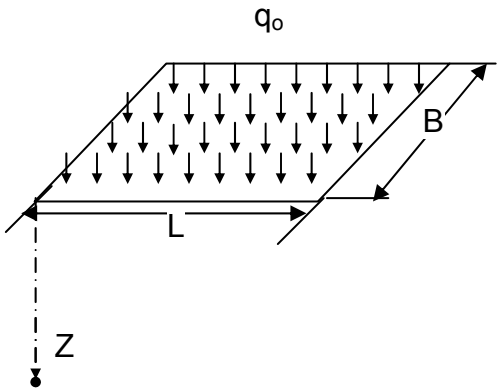

$\Delta p = \Delta\sigma_v = q_o \times I$

below the corner of a
flexible rectangular loaded area

$m = B/z$ $\quad$ $n = L/z$

Bowles Table 5.1 (p.294) Das Table 5.2 (p.228-229)

$\rightarrow$ I = *f* (m,n)

Stress at a point under different locations

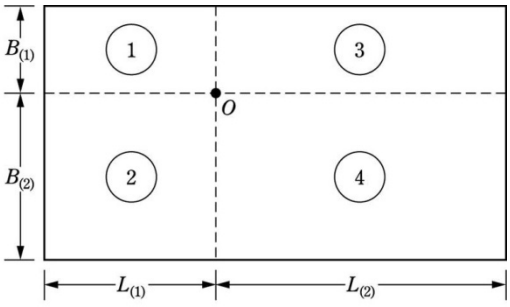

Figure 5.4 Stress below any point of a loaded flexible rectangular area (Das p.230)

use $B_1 \times L_1 \rightarrow m_1,n_1 \rightarrow I_2$
$B_1 \times L_2 \rightarrow m_1,n_2 \rightarrow I_1$
$B_2 \times L_1 \rightarrow m_2,n_1 \rightarrow I_3$
$B_2 \times L_2 \rightarrow m_2,n_2 \rightarrow I_4$

$\Delta p = \Delta\sigma_v = q_o (I_1 + I_2 + I_3 + I_4)$

Stress at a point under the center of the foundation

$\Delta p = \Delta\sigma_v = q_c \times I_c$

$I_c = f(m_1, n_1)$ $\quad$ $m_1 = L/B$ $\quad$ $n_1 = z/(B/2)$

- Bowles Table 5.1 (p.294), Das Table 5.3 (p.230) provides values of m_1 and n_1.
- See next page for a chart $\Delta p/q_0$ vs. z/B, f(L/B)

5. <u>General Charts of Stress Distribution Beneath a Rectangular and Strip Footings</u>

(a) $\rightarrow$ $\Delta P/q_o$ vs. z/B under the center of a rectangular footing with L/B = 1 (square) to L/B = ∞ (strip)

Stress Increase in a Soil Mass Caused by Foundation Load

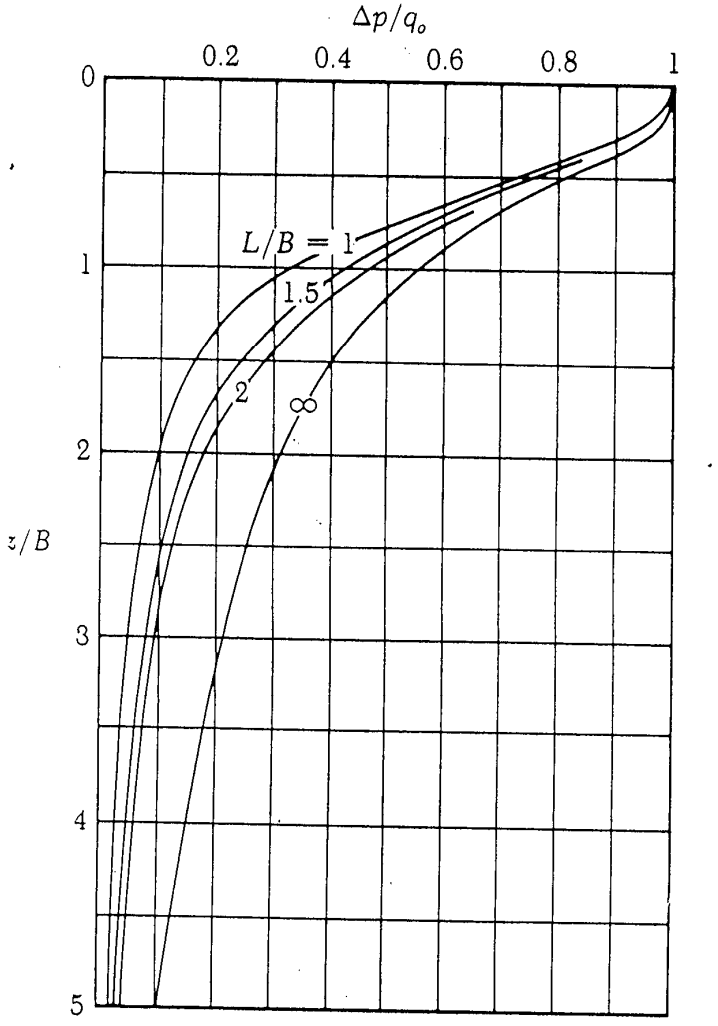

Figure 3.41 Increase of stress under the center of a flexible loaded rectangular area

Das “Principle of Foundation Engineering”, 3rd Edition

(b) Stress Contours (laterally and vertically) of a strip and square footings. Soil Mechanics, DM 7.1 – p. 167

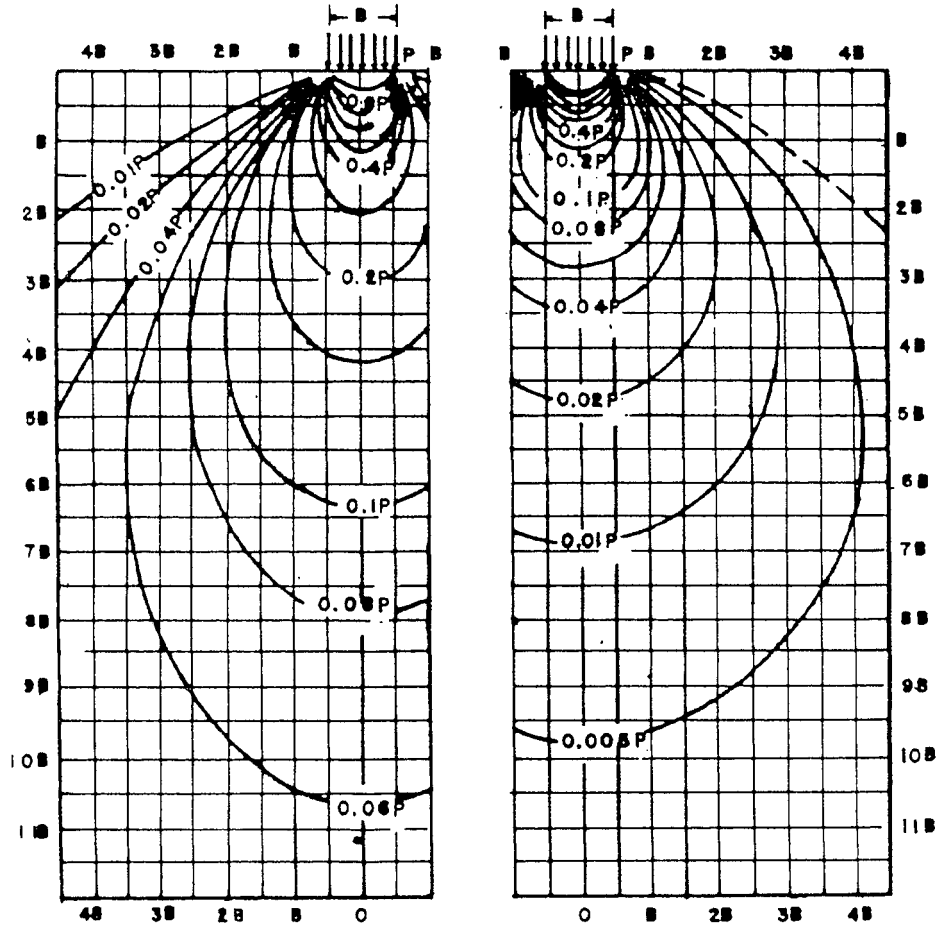

SQUARE FOOTING

GIVEN
FOOTING SIZE = 20'X 20'
UNIT PRESSURE P=2TSF

FIND
PROFILE OF STRESS INCREASE
BENEATH CENTER OF FOOTING
DUE TO APPLIED LOAD

B = 20' P = 2 TSF

Z (FT)	Z/B	σ_z TSF
10	0.5	0.70 X 2 = 1.4
20	1	0.38 X 2 = 0.76
30	1.5	0.19 X 2 = 0.38
40	2.0	0.12 X 2 = 0.24
50	2.5	0.07 X 2 = 0.14
60	3.0	0.05 X 2 = 0.10

FIGURE 3
Stress Contours and Their Application

Navy Design Manual

Example: size 8 x 8m, depth z = 4m

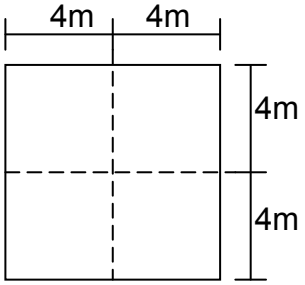

Find the additional stress under the center of the footing loaded with q_0

1. Generic relationship 4 x 4 x 4 m = 1, n = 1 } Bowles Table 5.1 and Das Table 5.2, I = 0.17522

   $\Delta p = (4 \times 0.17522)q_o = 0.7q_o$

2. Specific to center, m1 = 1, n1 = 1 $\rightarrow$ Table 5.3, Ic = 0.701
3. Use Figure 3 of the Navy $\rightarrow$ Square Footing z = B/2, $\sigma z \approx 0.7p$
4. Use figure 3.41 (class notes p.12) L/B = 1, Z/B = 0.5 $\rightarrow \Delta p / qo \approx 0.7$

6. Stress Under Embankment (Bowles Sect. 5.4 & Das Sect. 5.6)

Das Fig. 5.10 Embankment loading (text p.236)

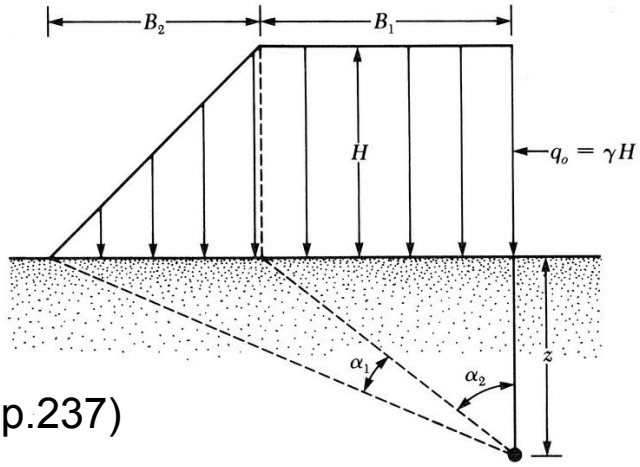

$\Delta p = \Delta\sigma = q_o I'$ (Das eq.5.23)

$I' = f\left(\frac{B_1}{z}, \frac{B_2}{z}\right)$ ➔ Das Fig. 5.11 (p.237)

Example:

$\gamma = 20\ kN/m^3$

$H = 3\ m \rightarrow q_o = \gamma H = 60\ kPa$

$B_1 = 4\ m \rightarrow \frac{B_1}{z} = \frac{4}{5} = 0.80$

$B_2 = 4\ m \rightarrow \frac{B_2}{z} = \frac{4}{5} = 0.80$

$z = 5\ m$

Fig. 5.11 (p.237) ➔ $I' \approx 0.43 \rightarrow \Delta p = 0.43 \times 60 = 25.8kPa$

7. Average Vertical Stress Increase due to a Rectangularly Loaded Area

Average increase of stress over a depth H under the corner of a rectangular foundation:

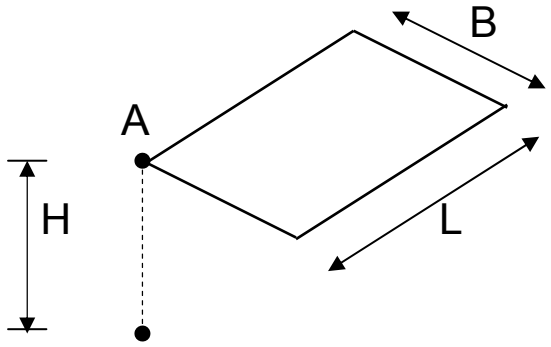

$I_a = f(m,n)$
$m = B/H$
$n = L/H$
use Das Fig. 5.7, p. 234

For the average depth between H_1 and H_2

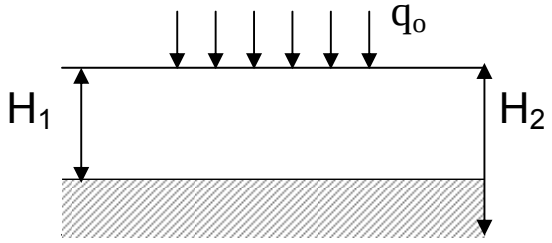

Use the following:

$$\Delta p_{avg} = \Delta\sigma_{avg} = qo\,[H_2 I_{a(H2)} - H_1 I_{a(H1)}]/(H_2 - H_1)$$

(eq. 5.19, p.233 in Das)

Example: 8x8m footing
H = 4m (H_1=0, H_2=4m)

Use 4x4x4 squares m = 1, n = 1

Das Fig. 5.7 (p.234) $I_a \approx 0.225$

$\Delta p_{avg} = 4 \times 0.225 \times q_o = 0.9\ q_o$

0.9 q_o is compared to 0.7q_o (see previous example) which is the stress at depth of 4m (0.5B). The 0.9 q_o reflects the average stress between the bottom of the footing (q_o) to the depth of 0.5B.

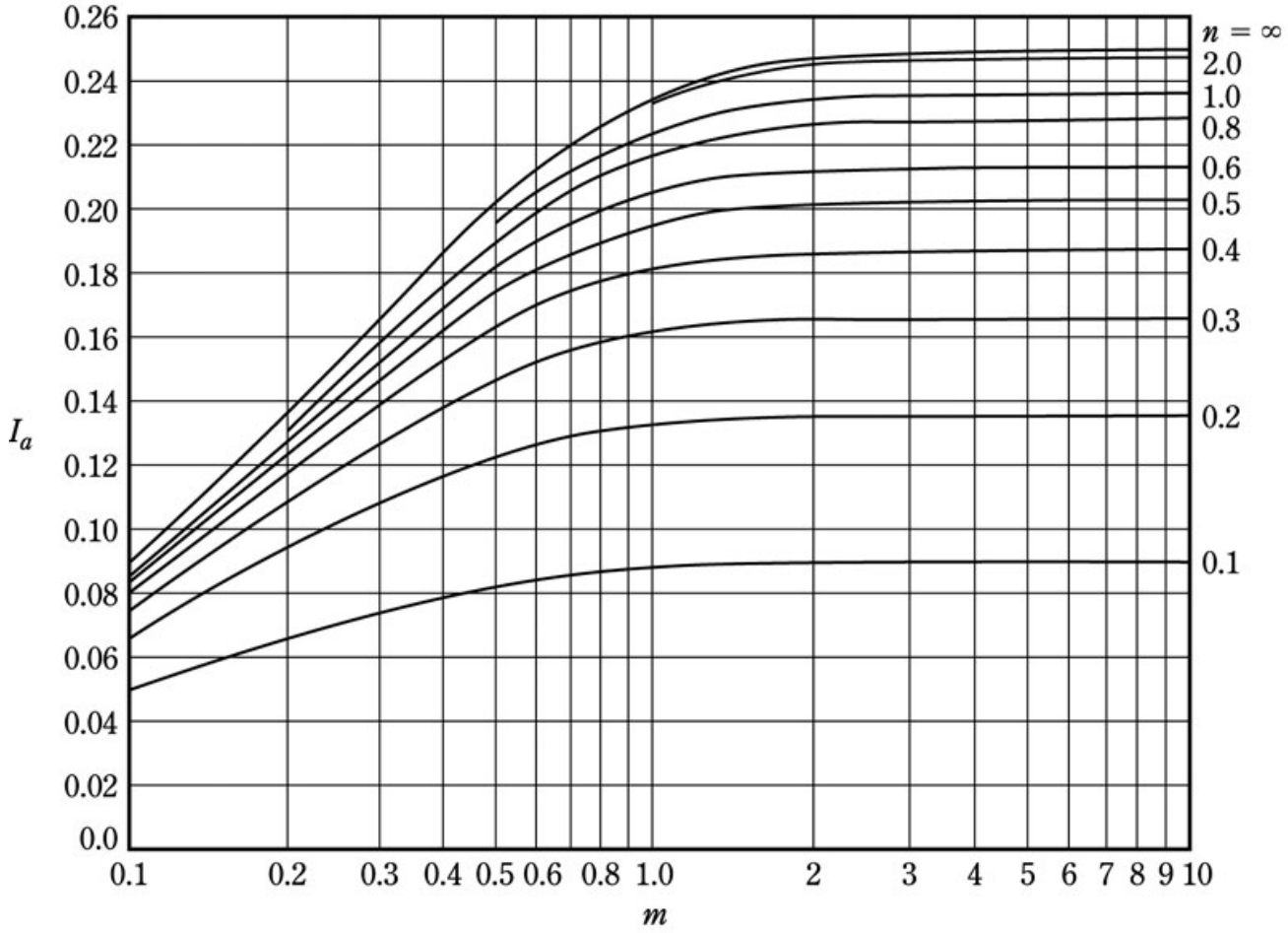

Figure 5.7 Griffiths' Influence factor I_a (Das p.234)

8. Influence Chart - Newmark's Solution (Bowles Figure 5.3)

Perform numerical integration of equation 5.1

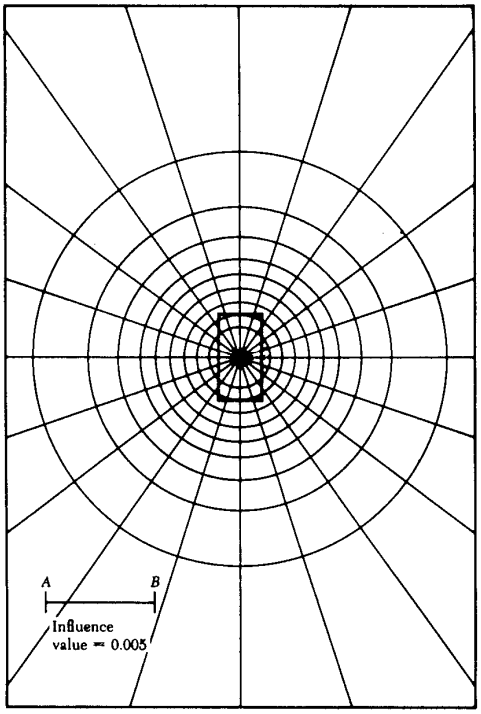

Influence value = $\frac{1}{200}$ (# of segments)

each segment contributes the same amount:

1. Draw the footing shape to a scale where z = length AB (2 cm = 20 mm)
2. The point under which we look for $\Delta\sigma_v'$, is placed at the center of the chart.
3. Count the units and partial units covered by the foundation
4. $\Delta\sigma_v' = \Delta p = q_o \times m \times I$

where m = # of counted units
q_o = contact stress
I = influence factor = $\frac{1}{200}$
= 0.005

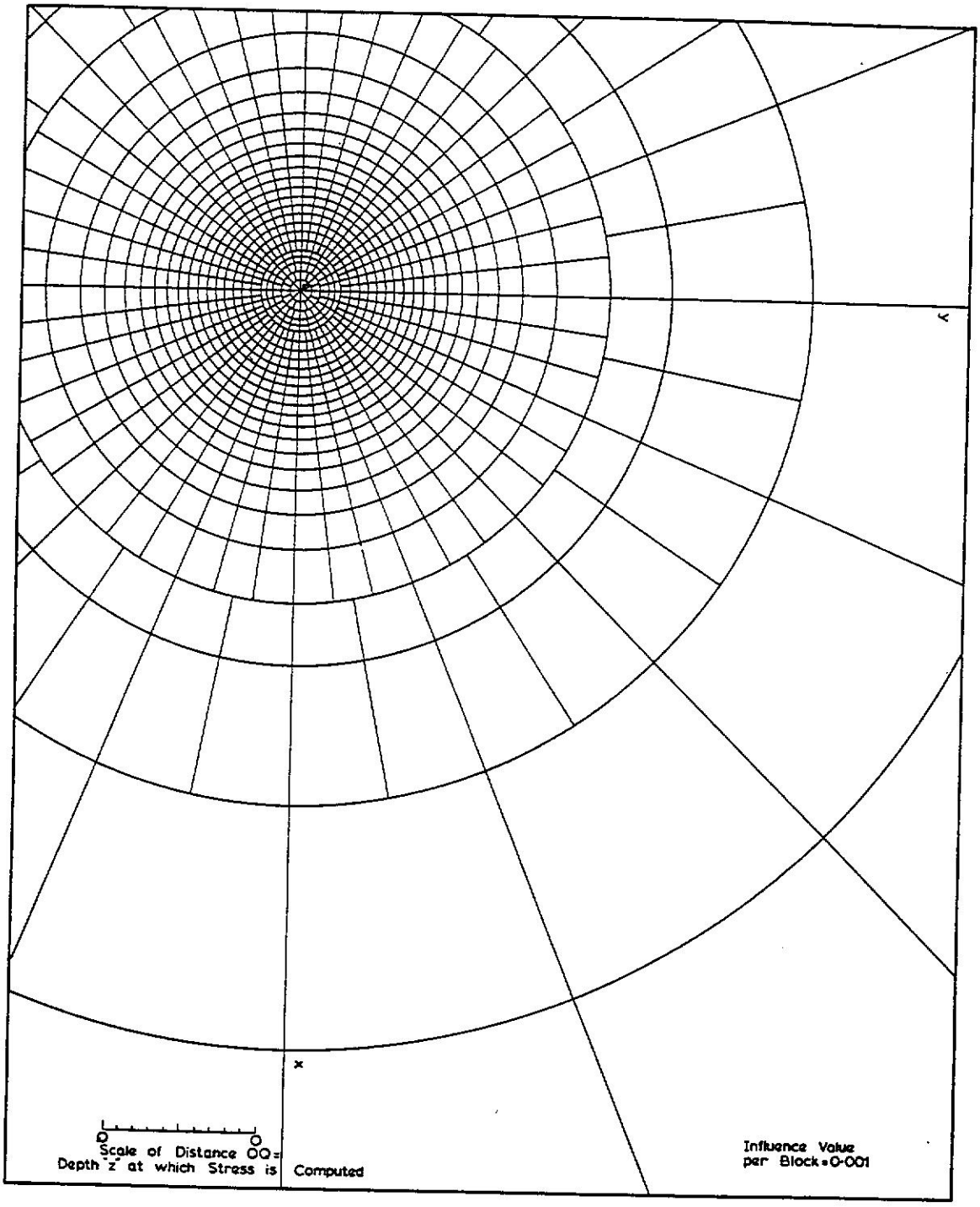

Fig. 3.50 Influence chart for vertical stress σ_z (Newmark, 1942)
(All values of ν) (Poulos and Davis, 1991)
$\sigma_z = 0.001N_p$ where N = no. of blocks

Example

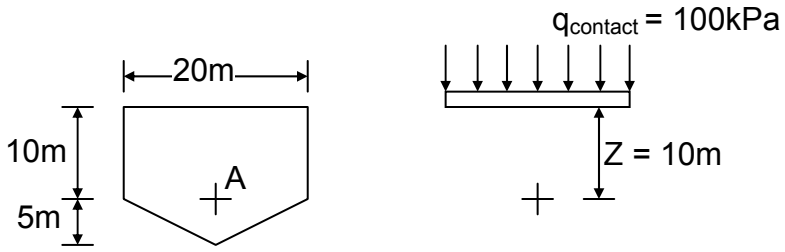

What is the additional vertical stress at a depth of 10 m under point A ?

1. z = 10 m scale 20 mm = 10 m

2. Draw building in scale with point A at the center

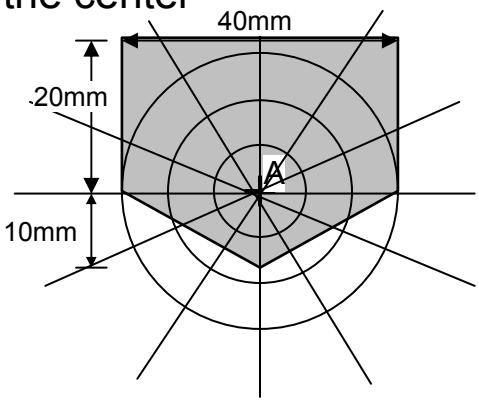

No. of elements - is (say) 76

$\Delta\sigma_v = \Delta p = 100 \times 76 \times \frac{1}{200} = 38$ kPa

9. Using Charts Describing Increase in Pressure

See figures from the Navy Design Manual, Bowles p.292 and Das 3rd edition Fig 3.41 (notes pp. 12 & 13)
Many charts exist for different specific cases like Das Fig. 5.11 (p.237) describing the load of an embankment (for extensive review see "Elastic Solutions for Soil and Rock Mechanics" by Poulus and Davis)

Most important to note:

1. What and where is the chart good for?
   e.g. under center or corner of footing?
2. When dealing with lateral stresses, what are the parameters used (mostly μ) to find the lateral stress from the vertical stress

10. Simplified Relationship

Back of an envelope calculations

2 : 1 Method (text p.231) (p.286)

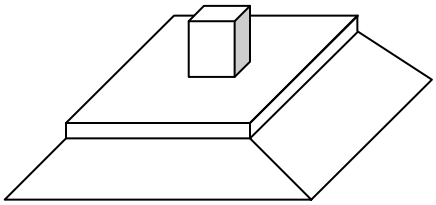

Bowles Figure 5.1,

Das Fig. 5.5, (p.231)

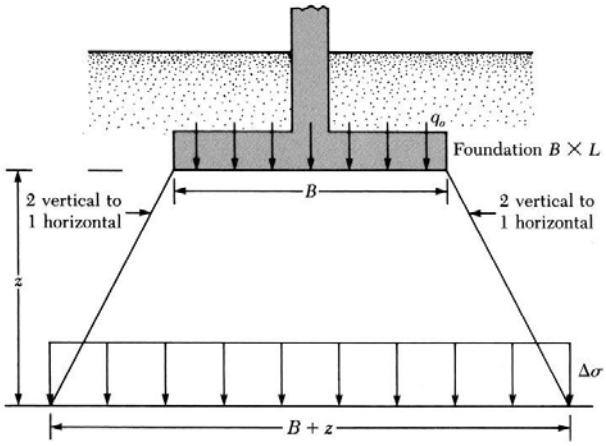

$$\Delta\sigma_v = \Delta P = \frac{Q}{(B+z)(L+z)}$$

Example:

What is the existing, additional, and total stress at the center of the loose sand under the center of the foundation ?

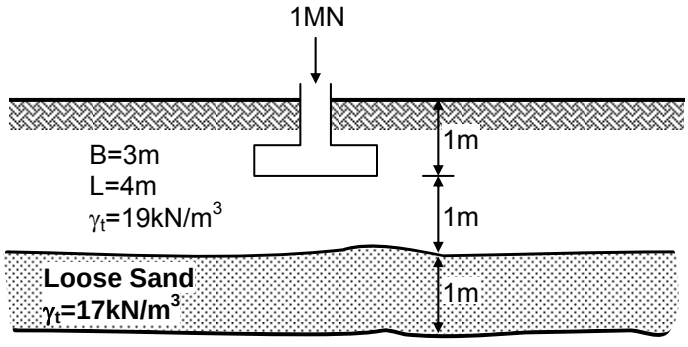

σ_v = (2 x 19) + (0.5 x 17) = 46.5 kPa

Using 2:1 method:

$\Delta\sigma_v = \frac{1000kN}{(3+1.5)(4+1.5)}$ = 40 kPa $q_{contact}$ = 83.3 kPa $\left(\Delta q / q_0 \cong 0.50\right)$

Total average stress at the middle of the loose sand σ_t = 86.5 kPa
Using Fig. 3.41 of these notes (p.12):

$\frac{z}{B} = \frac{1.5}{3} = 0.5$

$\frac{L}{B} = \frac{4}{3} = 1.33$ $\frac{\Delta p}{q_o} \approx 0.75$

$\Delta p = 0.75 \times 83.3 = 62.5$ kPa

The difference between the two values is due to the fact that the stress calculated by the 2:1 method is the <u>average</u> stress at the depth of 1.5m while the chart provides the stress at a <u>point,</u> under the center of the foundation.

This can be checked by examining the stresses under the corner of the foundation.

m = $\frac{3}{1.5}$ = 2 n = $\frac{4}{1.5}$ = 2.67

Bowles Table 5.1 (p.294), Das Table 5.2 (p.228-229)

I ≈ 0.23671 interpolated between

0.23614	0.23782
n = 2.5	n = 3

$\Delta p = 0.23671 \times 83.3 = 19.71$

Checking the average stress between the center and the corner:

$= \frac{\Delta p_{corner} + \Delta p_{center}}{2} = \frac{62.5+19.71}{2}$ = 41.1 kPa

the obtained value is very close to the stress calculated by the 2:1 method that provided the average stress at the depth of 1.5m. (40kPa)

IMMEDIATE SETTLEMENT ANALYSIS

(Bowles Sections 5.6-5.11, pp. 303-329)
(Das Sections 5.9-5.14, pp. 243-273)

1. General Elastic Relations

Different equations follow the principle of the analysis presented on p. 8.
For a uniform load (flexible foundation) on a surface of a deep elastic layer, the text presents the following detailed analysis:

$$S_e = q_0(\alpha B')\frac{1-\mu_s^2}{E_s} I_s I_f \qquad \text{(Das eq. 5.33)}$$

(Bowles eq. 5.16 & 5.16a)

q_o = contact stress

B' = $B'=B$ for settlement under the corner
= $B'=B/2$ for settlement under the center

E_s, μ = soil's modulus of elasticity and Poisson's ratio within zone of influence

α = factor depending on the settlement location
- for settlement under the center;
  $\alpha=4$, $m'=L/B$, $n'=H/(B/2)$
- for settlement under the corner;
  $\alpha=1$, $m'=L/B$, $n'=H/B$

I_s = shape factor, $I_s=F_1+\frac{1-2\mu}{1-\mu}F_2$
F_1 & F_2 f(n′ & m′) use Tables 5.8 and 5.9, pp.248-251

I_f = depth factor, $I_f=f(D_f/B, \mu_s, L/B)$, use Table 5.10 (pp.252); $I_f=1$ for $D_f=0$

For a rigid footing, $S_e \approx 0.93\ S_e$ (flexible footing)

2. Finding E_s, μ: the Modulus of Elasticity and Poisson's Ratio

For E_s : direct evaluation from laboratory tests (triaxial) or use general values and/or empirical correlation. For general values, use Table 5.8 from Das (6th ed., 2007) and see Bowles section 5.8 and Table 5.6.

Table 5.8 Elastic Parameters of Various Soils

Type of soil	Modulus of elasticity, E_s MN/m²	Modulus of elasticity, E_s lb/in²	Poisson's ratio, μ_s
Loose sand	10.5–24.0	1500–3500	0.20–0.40
Medium dense sand	17.25–27.60	2500–4000	0.25–0.40
Dense sand	34.50–55.20	5000–8000	0.30–0.45
Silty sand	10.35–17.25	1500–2500	0.20–0.40
Sand and gravel	69.00–172.50	10,000–25,000	0.15–0.35
Soft clay	4.1–20.7	600–3000	
Medium clay	20.7–41.4	3000–6000	0.20–0.50
Stiff clay	41.4–96.6	6000–14,000	

For μ (Poisson's Ratio): Cohesive Soils

Saturated Clays $\Delta V = 0$, $\mu = \nu = 0.5$

Other Soils, usually $\mu = \nu \cong 0.3$ to 0.4

Empirical Relations of Modulus of Elasticity

$$\frac{E_s}{p_a} = \alpha N_{60}$$ α = 5 to 15 (Das eq. 2.29)

(5–sands with fine s, 10–Clean N.C. sand, 15–clean O.C. sand)

Navy Design Manual (Use field values): E_s/N (E in tsf)

- Silts, sandy silts, slightly cohesive silt-sand mixtures 4
- Clean, fine to medium, sands & slightly silty sands 7
- Coarse sands & sands with little gravel 10
- Sandy gravels with gravel 12

E_s = 2 to 3.5q_c (cone resistance) CPT General Value

(Some correlation suggest 2.5 for equidimensional foundations and 3.5 for a strip foundation.)

General range for clays:

N.C. Clays Es = $250c_u$ to $500c_u$

O.C. Clays Es = $750c_u$ to $1000c_u$

See Das Table 5.7 for $E_s = \beta \cdot C_u$ and β = f(PI, OCR)

3. Improved Equation for Elastic Settlement (Mayne and Poulos, 1999)

Considering: foundation rigidity, embedment depth, increase of E_s with depth, location of rigid layers within the zone of influence.

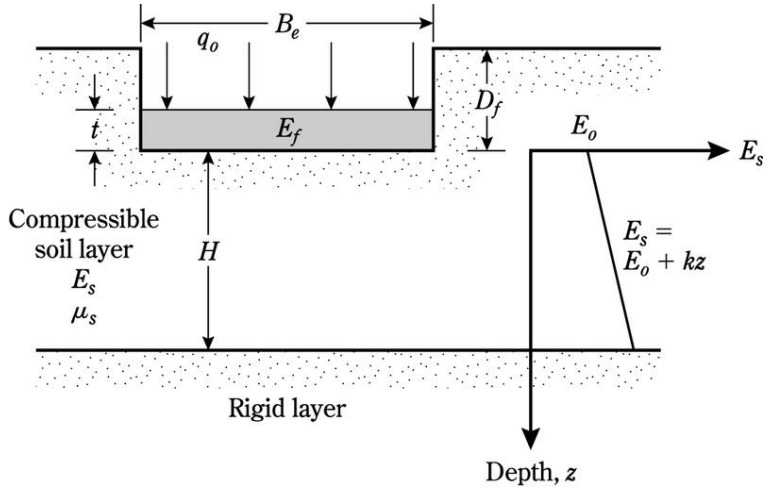

The settlement below the center of the foundation:

$$S_e = \frac{q_0 B_e I_G I_F I_E}{E_0}\left(1-\mu_s^2\right) \qquad \text{(Das eq. 5.46)}$$

- $B_e = \sqrt{\frac{4BL}{\pi}}$ or for a circular foundation $B_e = B$
- $E_s = E_0 + kz$ being considered through I_G
- I_G = f(B, H/B_e), $\beta = E_0/kB_e$

Das Figure 5.18 (p.255)
Variation of I_G with β

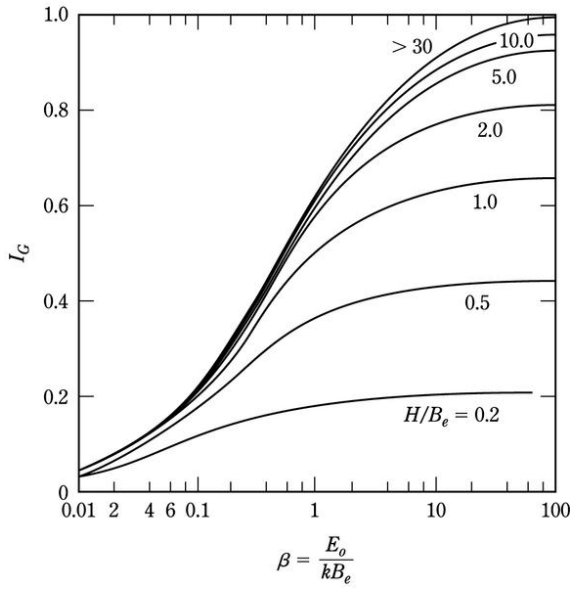

- Effect of foundation rigidity is being considered through I_F

I_F = f(k_f) flexibility factor $k_F = \left(\frac{E_f}{E_0 + \frac{B_e}{2}k}\right)\left(\frac{2t}{B_e}\right)^3$

k needs to be estimated

Das Figure 5.19 (p.256)
Variation of rigidity correction factor I_F with flexibility factor k_F [Eq.(5.47)]

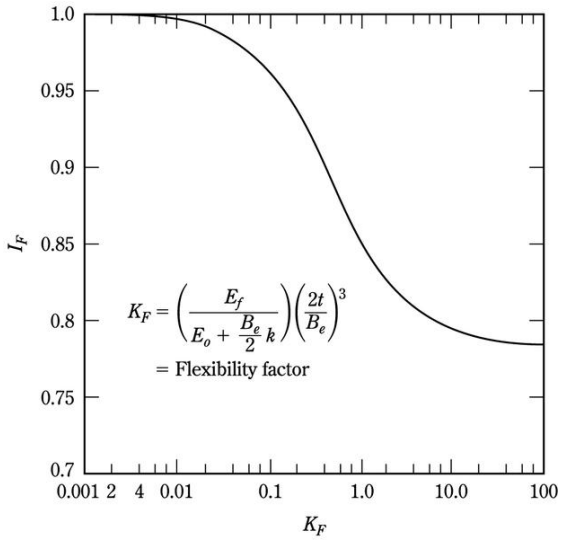

E_f = modulus of foundation material

t = thickness of foundation

- Effect of embedment is being considered through I_E;

  $I_E = f(\mu_s, D_f, B_e)$

  Das Fig. 5.20 (p.256)
  Variation of embedment correction factor I_E with D_f/B_e [Eq.(5.48)]
  Note: Figure in the text shows I_F instead of I_E.

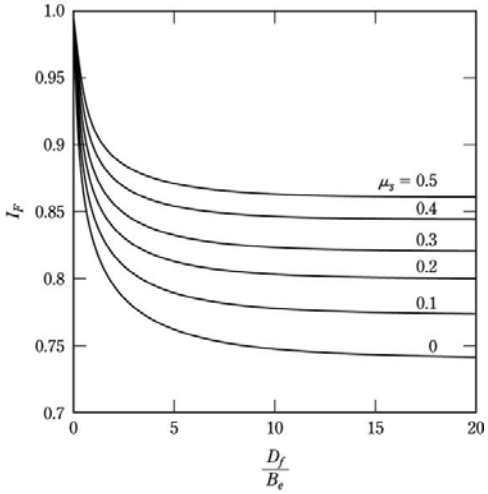

4. <u>Immediate (elastic) Settlement of Sandy Soil – The Strain Influence Factor (Schmertmann and Hartman, 1978)</u>
   (Das Section 5.12, pp. 258-263)

The surface settlement

(i) $s_i = \int_{z=0}^{\infty} \varepsilon_z dz$

From the theory of elasticity, the distribution of vertical strain ε_z under a linear elastic half space subjected to a uniform distributed load over an area:

(ii) $\varepsilon_z = \frac{\Delta q}{E} I_z$

Δq = the contact load
E = modulus of elasticity - the elastic medium
I_z = strain influence factor = f (μ, point of interest)

- From stress distribution (see Figure 3.41, p.12 of notes):
  influence of a square footing ≈ 2B
  influence of a strip footing ≈ 4B
  (both for $\frac{\Delta q}{q_{contact}} \approx 10\%$)

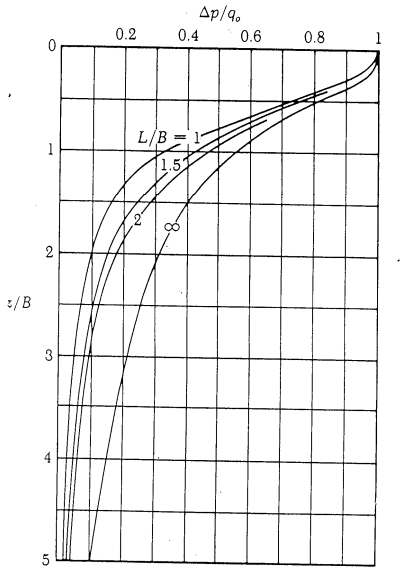

- From FEM and test results. The influence factor I_z:

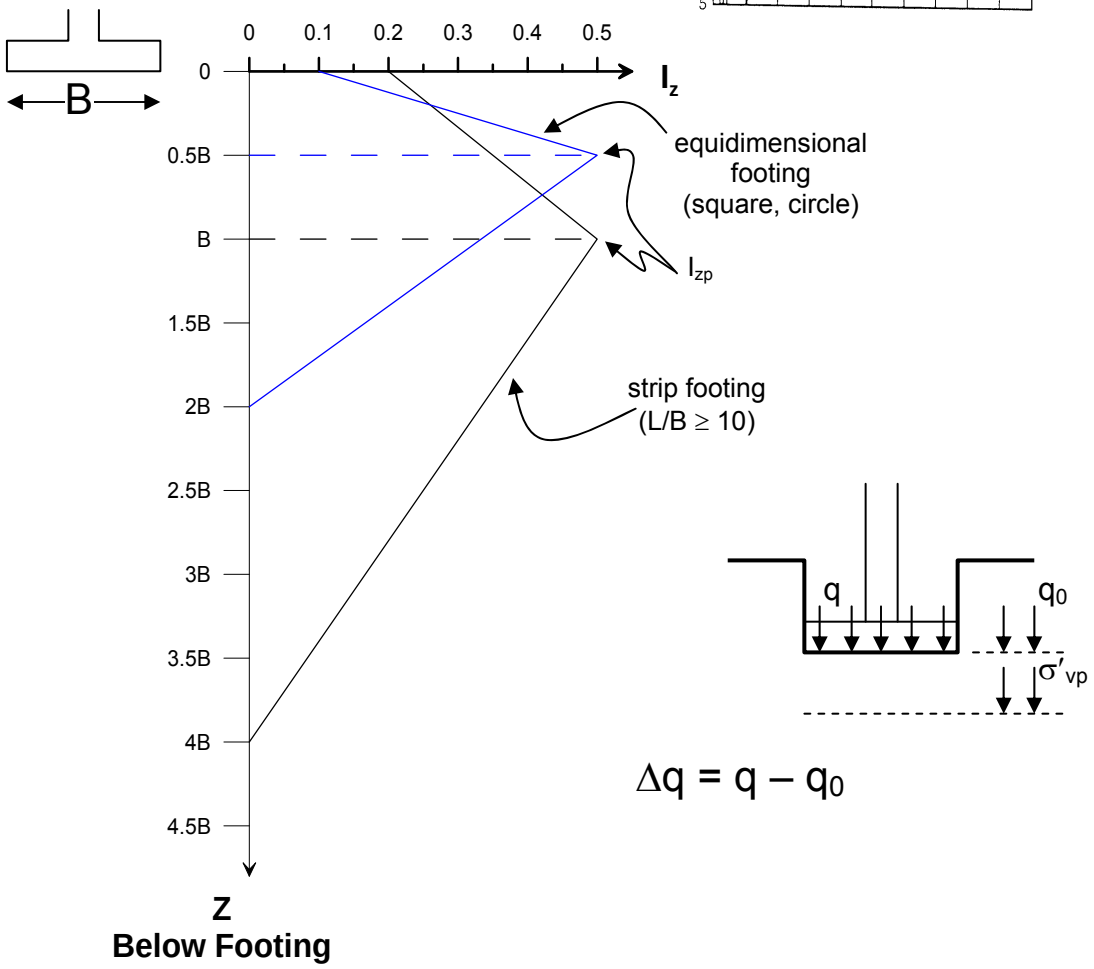

substituting the above into Eq. (i).

For square $s_i = \Delta q \int_0^{2B} \frac{I_z}{E} dz$

Approximating the integral by summation and using the above simplified ε vs. D/B relations we get to equation 5.49 of Das.

$$S_e = C_1 C_2 \Delta q \sum_{i=1}^{n} \left(\frac{I_z}{E_s} \right) \Delta z_i$$

Δq = contact stress (net stress = stress at found – q_0)

$$c_1 = 1 - 0.5 \left[\frac{\sigma'_{vo}}{\Delta q} \right]$$

σ'_{vo} is calculated at the foundation depth

I_z = strain influence factor from the distribution

E_s = modulus in the middle of the layer

C_2 - (use 1.0) or $C_2 = 1 + 0.2 \log (10t)$

Creep correction factor t = elapsed time in years

e.g. t = 5 years, C_2 = 1.34

5. The Preferable Iz Distribution for the Strain Influence Factor

The distribution of I_z provided in p.27 of the notes is actually a simplified version proposed by Das (Figure 5.21, p.259). The more complete version of I_z distribution recommended by Schmertmann et al. (1978) is

$$I_{zp} = 0.5 + 0.1 \sqrt{\frac{\Delta q}{\sigma'_{vp}}}$$

Where σ'_{vp} is the effective vertical stress at the depth of I_{zp} (i.e. 0.5B and 1B below the foundation for axisymmetric and strip footings, respectively).

6. Immediate Settlement in Sandy Soils Using Burland and Burbridge's (1985) Method
(Das Section 5.13, pp.265-267)

$$\frac{S_e}{B_R} = \alpha_1 \alpha_2 \alpha_3 \left[\frac{1.25\left(L/B\right)}{0.25 + \left(L/B\right)} \right]^2 \left(\frac{B}{B_R} \right)^{0.7} \left(\frac{q'}{p_a} \right) \qquad \text{(Das eq.5.70)}$$

1. Determine N SPT with depth (Das eq. 5.67, 5.68)
2. Determine the depth of stress influence - z′ (Das eq. 5.69)
3. Determine α_1, α_2, α_3 for NC or OC sand (Das p.266)

7. Case History - Immediate Settlement in Sand
A rectangular foundation for a bridge pier is of the dimensions L=23m and B=2.6m, supported by a granular soil deposit. For simplicity it can be assumed that L/B ≈ 10 and, hence, it is a strip footing.
- Provided q_c with depth (next page)
- Loading $\bar{q}$ = 178.54kPa, q = 31.39kPa (at D_f=2m)

Find the settlement of the foundation
(a-1) The Strain Influence Factor (as in the text)

$$C_1 = 1 - 0.5 \frac{q}{\bar{q} - q} = 1 - 0.5 \frac{31.39}{178.54 - 31.39} = 0.893$$

$$C_2 = 0.2 \log\left(\frac{t}{0.1}\right) \rightarrow \quad t = 5\text{years} \quad C_2 = 1.34$$

$$t = 10\text{years} \quad C_2 = 1.40$$

Using the attached Table for the calculation of Δz (see next page)

$$S_e = C_1 \cdot C_2 \, (\bar{q} - q) \sum \frac{Iz}{Es} \Delta z = 0.893 \cdot 1.34 \cdot (178.54 - 31.39) \cdot 18.95 \cdot 10^{-5} \text{m}$$

$$S_e = 0.03336\text{m} \cong 33\text{mm}$$

For t = 10years → S_e = <u>34.5mm</u>

For the calculation of the strain in the individual layer and it's integration over the entire zone of influence, follow the influence chart (notes p.27) and the figure and calculation table below.

Example:

$z = 0 \rightarrow I_z = 0.2$

$z = 1B = 2.6m \rightarrow I_z = 0.5$

$z_1 = 0.5m \rightarrow I_z = 0.2 + \frac{0.5 - 0.2}{2.6} \times 0.5 = 0.2577$

note: sublayer 1 has a thickness of 1m and we calculate the influence factor at the center of the layer.

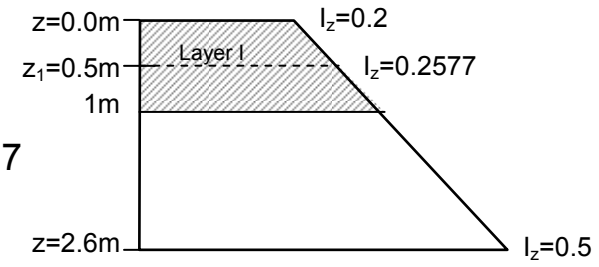

Layer	Δz (m)	q_c (kN/m²)	E_s[a] (kN/m²)	z to the center of the layer (m)	I_z at the center of the layer	$(I_z/E_s)\,\Delta z$ (m²/kN)
1	1	2,450	8,575	0.5	0.258	3.00×10^{-5}
2	1.6	3,430	12,005	1.8	0.408	5.43×10^{-5}
3	0.4	3,430	12,005	2.8	0.487	1.62×10^{-5}
4	0.5	6,870	24,045	3.25	0.458	0.95×10^{-5}
5	1.0	2,950	10,325	4.0	0.410	3.97×10^{-5}
6	0.5	8,340	29,190	4.75	0.362	0.62×10^{-5}
7	1.5	14,000	49,000	5.75	0.298	0.91×10^{-5}
8	1	6,000	21,000	7.0	0.247	1.17×10^{-5}
9	1	10,000	35,000	8.0	0.154	0.44×10^{-5}
10	1.9	4,000	14,000	9.45	0.062	0.84×10^{-5}
	Σ 10.4 m = $4B$					Σ 18.95×10^{-5}

[a] $E_s \approx 3.5 q_c$

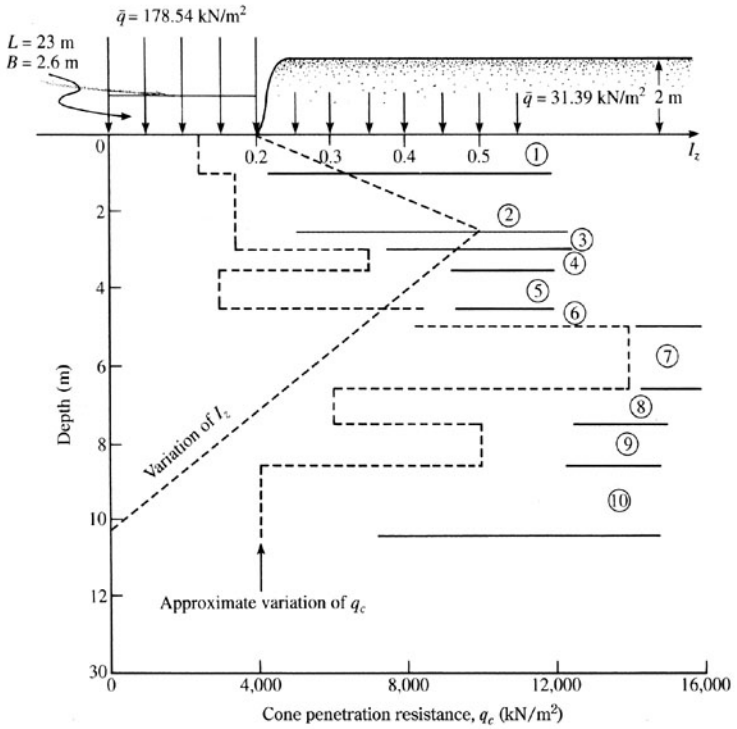

Variation of I_z and q_c below the foundation

(a-2) The Strain Influence Factor (Schmertmann et al., 1978)

$$I_{zp} = 0.5 + 0.1\sqrt{\frac{\Delta q}{\sigma'_{vp}}}$$

q = 31.39kPa $\rightarrow$ γ_t = 15.70kN/m^3

Δq = 178.54 – 31.39 = 147.15

σ'_{vp} @ 1B below the foundation = 31.39 + 2.6 (15.70) = 72.20kPa

$$I_{zp} = 0.5 + 0.1\sqrt{\frac{147.15}{72.2}} = 0.50 + 0.14 = 0.64$$

This change will affect the table on p. 30 in the following way:

Layer	I_z	$(I_z/E_z)\Delta z$ [(m^2/kN)x10^{-5}]
1	0.285	3.31
2	0.505	6.72
3	0.624	2.08
4	0.587	1.22
5	0.525	5.08
6	0.464	0.79
7	0.382	1.17
8	0.279	1.32
9	0.197	0.56
10	0.078	1.06
		Σ 23.31x10^{-5}

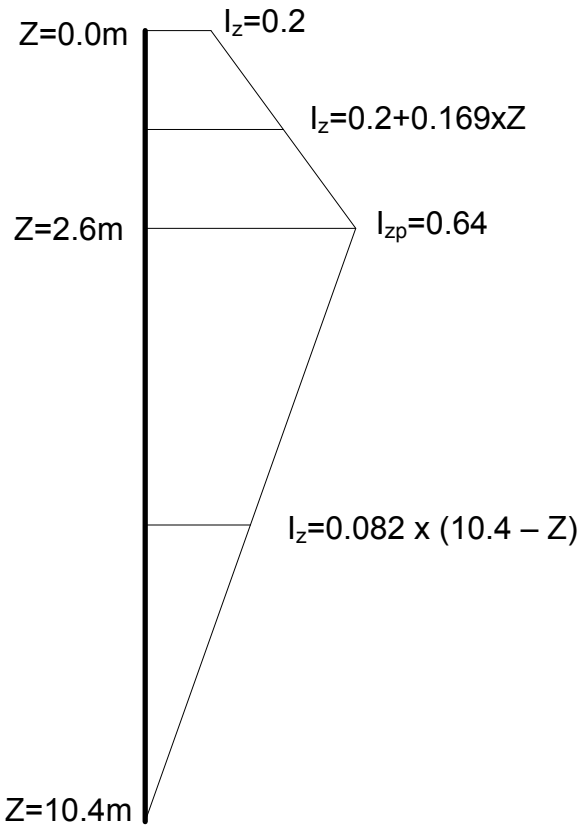

$$S_e = C_1 \cdot C_2 (\bar{q} - q) \cdot \sum \frac{I_z}{E_s} \Delta z$$

Using the I_{zp}

S_e = 40.6mm

for t = 10 years, S_e = 42.4mm

Using the previously presented elastic solutions for comparison:

(b) The elastic settlement analysis presented in Das sect. 5.10

$$S_e = q_0(\alpha B')\frac{1-\mu_s^2}{E_s} I_s I_f \qquad \text{(Das eq.5.33)}$$

$B' = 2.6/2 = 1.3$m for center
$B = 2.6$m for corner
$q_0 = 178.54$kPa (stress applied to the foundation)

Strip footing, zone of influence $\approx 4B = 10.4$m
From the problem figure ➔ $q_c \approx 4000$kPa. Note the upper area is most important and the high resistance zone between depths 5 to 6.3m is deeper than 2B, so choosing 4,000kPa is on the safe side. Can also use weighted average (Das Eq. 5.34)

$q_c \approx 4{,}000$kPa, general, use notes p.23-24:
$E_s = 2.5q_c = 104{,}000$kPa, matching the recommendation for a square footing
$\mu_s \approx 0.3$ (the material dense)

For settlement under the center:

α=4, m′=L/B=23/2.6 = 8.85, n′=H/(B/2)= (>30m)/(2.6/2) > 23

Das Table 5.8

m′ = 9	n′ = 12	F_1 = 0.828	F_2 = 0.095
m′ = 9	n′ = 100	F_1 = 1.182	F_2 = 0.014

the difference between the values of m′=8 or m′=9 is negligible so using m′=9 is ok. For n′ one can interpolate. For accurate values one can follow Das Eqs. 5.34 to 5.39.

interpolated values for n′=23 ➔ F_1=0.872, F_2=0.085

for exact calculations:

$$I_s = F_1 + \frac{1-2\mu_s}{1-\mu_s} F_2 = 0.872 + \frac{1-2(0.3)}{1-0.3}(0.085) \cong 0.921$$

As the sand layer extends deep below the footing H/B >> and F_2 is quite negligible.

For settlement under corner:

α=1, m′=L/B= 8.85, n′=H/(B)= (>30m)/2.6 > 11.5

Das Tables 5.8 & 5.9

m′ = 9 n′ = 12 F_1 = 0.828 F_2 = 0.095

$$I_s = 0.828 + \frac{1-2(0.3)}{1-0.3}(0.095) \cong 0.882$$

D_f/B = 2/2.6 = 0.70, L/B = 23/2.6 = 8.85

Das Table 5.10

➔ μ_s = 0.3, B/L = 0.2, D_f/B = 0.6 ➔ I_f = 0.85,

- Settlement under the center (B′ = B/2, α = 4)

$$S_e = 178.54(4)(1.15)\frac{1-(0.3)^2}{10,000}(0.921)(0.85) = 0.0585m = \underline{58\text{mm}}$$

- Settlement under the corner (B′ = B, α = 1)

$$S_e = 178.54(1)(2.3)\frac{1-(0.3)^2}{10,000}(0.882)(0.85) = 0.0280m = \underline{28\text{mm}}$$

Average Settlement = **<u>43mm</u>**

Using Das eq. 5.41 settlement for flexible footing = (0.93)(43)

= <u>40mm</u>

(c) The elastic settlement analysis presented in Das sect. 5.11:

$$S_e = \frac{q_0 B_e I_G I_F I_E}{E_0}\left(1-\mu_s^2\right) \qquad \text{(Das eq. 5.46)}$$

$$B_e = \sqrt{\frac{4BL}{\pi}} = \sqrt{\frac{4(2.6)(23)}{\pi}} = 8.73m$$

$$\beta = \frac{E_0}{kB_e}$$

Using the given figure of q_c with depth, an approximation of q_c with depth can be made such that $q_c=q_0+z(q/z)$ where $q_0 \approx$ 2200kPa, $q/z \approx$ 6000/8 = 750kPa/m

Using the ratio of E_s/q_c = 2.5 used before, this relationship translates to E_0 = 5500kPa and k = E/z = 1875kPa/m

$$\beta = \frac{5500}{(1875)(8.73)} = 0.336$$

H/B_e = >10/8.73 > 1.15 no indication for a rigid layer and actually a less dense layer starts at ≈9m ($q_c \approx$ 4000kPa)

Das Figure 5.18, $\beta \approx 0.34 \rightarrow \underline{I_G \approx 0.35}$ (note; H/B_e has almost no effect in that zone when greater than 1.0)

$$k_F = \frac{E_f}{E_0 + \frac{B_e}{2}k}\left(\frac{zt}{B_e}\right)^3$$

Using $E_f = 15x10^6$kPa, t = 0.5m

$$k_F = \frac{15x10^6}{5500 + \frac{8.73}{2}1875}\left(\frac{2x0.5}{8.73}\right)^3 = 1.65$$

$$I_F = \frac{\pi}{4} + \frac{1}{4.6x10k_F} = \frac{\pi}{4} + \frac{1}{4.6x10x1.65} = 0.80$$

$$I_E = 1 - \frac{1}{3.5e^{(1.22\mu_s - 0.4)}\left(B_e/D_f + 1.6\right)}$$

$$I_E = 1 - \frac{1}{3.5e^{(1.22x0.3 - 0.4)}\left(8.73/2 + 1.6\right)} = 1 - \frac{1}{20.18} = 0.95$$

$$S_e = \frac{178.54x8.73x0.35x0.80x0.95}{5500}\left(1 - 0.3^2\right) = 0.0686m = \underline{\mathbf{69mm}}$$

(d) Burland and Burbridge's Method presented in Das section 5.13, p.265

1. Using $q_c \approx 4{,}000$kPa = 41.8tsf and as $E_s \cong 7N$ and $E_s \cong 2q_c$ we can also say that: $N \approx q_c$(tsf)/3.5
   $\therefore N \approx 12$

2. The variation of q_c with depth suggests increase of q_c to a depth of ~6.5m (2.5B) and then decrease. We can

assume that equation 5.69 is valid as the distance to the "soft" layer (z″) is beyond 2B.

$$\frac{z'}{B_R} = 1.4\left(\frac{B}{B_R}\right)^{0.75}$$

B_R = 0.3m
B = 2.6m

3. Elastic Settlement (Das eq.5.70)

$$S_e = B_R \alpha_1 \alpha_2 \alpha_3 \left[\frac{1.25\frac{L}{B}}{0.25+\frac{L}{B}}\right]^2 \left(\frac{B}{B_R}\right)^{0.7} \left(\frac{q'}{p_a}\right)$$

Assuming N.C. Sand:

α_1 = 0.14, $\alpha_2 = \frac{1.71}{(12)^{1.4}} = 0.049$ α_3 = 1

$$S_e = 0.3(0.14)(0.049)(1)\left[\frac{1.25\frac{23}{2.6}}{0.25+\frac{23}{2.6}}\right]^2 \left(\frac{2.6}{0.3}\right)\left(\frac{178.54}{100}\right)$$

$$S_e = 0.00206\left[\frac{12.5}{9.1}\right]^2 (8.67)(1.7854) = 0.060m = \underline{\mathbf{60mm}}$$

(e) Summary and Conclusions

Method	Case	Settlement (mm)
Strain Influence Das sect. 5.12, 5 years	I_z (Das)	33
	I_{zp} (Schmertmann et al.)	41
Elastic Das sect. 5.10	Center	58
	Corner	28
	Average	40
Elastic Das sect. 5.11		69
B & B Das sect. 5.13		60

- The elastic solution (section 5.10), the improved equation (section 5.11) and B&B (section 5.13) resulted with a similar settlement analysis under the center of the footing (57, 69, and 60mm respectively). This settlement is about twice that of the strain influence factor method as presented by Das.
- Averaging the elastic solution method result for the center and corner and evaluating "flexible" foundation resulted with a settlement similar to the strain influence factor as proposed by Schmertmann (39 vs. 41mm). The improved method considers the foundation stiffness.
- The elastic solutions of sections 5.10 and 5.11 are quite complex and take into considerations many factors compared to common past elastic methods.
- The major shortcoming of all the settlement analyses is the accuracy of the soil's parameters, in particular the soil's modulus and its variation with depth. As such, many of the refined factors (e.g. for the elastic solutions of sections 5.10 and 5.11) are of limited contribution in light of the soil parameter's accuracy.
- What to use?
  (1) From a study conducted at UML Geotechnical Engineering Research Lab, the strain influence method

using I_{zp} recommended by Schmertmann provided the best results with the mean ratio of load measured to load calculated for a given settlement being about 1.28 $\pm$ 0.77 (1 S.D.) for 231 settlement measurements on 53 foundations.

(2) Check as many methods as possible, make sure to examine the simple elastic method.

(3) Check ranges of solutions based on the possible range of the parameters (e.g. E_0).

For example, in choosing q_c we could examine the variation between 3,500 to 6,000 and then the variation in the relationship between q_c and E_s between 2 to 3.5. The results would be:

E_{smin} = 2 x 3,500 = 7,000kPa
E_{smax} = 3.5 x 6,000 = 21,000kPa

As S_e of equation 5.33 is directly inverse to E_s, this range will result with:

S_{emin} = 27mm, S_{emax} = 81mm (compared to 57mm)

8. <u>Immediate (Elastic) Settlement of Foundations on Saturated Clays</u>: (Junbu et al., 1956), Das section 5.9, p.243

$\mu = \nu_s = 0.5$ Flexible Footings

$$Se = A_1 A_2 \frac{q_0 B}{E_s} \qquad \text{(Das eq.5.30)}$$

A_1 = Shape factor and finite layer - $A_1 = f(H/B, L/B)$
A_2 = Depth factor - $A_2 = f(D_f/B)$

Note: H/B >>> deep layer the values become asymptotic
e.g. for L = B (square) and H/B $\geq$ 10 $A_1 \approx 0.9$

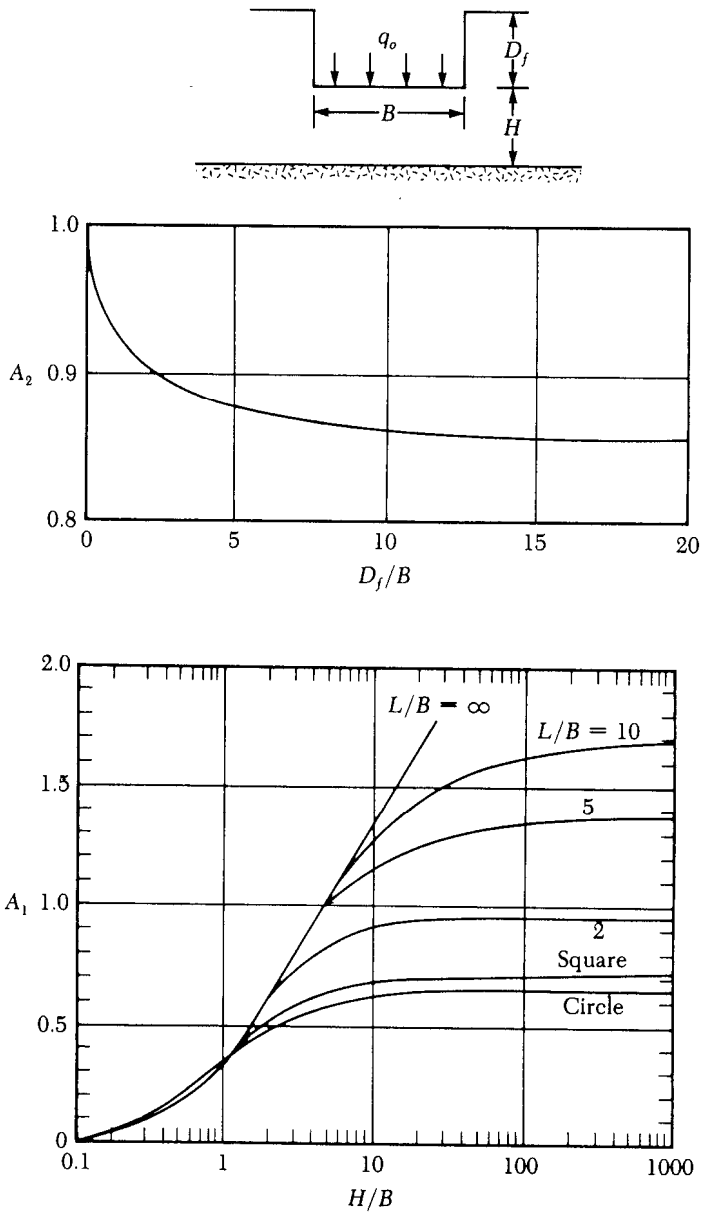

Das Figure 5.14 Values of A_1 and A_2 for elastic settlement calculation – Eq. (5.30) (after Christian and Carrier, 1978)

CONSOLIDATION SETTLEMENT - LONG TERM SETTLEMENT

Consolidation General, Bowles Sect. 2.10 (pp.54-66) and Das Sect. 1.13 (pp.32-37)
Consolidation Settlement for Foundations, Das Sects. 5.15–5.20 (pp.273-285)

1. Principle and Analogy

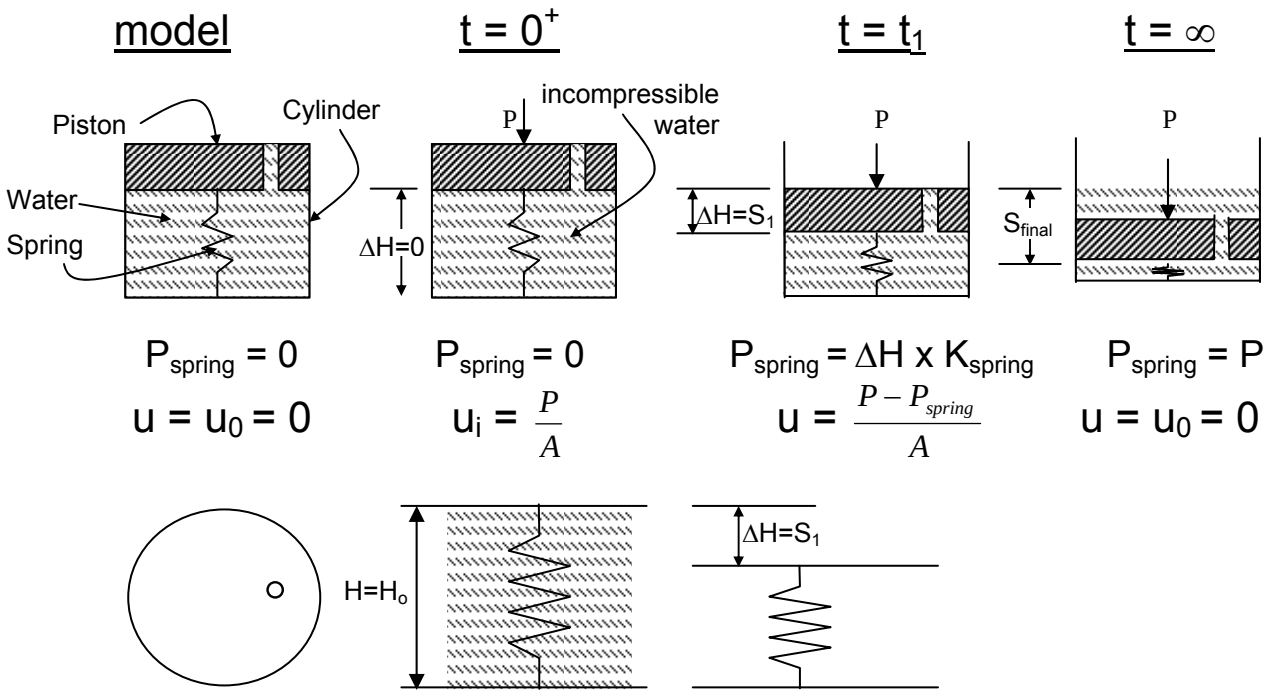

We relate only to changes, i.e. the initial condition of the stress in the soil (force in the spring) and the water are being considered as zero. The water pressure before the loading and at the final condition after the completion of the dissipation process is hydrostatic and is taken as zero, ($u_0 = u_{hydrostatic} = 0$). The force in the spring before the loading is equal to the weight of the piston (effective stresses in the soil) and is also considered as zero for the process, $P_{spring} = P_o$ = effective stress before loading= $P_{at\ rest}$. The initial condition of the process is full load in the water and zero load in the soil (spring), at the end of the process there is zero load in the water and full load in the soil.

Analogy Summary

model	soil
water →	water
spring →	soil skeleton/effective stresses
piston →	foundation
hole size→	permability
force P →	load on the foundation or at the relevant soil layer due to the foundation

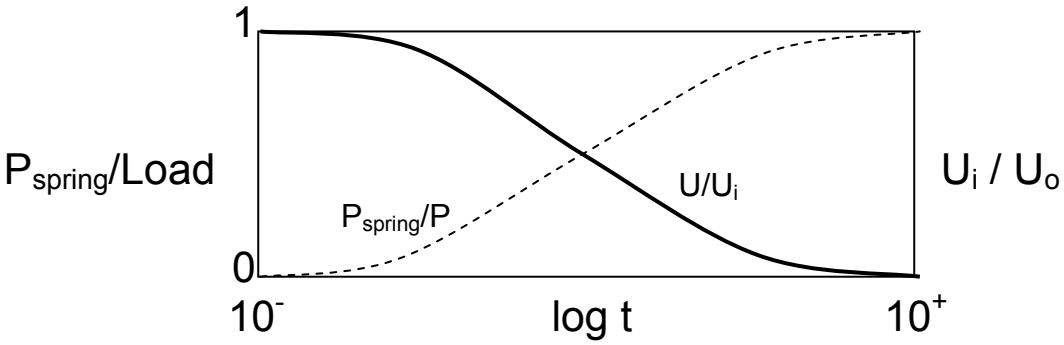

2. Final Settlement Analysis

(a) Principle of Analysis

$$e = \frac{V_v}{V_s}$$

$$\omega = \frac{W_w}{W_s}$$

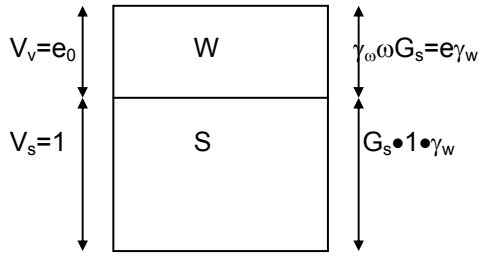

weight - volume relations
saturated clay

initial soil volume = $V_o = 1 + e_o$

final soil volume = $V_f = 1+e_o-\Delta e$

$\Delta V = V_o - V_f = \Delta e$

As area A = Constant:

$V_o = H_o \times A$ and $V_f = H_f \times A$

$\Delta V = V_o - V_f = A(H_o - H_f) = A \times \Delta H$

$\Delta H = \frac{\Delta V}{A}$

for 1-D (note, we do not consider 3-D effects and assume pore pressure migration and volume change in one direction only).

$$\varepsilon_v = \frac{\Delta H}{H_o} = \frac{\frac{\Delta V}{A}}{\frac{V_o}{A}} = \frac{\Delta V}{V_o}, \text{ substituting for V, e relations}$$

$$\varepsilon_v = \frac{\Delta V}{V_o} = \frac{\Delta e}{V_o} = \frac{\Delta e}{1 + e_o}$$

$$\boxed{\Delta H = \varepsilon_v \times H_o = \frac{\Delta e}{1 + e_o} \times H_o}$$

Calculating Δe

We need to know:

(i) Consolidation parameters c_c, c_r at a representative point(s) of the layer, based on odometer tests on undisturbed samples.

(ii) The additional stress at the same point(s) of the layer, based on elastic analysis.

(b) Consolidation Test (1-D Test)

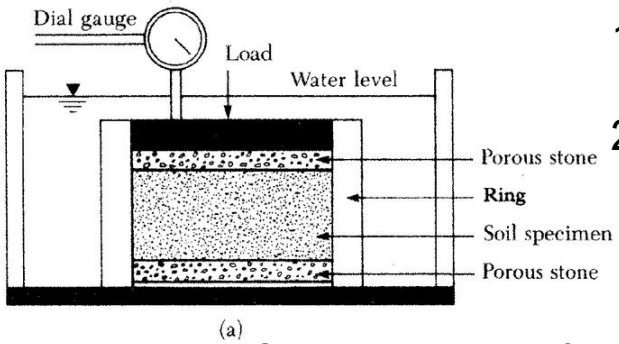

Das Fig. 1.15a Schematic Diagram of consolidation test arrangement (p.33)

1. Oedometer = Consolidometer

2. Test Results

a) final settlement with load after 24 hours

b) settlement with time under a certain load

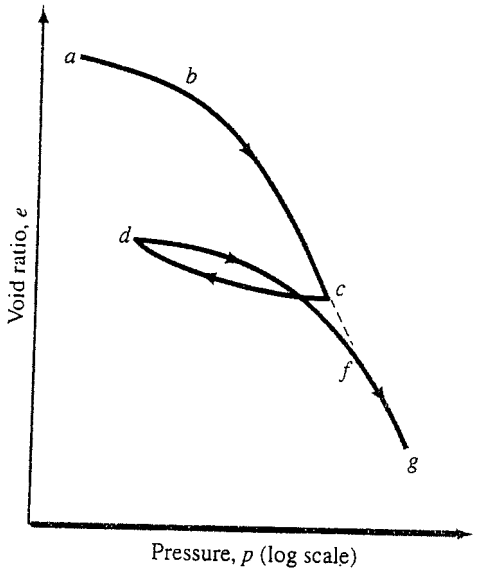

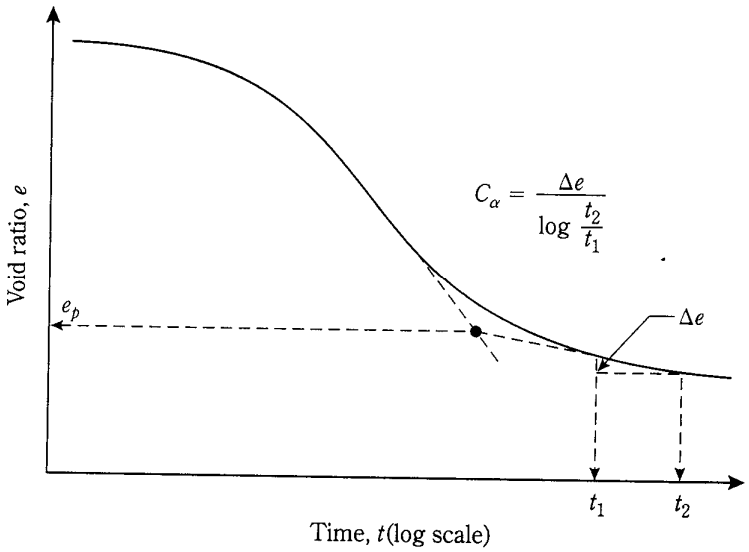

$e = \frac{V_v}{V_s}$ e << $\rightarrow$ V_v << $\rightarrow$ denser material

γ_d >> $\gamma_d = \frac{W_s}{V}$ (V <<)

(c) Obtaining Parameters from Test Results

analysis of e-log p results.

1st Stage - Casagrande's procedure to find max. past pressure.
(see Das Figs. 1.15 to 1.17, pp.33 to 37, respectively)
(see Bowles Figs. 2.16a and b, pp.74 and 75, respectively)

1. find the max. curvature.
   - use a constant distance and look for the max. normal.
   - draw tangent to the curve at that point.
2. draw horizontal line through that point and divide the angle.
3. extend (if doesn't exist) the e-log p line to e = 0.42eo
4. extend the tangent to the curve and find its point of intersection with the bisector of stage 2. $\rightarrow P_c'$ = max. past pressure.

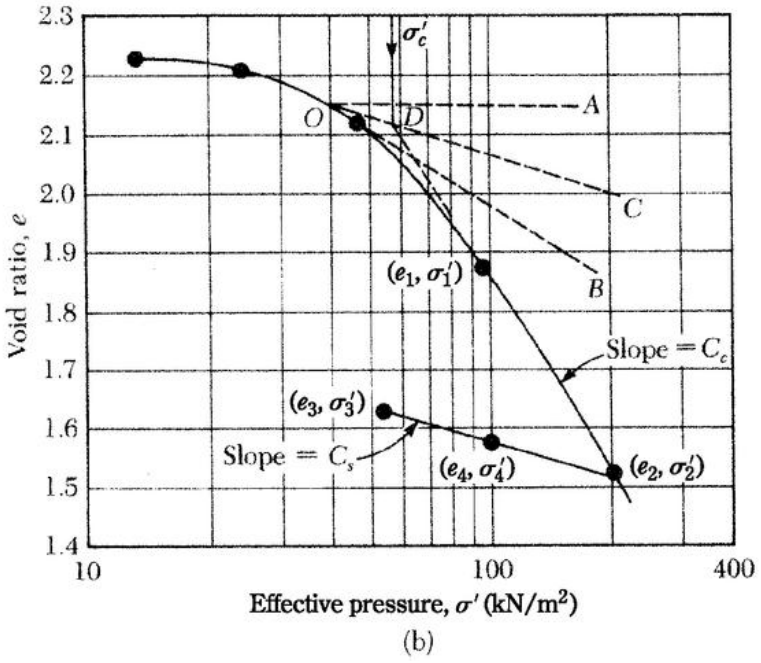

Das Figure 1.15 (b) e-log σ′ curve for a soft clay from East St. Louis, Illinois (note: at the end of consolidation, σ = σ′

2nd Stage - Reconstructing the full e-log p' (undisturbed) curve (Schmertmann's Method; See Das Figs. 1.16 & 1.17, pp.35 & 37, and Bowles Figure 2.17, p.76)

OCR = $\frac{p_c'}{p_o'}$

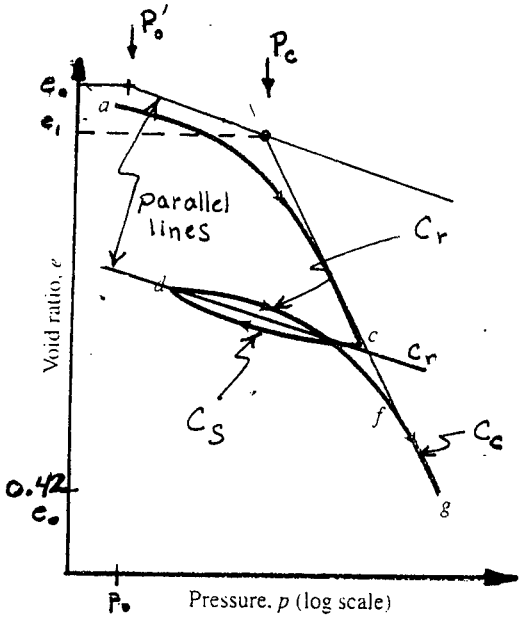

1. find the point e_o, p'_o
   $e_o = \omega_n \times G_s$ $\quad p'_o = \gamma' z$
2. find the avg. recompression curve and pass a parallel line through point 1.
3. find point p_c' & e.
4. connect the above point to $e = 0.42e_o$

Compression index (or ratio)

$$C_c = \frac{\Delta e}{\log\left(p_2/p_1\right)} = \frac{e_1 - e_2}{\log\left(p_2/p_c\right)}$$

Recompression index (or ratio)

$$C_r = \frac{\Delta e}{\log\left(p_c/p_o\right)} = \frac{e_o - e_1}{\log\left(p_c/p_o\right)}$$

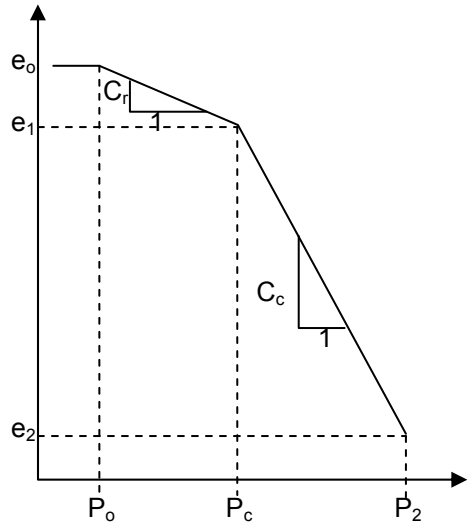

- See Das p.35-37 and Bowles Table 2.5 for C_s & C_c values.
- natural clay $C_c \approx 0.09(LL - 10)$ where LL is in (%) (eq.1.50)
- B.B.C $C_c = 0.35$ $C_s = 0.07$

(d) Final Settlement Analysis (Bowles p. 83-84)

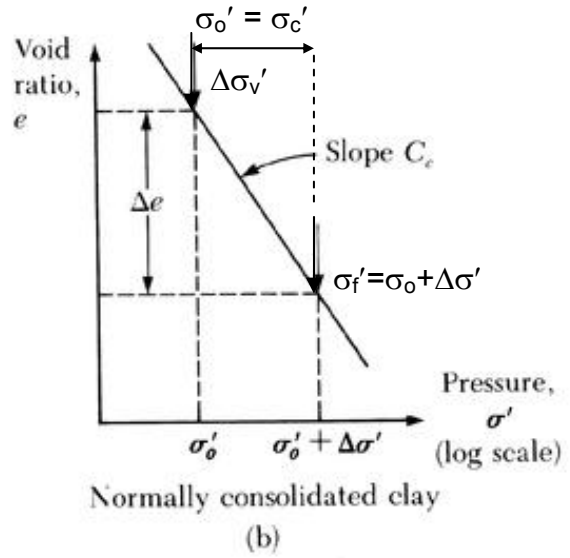

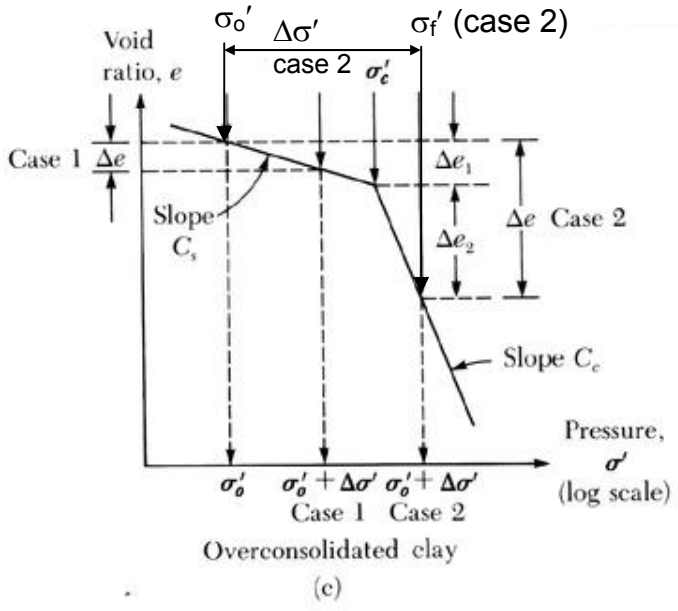

$$\Delta e = C_c \log \frac{\sigma'_o + \Delta\sigma'}{\sigma'_o} \qquad \Delta e = \overbrace{C_s \log \frac{\sigma_c'}{\sigma_o'}}^{\Delta e_1} + \overbrace{C_c \log \frac{\sigma_o' + \Delta\sigma}{\sigma_c'}}^{\Delta e_2}$$

(for $\sigma'_o + \Delta\sigma' > \sigma'_c$)

Solution:

1. Subdivide layers according to stratification and stress variation
2. In the center of each layer calculate $\sigma'_{vo}(\sigma'_o)$ and $\Delta\sigma'$
3. Calculate for each layer Δe_i

$$H = \sum_{i=1}^{n} H_i \frac{\Delta e_i}{1+e_o}$$

replace p_c by $\sigma'_{v\,max}$ and p_o by $\sigma'_{v\,o}$

The average increase of the pressure on a layer ($\Delta\sigma' = \Delta\sigma'_{av}$) can be approximated using Das eq. 5.84 (p.274)

$$\Delta\sigma'_{av} = \frac{1}{6}(\Delta\sigma'_t + 4\Delta\sigma'_m + \Delta\sigma'_b)$$

↑ top ↑ middle ↑ bottom

Skempton - Bjerrum Modification for Consolidation Settlement
Das Section 5.16 p. 275 - 279

The developed equations are based on 1-D consolidation in which the increase of pore pressure = increase of stresses due to the applied load. Practically we don't have 1-D loading in most cases and hence different horizontal and vertical stresses.

$\Delta u = \sigma_c + A[\sigma_1 - \sigma_c]$

A = Skempton's pore pressure parameter

For example: Triaxial Test

N.C. OCR = 1 0.5<A<1

OCR < 4 0.25<A<0.5

OCR ≈ 5 0

OCR > 6 -0.5<A<0

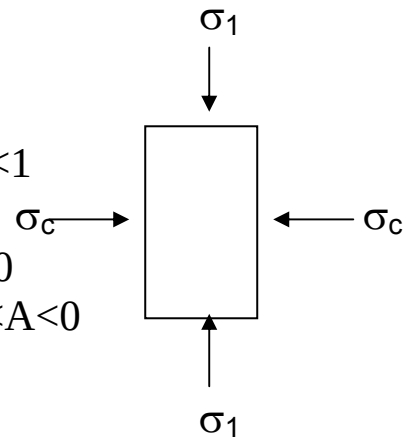

considering the partial pore pressure build up, we can modify our calculations:

1) calculate the consolidation settlement the same way as was shown earlier
2) determine pore water pressure parameter → lab test or see the table on p. 52 in Das
3) H_c/B = consolidation depth / foundation width
4) use Das Fig. 5.31, p.276, (A & H_c/B) → settlement ratio (<1)
   (Note circular or continuous)
5) $S_c = S_{c\ calc}$ x Settlement Ratio

Note: Das Table 5.14, p.277 provides the settlement ratio as a function of B/H_c and OCR based on Leonards (1976) field work. It is an alternative to Figure 5.31 as A = f(OCR), (see above) for which an equivalent circular foundation can be calculated (e.g. $B_{eq} = \sqrt{L \times B}$)

From Das, Figure 5.31 and Table 5.14

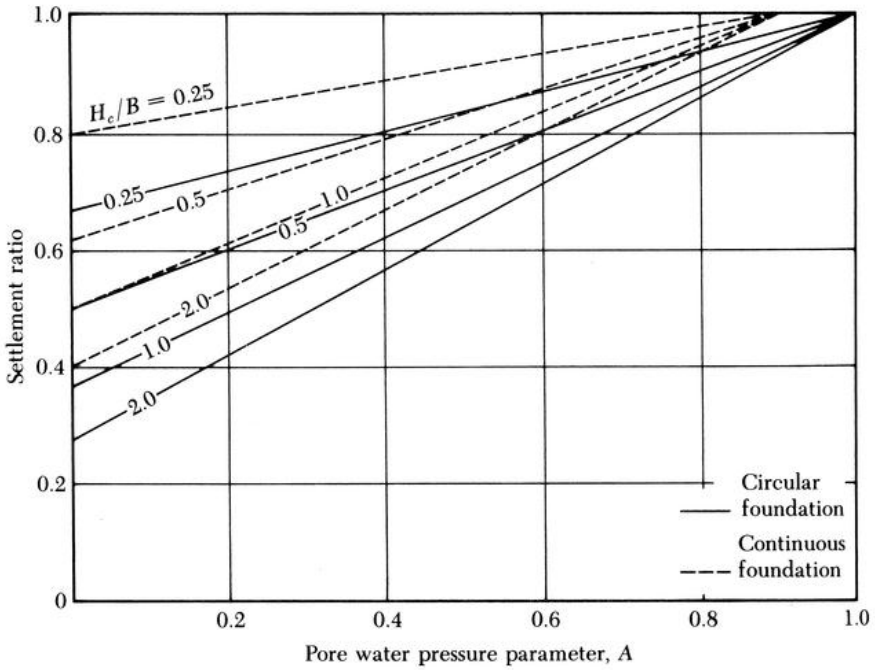

Figure 5.31 Settlement ratios for circular (K_{cir}) and continuous (K_{str}) foundations

Table 5.14 Variation of $K_{cr(OC)}$ with OCR and B/H_c

	$K_{cr(OC)}$		
OCR	**B/H_c = 4.0**	**B/H_c = 1.0**	**B/H_c = 0.2**
1	1	1	1
2	0.986	0.957	0.929
3	0.972	0.914	0.842
4	0.964	0.871	0.771
5	0.950	0.829	0.707
6	0.943	0.800	0.643
7	0.929	0.757	0.586
8	0.914	0.729	0.529
9	0.900	0.700	0.493
10	0.886	0.671	0.457
11	0.871	0.643	0.429
12	0.864	0.629	0.414
13	0.857	0.614	0.400
14	0.850	0.607	0.386
15	0.843	0.600	0.371
16	0.843	0.600	0.357

(e) EXAMPLE - Final Consolidation Settlement

Calculate the final settlement of the footing shown in the figure below. Note, OCR = 2 for all depths. Give the final settlement with and without Skempton & Bjerrum Modification

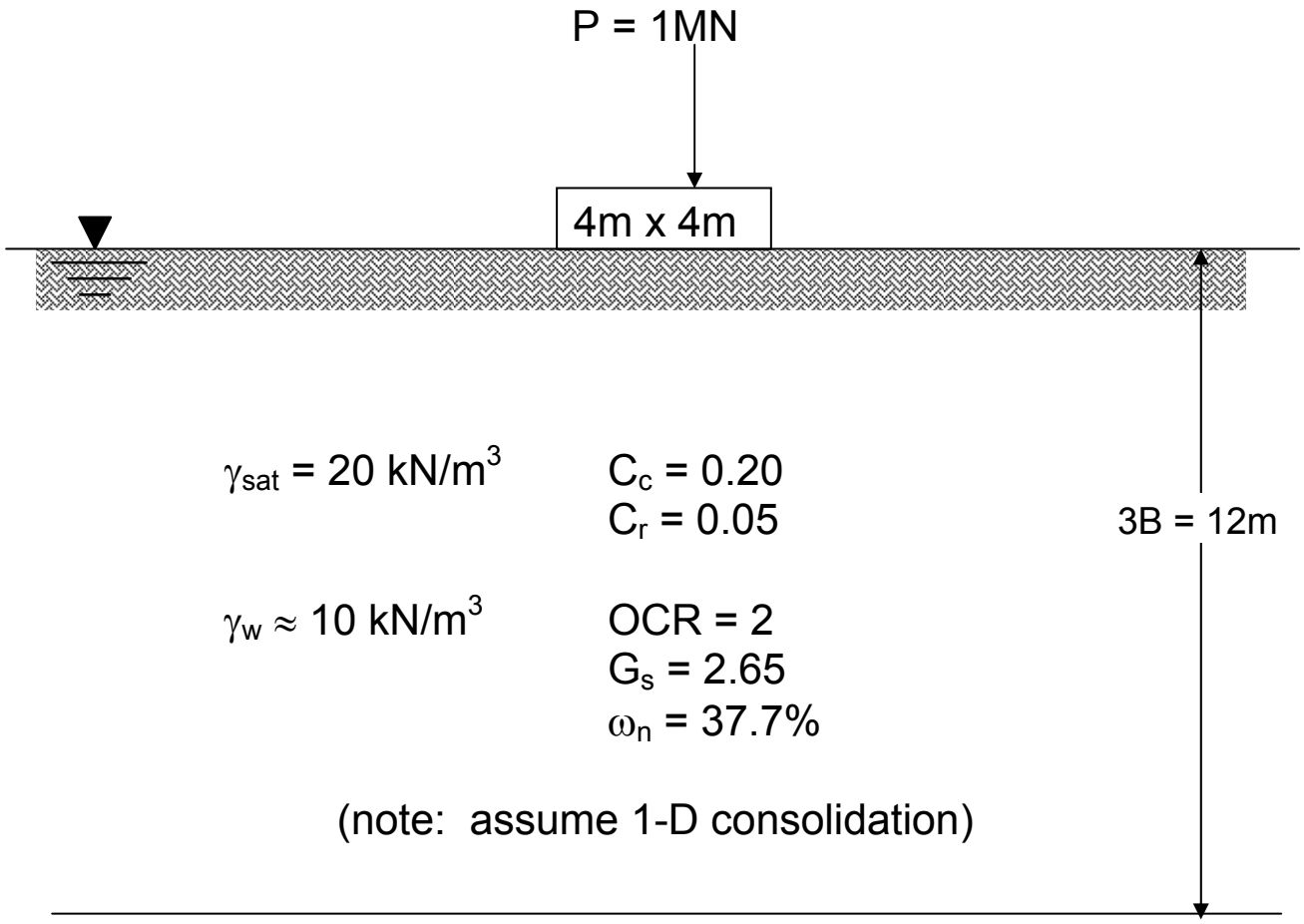

γ_{sat} = 20 kN/m^3

$\gamma_w \approx$ 10 kN/m^3

C_c = 0.20

C_r = 0.05

OCR = 2

G_s = 2.65

ω_n = 37.7%

(note: assume 1-D consolidation)

P=1MN, B=4mx4m, q_0 = 1000/16=62.5kPa

	z (m)	z/B	$\Delta q/q_o$	Δq	P_o' (kPa)	P_c' (kPa)	$P_o' + \Delta q = P_f'$	Δe	$\frac{\Delta e}{1+eo} \bullet \Delta H$
Layer I	1	(0.25) +	0.90	56.3	10	20	66.3	0.1188	0.1188
----------	2	----------							
Layer II	3	(0.75) +	0.50	31.3	30	60	61.3	0.0165	0.0165
----------	4	----------							
Layer III	6	(1.50) +	0.16	10.0	60	120	70.0	0.003	0.006
----------	8	----------							
Layer IV	10	(2.5) +	0.07	4.4	100	200	104.4	0.001	0.002
----------	12	----------							

$\sum$ = 0.1433m

1) From Figure 3.41, Notes p. 12
$\rightarrow$ influence depth {10% $\rightarrow$ 2B, $\cong$ 5% $\rightarrow$ 3B} = 12 m.

2) Subdivide the influence zone into 4 sublayers 2 of 2m in the upper zone (major stress concentration) and 2 of 4 m below.

3) Calculate for the center of each layer: Δ_q, P_o', P_c', P_f'

4) $e_o = \omega_n \cdot G_s = 1.0$

5) Calculate Δe for each layer:

$$\Delta e_1 = c_r \log\frac{20}{10} + C_c \log\frac{66}{20} = 0.1188$$

$$\Delta e_2 = c_r \log\frac{60}{30} + C_c \log\frac{61}{60} = 0.0165$$

$$\Delta e_3 = c_r \log\frac{70}{60} = 0.003$$

$$\Delta e_4 = c_r \log\frac{104}{100} = 0.001$$

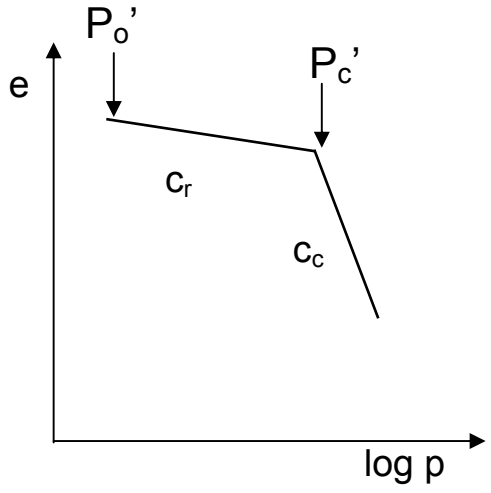

For the evaluation of the increased stress, use general Charts of Stress distribution beneath a rectangular and strip footings

(a) Use Figure 3.41 (p.12 of notes)

$\rightarrow \Delta P/q_o$ vs. z/B under the center of a rectangular footing

(use L/B = 1)

Stress Increase in a Soil Mass Caused by Foundation Load

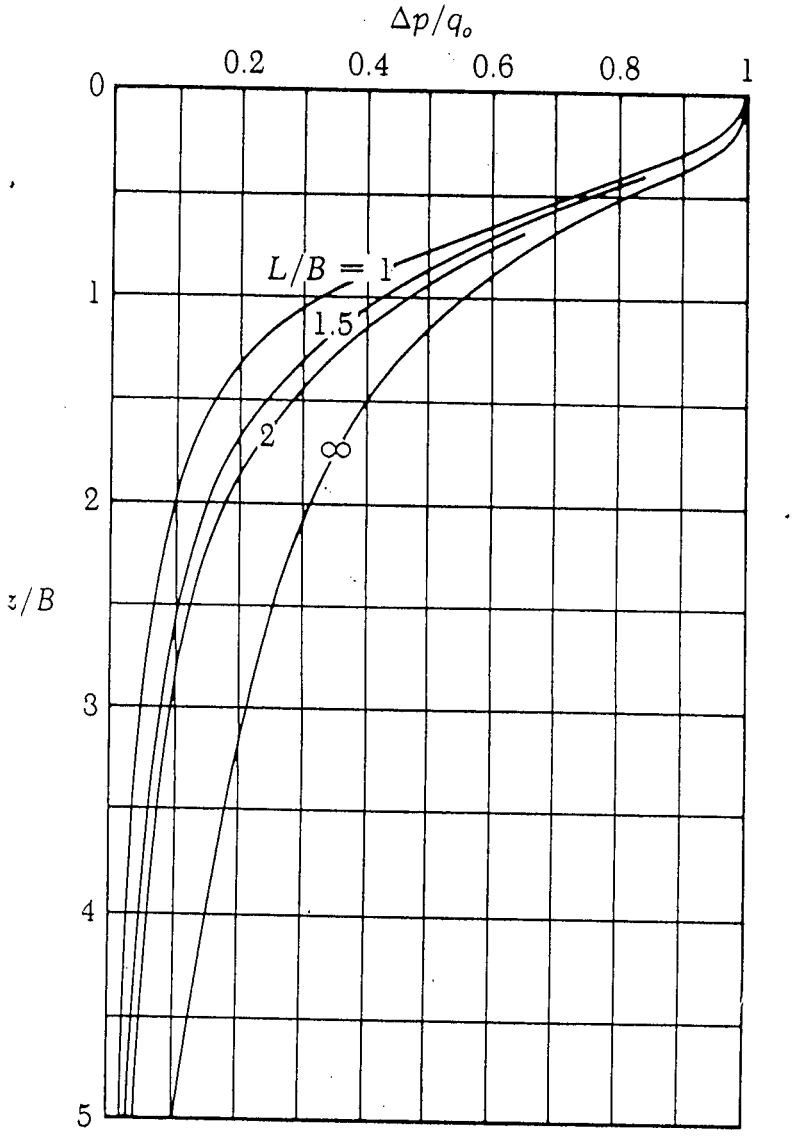

Das "Principle of Foundation Engineering", 3rd Edition

Figure 3.41 Increase of stress under the center of a flexible loaded rectangular area

6) The final settlement, not using the table:

$$\Delta H = \Sigma\, \Delta Hi\, \frac{\Delta ei}{1+eo} = 2m \times \frac{0.1188}{1+1} + 2m \times \frac{0.0165}{1+1} + 4m \times \frac{0.003}{1+1}$$

$$+4 \times \frac{0.001}{1+1} = 0.14m = 14cm$$

note: upper 2m contributes ≈85% of the total settlement

Skempton - Bjerrum Modification

Use Das Figure 5.31, p. 276

$A \cong 0.4$ $Hc/B >>> 2$ Settlement ratio < 0.57

$Sc < 0.57 \times 14 = 8cm$ $Sc < 8cm$

- **Check solution when using Das equation 5.84 and the average stress increase:**

$$\Delta\sigma'_{av} = \frac{1}{6}(\Delta\sigma'_t + 4\Delta\sigma'_m + \Delta\sigma'_b)$$

Like before, assume a layer of 3B = 12m

$$\Delta\sigma'_t = q_o = \frac{1000\text{kN}}{16} = 62.5\ \text{kPa}$$

$\Delta\sigma'_m$ (@6m = 1.5B) $\cong 0.16q_o$

$\Delta\sigma'_b$ (@12m = 3B) $\cong 0.04q_o$

$\Delta\sigma'_{av} = 1/6\ (1 + 4 \times 0.16 + 0.04)q_o = 1/6 \times 1.68 \times 62.5 = 0.28 \times 62.5$
$= 17.5$ kPa

$\Delta\sigma'_{av} = 17.5$ kPa

$Z = 6m$, $Z/B = 1.5$, $\frac{\Delta q}{q_o} = 0.28$ $\Delta q = 17.5$ kPa

P_o' = 60kPa, P_c' = 120kPa P_f' =77.5kPa

$$\Delta e = C_r \log \frac{77.5}{60} = 0.05 \times 0.111 = 0.0056$$

$$\frac{\Delta e}{1+e_o} \times \Delta H = \frac{0.0056}{1+1} \times 12m = 0.033m = 3.33\ cm$$

Why is there so much difference?

As OCR does not change with depth, the influence of the additional stresses decrease very rapidly and hence the concept of the "average point" layer does not work well in this case. The additional stresses at the representative point remain below the maximum past pressure and hence large strains do not develop. The use of equation 5.84 is more effective with a layer of a final thickness.

(f) Terzaghi's 1-D Consolidation Equation

Terzaghi used the known diffusion theory (e.g. heat flow) and applied it to consolidation.

Assumptions:

6. The soil is homogenous and fully saturated.
7. The solid and the water are incompressible.
8. Darcy's Law governs the flow of water out of the pores.
9. Drainage and compression are one dimensional.
10. The strains are calculated using the small strain theory, i.e. load increments produces small strains.

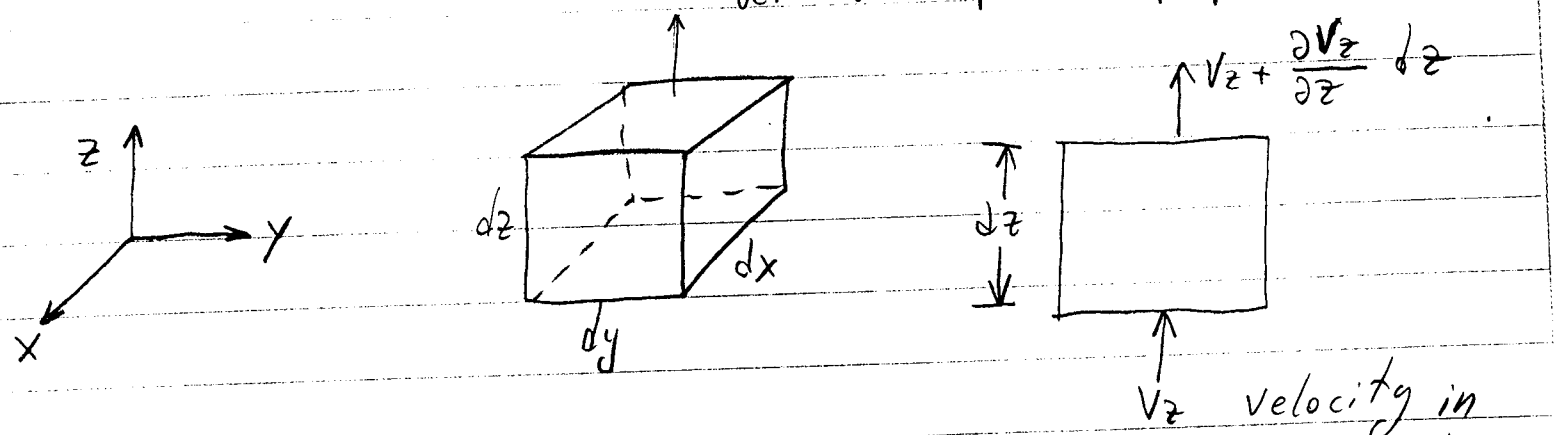

(I) continuity, the volume change is the difference between what comes in and goes out.

$$\Delta V_z = \left[V_z - \left(V_z + \frac{\partial V_z}{\partial z} dz\right)\right] dx\, dy$$

(II) Darcy

$$V_z = K_z \cdot i_z = K_z \frac{\partial h}{\partial z}$$

K = coeff. of permeability.

(I) $$\Delta V_z = -\frac{\partial V_z}{\partial z} dx\, dy\, dz$$

subst (II) into (I)

$$\Delta V_z = -\frac{\partial}{\partial z}\left(K_z \frac{\partial h}{\partial z}\right) dx\, dy\, dz$$

(a) $$\Delta V_z = -K_z \frac{\partial^2 h}{\partial z^2} dx\, dy\, dz$$

The volume of the water in the element:

$$V_w = \frac{S \cdot e}{1+e_0} \cdot V_T = \frac{S \cdot e}{1+e_0} dx\, dy\, dz$$

$$\Delta V_z = \frac{\partial V_w}{\partial t} = \frac{\partial}{\partial t}\left(\frac{S \cdot e}{1+e_0} dx\, dy\, dz\right)$$ (b) rate of change of water volume.

$$V_S = \frac{V_T}{1+e_0} = \frac{dx\, dy\, dz}{1+e_0}$$

Volume of solid in the element = constant.

$$\Delta V_z = -k_z \frac{\partial^2 h}{\partial z^2}\,dx\,dy\,dz = \frac{1}{1+e_0}\frac{\partial}{\partial t}(s\cdot e)\,dx\,dy\,dz$$

(a) (b)

$$-k_z \frac{\partial^2 h}{\partial z^2} = \frac{1}{1+e_0}\frac{\partial}{\partial t}(s\cdot e) \qquad (c)$$

r.h.s

$$\frac{\partial}{\partial t}(s\cdot e) = \left(e\frac{\partial s}{\partial t} + s\frac{\partial e}{\partial t}\right)$$

$\frac{\partial s}{\partial t} = 0$ full saturation all the time. $S=1$

$$\frac{\partial}{\partial t}(s\cdot e) = s\frac{\partial e}{\partial t} = \frac{\partial e}{\partial t}$$

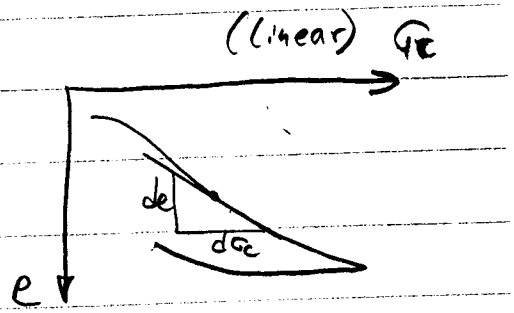

change of variables

$$\frac{\partial e}{\partial t} = \frac{\partial e}{\partial \sigma_v'}\frac{\partial \sigma_v'}{\partial t} = a_v \frac{\partial \sigma_v'}{\partial t}$$

a_v = Coeff. of compressibility from e vs. σ_z' (linear)

relations $a_v = -\frac{de}{d\sigma_c'} \neq \text{const.} \cong \frac{\Delta e}{\Delta \sigma_c'}$

$k_z = k_x = k_y = k$ assuming isotropic permeability

subst. in eq. (c)

$$-k\frac{\partial^2 h}{\partial z^2} = \frac{1}{1+e_0} a_v \frac{\partial \sigma_v'}{\partial t}$$

rearrange:

$$\frac{k(1+e_0)}{a_v}\frac{\partial^2 h}{\partial z^2} = -\frac{\partial \sigma_v'}{\partial t}$$

convinient change in h:

$$h = h_e + h_p = h_e + \frac{u}{\gamma_w} = h_e + \frac{1}{\gamma_w}(u_{ss} + u_e)$$

$$\frac{\partial^2 h}{\partial z^2} = \frac{\partial^2}{\partial z^2}\left[h_e + \frac{1}{\gamma_w}(u_{ss} + u_e)\right]$$

u_s = (mostly hydrostatic) = steady state

u_e = excess pore pressure

$$\frac{\partial^2 he}{\partial z^2} = 0$$

u_{ss} varies linearly so $\frac{\partial u_{ss}}{\partial z} = \text{const}$ & $\frac{\partial^2 u_{ss}}{\partial z^2} = 0$

Hence:

$$\frac{k(1+e_0)}{a_v} \frac{\partial^2 u_e}{\partial z^2} \frac{1}{\gamma_w} = \frac{\partial \sigma_v'}{\partial t}$$

$$\frac{k(1+e_0)}{\gamma_w a_v} = c_v = \text{coefficient of consolidation.} \quad [L^2/T] \quad (m^2/sec)$$

$$c_v \frac{\partial^2 u_e}{\partial z^2} = -\frac{\partial \sigma_v'}{\partial t}$$

$$\sigma_v' = \sigma_t - u = \sigma_t - (u_{ss} + u_e)$$

$$\frac{\partial \sigma_t}{\partial t} = 0 \qquad \frac{\partial u_{ss}}{\partial t} = 0$$

$$-\frac{\partial \sigma_v'}{\partial t} = \frac{\partial u_e}{\partial t}$$

$$\boxed{c_v \frac{\partial^2 u_e}{\partial z^2} = \frac{\partial u_e}{\partial t}} \qquad 1\text{-D consolidation}$$

c_v is a diffusion constant usually obtained directly from the consolidation test. It is actually not a constant but only due to our simplifications saying a_v, k and e_0 constants, it's becomes one.

(9) Time rate consolidation - chart solution.

$$C_v \frac{\partial^2 u_e}{\partial z^2} = \frac{\partial u_e}{\partial t} \qquad C_v = \frac{k(1+e_0)}{\gamma_w a_v}$$

Using simple, uniform inital excess pore pressure distribution we introduce nonedimensional variables

$$Z_1 = \frac{z}{H_{dr}} \qquad T = \frac{C_v \cdot t}{H_{dr}^2}$$

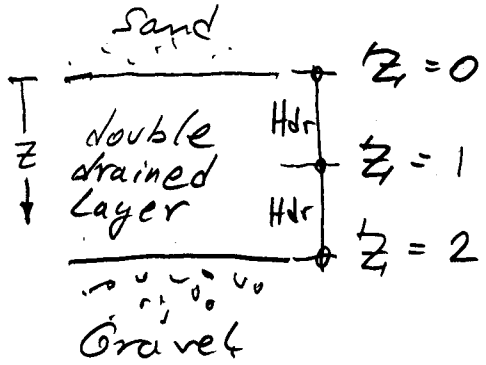

The consolidation equation then becomes:

$$\frac{\partial^2 u_e}{\partial Z_1^2} = \frac{\partial u_e}{\partial T}$$

The solution of that equation has to satisfy the following Boundry Conditions (B.C.)

at $t = 0$ $\quad T = 0$ $\quad u_e = u_i$ $\quad$ for $0 < Z < 2$

at all t $\quad u_e = 0$ $\quad$ for $Z_1 = 0$ & $Z_1 = 2$

The solution is (Taylor 1948)

$$u_c = \sum_{m=0}^{m=\infty} \frac{2u_i}{M} (\sin M Z_1) e^{-M^2 T}$$

$M = \frac{\pi}{2}(2m+1)$ $\quad$ m = dummy variable taking on values 1, 2, 3, ...

We can show the solution on a graph where we present the Consolidation Ratio $U_z = 1 - \frac{u_e}{u_i} = f(Z_1, T)$

3. Time Rate Consolidation (Das Sects. 1.15 & 1.16, pp. 38-47)

(a) Outline of Analysis

The consolidation equation is based on homogeneous completely saturated clay-water system where the compressibility of the water and soil grains is negligible and the flow is in one direction only, the direction of compression.

Utilizing Darci's Law and a mass conservation equation ➔ rate of outflow - rate of inflow = rate of volume change; leads to a second order differential equation

$$C_v \frac{\partial^2 u_e}{\partial z^2} = \frac{\partial u_e}{\partial t} - \frac{\partial \sigma_v}{\partial t}$$

u_e = excess pore pressure
σ_v = vertical effective stress

Practically, we use either numerical solution or the following two relationships related to two types of problems:

Problem 1: Time and Average Consolidation

Equation 1) $$\boxed{t_i = \frac{T_v H_{dr}^2}{C_v}}$$

t_i - The time for which we want to find the average consolidation settlement.
See Fig. 1.21 (p.42) in Das, and the tables on p.42-43 in the notes.

T_v = time factor $\rightarrow$ T = *f* (U_{avg})

(L) H_{dr} = the layer thickness of drainage path.

$\left(\frac{L}{t}\right)$ C_v = coeff. of consolidation = $\frac{k}{\gamma_w m_v}$

m_v = coeff. of volume comp. = $\frac{a_v}{1+e_o}$

a_v = coeff. of compression = $\frac{\Delta e}{\Delta p}$

Equation 2) Average Consolidation

$$U_{avg} = S_t/S_\infty = \frac{\text{Settlement of the layer at time t}}{\text{Final settlement due to primary consolidation}}$$

For initial constant pore pressure with depth

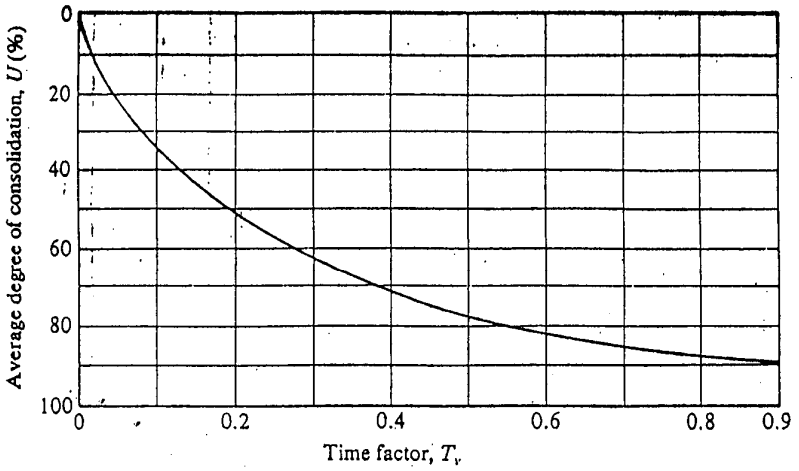

Figure 7.25 Variation of average degree of consolidation with time factor, T_v (u_o constant with depth)

Table 7.3 Variation of Time Factor with Degree of Consolidation* (p.42)

Degree of consolidation U%	Time factor, T_v
0	0
10	0.008
20	0.031
30	0.071
40	0.126
50	0.197
60	0.287
70	0.403
80	0.567
90	0.848
100	∞

*u_o is constant with depth

Problem 2: Time related to a consolidation at a specific point

Equation 3) Degree of consolidation at a point $\quad U_{z,t} = 1 - \frac{u_{z,t}}{u_{z,o}}$

Pore pressure at a point (distance z, time t) $\quad U_{z,t} = \gamma_w \text{ x } hw_{z,t}$

For initial linear distribution of Δui the following distribution of pore pressures with depths and time is provided.

Das Fig. 1.20 (c) Plot of $\Delta u/\Delta u_o$ with T_v and H/H_c (p.39)

$$\frac{H}{H_{dr}}$$

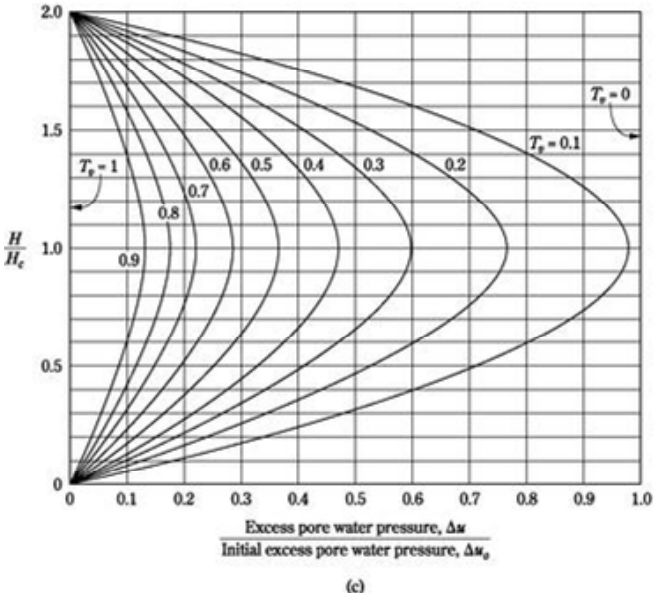

(c)

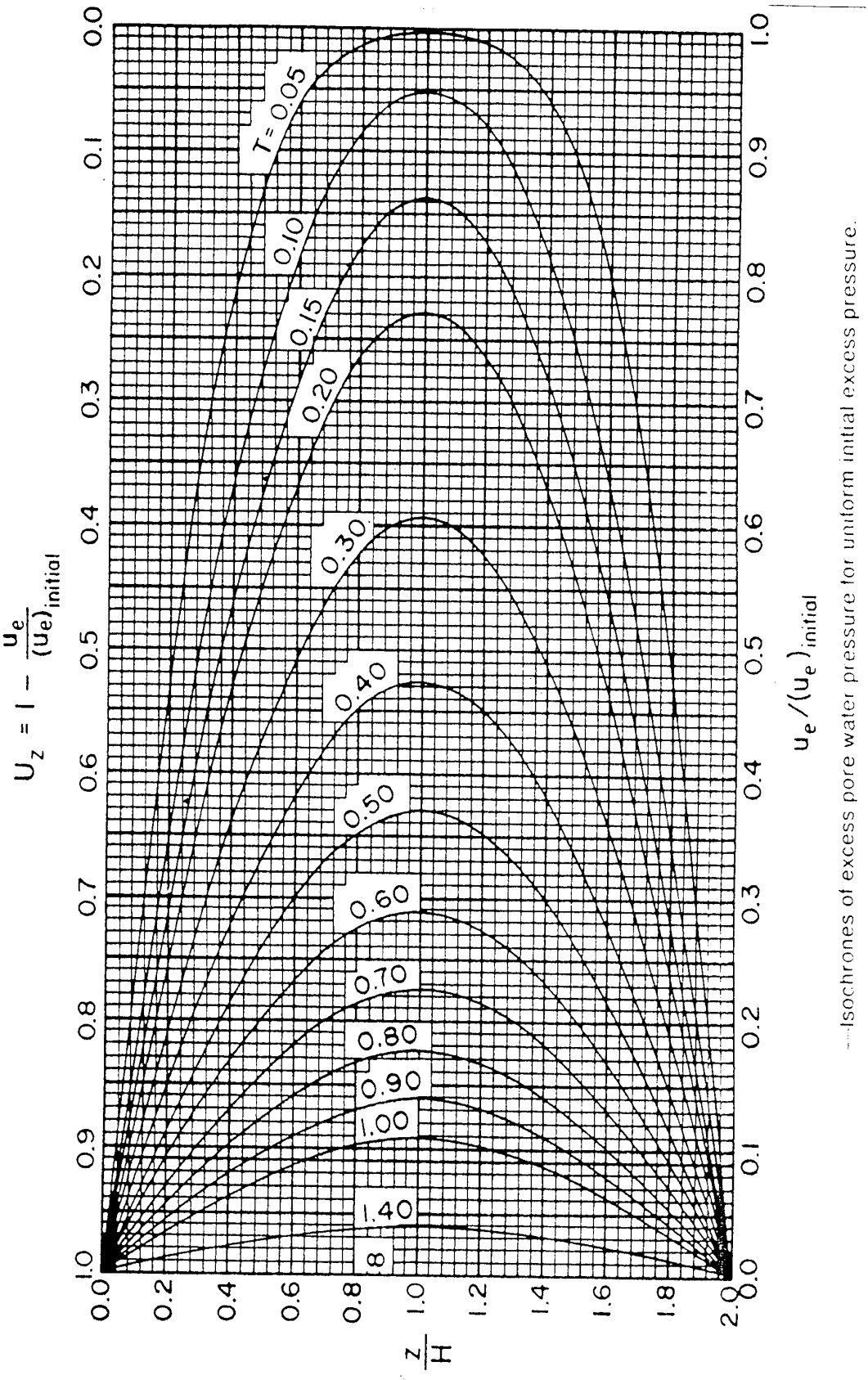

Isochrones of excess pore water pressure for uniform initial excess pressure.

Table 1

One-Dimensional Consolidation Theory: Solutions for Four Cases of Initial Excess Pore Water Pressure Distribution in Double-Drained Stratum.

Average Degree of Consolidation for Various Values of T					Distributions of Initial Excess Pore Water Pressure
	Average Degree of Consolidation, U (%)				
T	Case 1	Case 2	Case 3	Case 4	
0.004	7.14	6.49	0.98	0.80	2H Constant
0.008	10.09	8.62	1.95	1.60	
0.012	12.36	10.49	2.92	2.40	
0.020	15.96	13.67	4.81	4.00	
0.028	18.88	16.38	6.67	5.60	
0.036	21.40	18.76	8.50	7.20	Linear Variation
0.048	24.72	21.96	11.17	9.60	
0.060	27.64	24.81	13.76	11.99	
0.072	30.28	27.43	16.28	14.36	
0.083	32.51	29.67	18.52	16.51	CASE 1
0.100	35.68	32.88	21.87	19.77	Half Sine Curve
0.125	39.89	36.54	26.54	24.42	
0.150	43.70	41.12	30.93	28.86	
0.175	47.18	44.73	35.07	33.06	
0.200	50.41	48.09	38.95	37.04	CASE 2
0.250	56.22	54.17	46.03	44.32	Sine Curve
0.300	61.32	59.50	52.30	50.78	
0.350	65.82	64.21	57.83	56.49	
0.400	69.79	68.36	62.73	61.54	
0.500	76.40	76.28	70.88	69.95	CASE 3
0.600	81.56	80.69	77.25	76.52	Triangular
0.700	85.59	84.91	82.22	81.65	
0.800	88.74	88.21	86.11	85.66	
0.900	91.20	90.79	89.15	88.80	
1.000	93.13	92.80	91.52	91.25	CASE 4
1.500	98.00	97.90	97.53	97.45	
2.000	99.42	99.39	99.28	99.26	

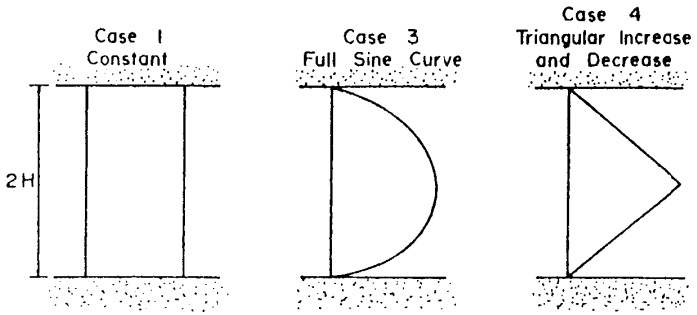

a) - Double - Drained Stratum

One-Dimensional Consolidation Theory: Time Factor for Various Average Degrees of Consolidation Double-Drained Stratum

	Time Factor T			
U (%)	Case 1	Case 2	Case 3	Case 4
0	0	0	0	0
5	0.0020	0.0030	0.0208	0.0250
10	.0078	.0111	.0427	.0500
15	.0177	.0238	.0659	.0753
20	.0314	.0405	.0904	.101
25	.0491	.0608	.117	.128
30	.0707	.0847	.145	.157
35	.0962	.112	.175	.187
40	.126	.143	.207	.220
45	.159	.177	.242	.255
50	.197	.215	.281	.294
55	.239	.257	.324	.336
60	.286	.305	.371	.384
65	.342	.359	.425	.438
70	.403	.422	.488	.501
75	.477	.495	.562	.575
80	.567	.586	.652	.665
85	.684	.702	.769	.782
90	0.848	0.867	0.933	0.946
95	1.129	1.148	1.214	1.227
100	∞	∞	∞	∞

see Table 1 for initial excess pore pressure distribution

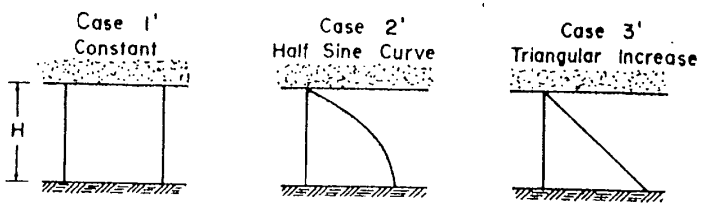

b) - Single - Drained Stratum

Fig. 7.8—Initial excess pore water pressure distribution for double-drained and single-drained strata for which Table 1 is applicable.

(b) Obtaining Parameters from the Analysis of e-log t Consolidation Test Results

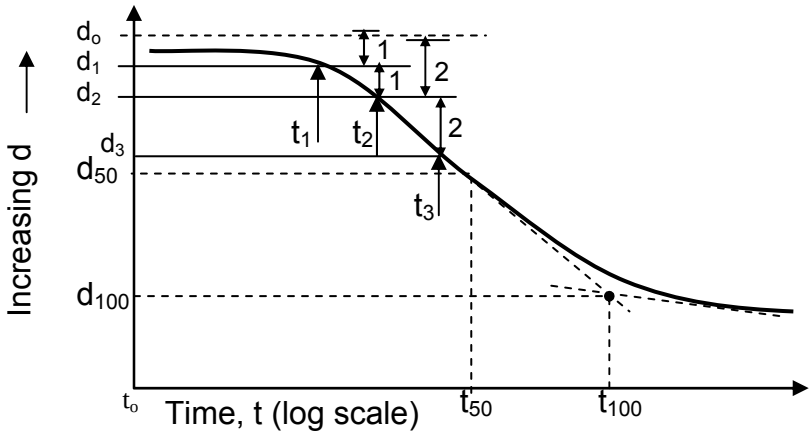

1. find d_o - 0 consolidation time t = 0
   set time t_1, $t_2 = 4t_1$, $t_3 = 4t_2$
   find corresponding d_1, d_2, d_3
   offset $d_1 - d_2$ above d_1 and $d_2 - d_3$ above d_2

2. find d_{100} - 100% consolidation
   referring to primary consolidation (not secondary).

3. find d_{50} and the associated t_{50}

Coefficient of Consolidation

$$C_v = \frac{T_i H_{dr}^2}{t_i}$$

T_i = time factor (equation 1.75, p.41 of Das)

H_{dr} = drainage path = ½ sample
t_i = time for i% consolidation

Using 50% consolidation and case I

$$C_v = \frac{0.197 H_{dr}^2}{t_{50}}$$

T for Uavg = 50%

And linear initial distribution

(A) Finite Differences solution

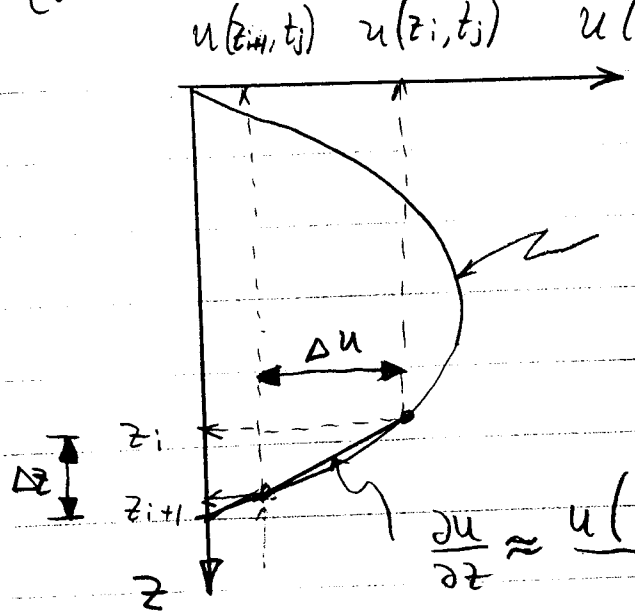

distribution of excess pore water pressure with depth for a certain time t_j $(u - u_e)$

$$\frac{\partial u}{\partial z} \approx \frac{u(z_{i+1}, t_j) - u(z_i, t_j)}{\Delta z}$$

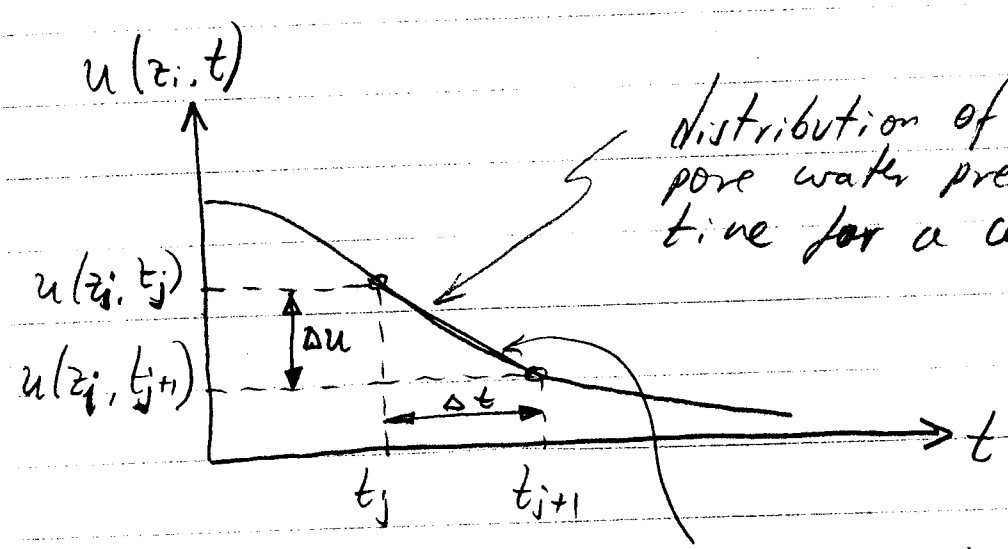

distribution of excess pore water pressure with time for a certain depth z_j

$$\frac{\partial u}{\partial t} = \frac{u(z_i, t_{j+1}) - u(z_i, t_j)}{\Delta t}$$

$$\frac{\partial^2 u}{\partial z^2} = \frac{u(z_{i+1}, t_j) - 2u(z_i, t_j) + u(z_{i-1}, t_j)}{(\Delta z)^2}$$

$u(z,t) = u_{i,j}$

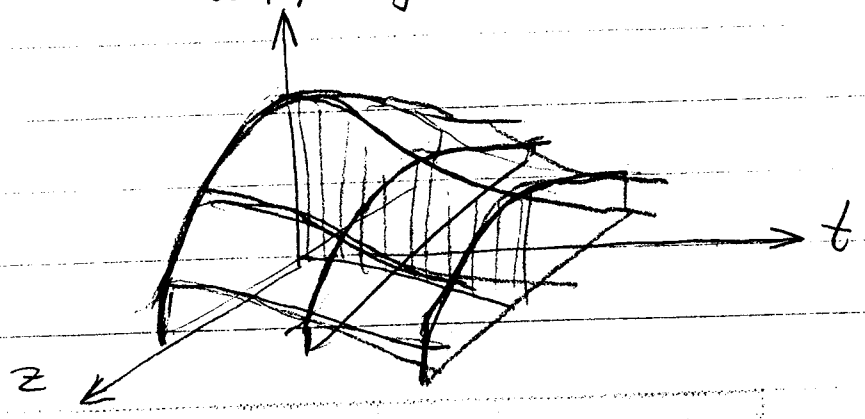

For simplicity we can write $u(z_{iH}, t_j) = u_{i+1,j}$

$$C_v \frac{\partial^2 u}{\partial z^2} = \frac{\partial u}{\partial t}$$

Substitute

$$C_v \frac{\left(u_{i+1,j} - 2u_{i,j} + u_{i-1,j}\right)}{\Delta z^2} = \frac{\left(u_{i,j+1} - u_{i,j}\right)}{\Delta t}$$

which can easily by solved by a computer. For simplicity we can rewrite the above equation as:

$u_{i+1,j} = \alpha u_{i+1,j} + (1-2\alpha)u_{i,j} + \alpha u_{i-1,j}$

for which:

$$\alpha = \frac{C_v \bullet \Delta t}{(\Delta z)^2} \leq 0.5$$

for $\alpha = 0.5$ we get:

$$\boxed{u_{i,j+1} = \frac{1}{2}\left(u_{i-1,j} + u_{i+1,j}\right)}$$

this form allows for hand calculations
e.g. for i = 2, j = 3 $u_{2,4} = ½(u_{1,3} + u_{3,3})$

Example

Find $u(z,t)$ using the simplified finite differences solution for double drainage and rectangular initial pore pressure distribution

$n = 10$ no. of sublayers

$C_v = 10^{-5}$ m²/min.

$\Delta\sigma' = 5.0$ t/m²

$H = 25$ m

$$\Delta t = \frac{\alpha(\Delta z)^2}{C_v} = \frac{0.5 \times 2.5^2}{10^{-5}} = 3.125 \cdot 10^5 \text{ minutes} = 217 \text{ days}$$

i	0	1	2	3	4	5	6	7	8	9	10
z_i meter מטר	0	2.5	5.0	7.5	10.0	12.5	15.0	17.5	20.0	22.5	25.0
time זמן j	t_j זמן days	$u(z,t)$ pore pressure תלחץ הנקבובי									
	0^-	5.00	5.00	5.00	5.00	5.00	5.00	5.00	5.00	5.00	5.00
0	0	2.50	5.00	5.00	5.00	5.00	5.00	5.00	5.00	5.00	2.50
1	217	0	3.75	5.00	5.00	5.00	5.00	5.00	5.00	3.75	0
2	434	0	2.50	4.37	5.00	5.00	5.00	5.00	4.37	2.50	0
3	651	0	2.18	3.75	4.69	5.00	5.00	4.69	3.75	2.90	0
4	868	0	1.87	3.44	4.37	4.84	5.00	4.84	4.37	3.44	1.88	0
5	1085	0	1.72	3.12	4.14	4.69	4.84					0
6	1302	0	1.56	2.93	3.91	4.49	4.69					0
7	1519	0	1.46	2.73	3.71	4.30	4.49					0
8	1736	0	1.38	2.59	3.51	4.10	4.30					0
9	1953	0	1.29	2.44	3.34	3.90	4.10					0
10	2170	0	1.20	2.32	3.17	3.72	3.90					0

4. Consolidation Example

The construction of a new runway in Logan Airport requires the pre-loading of the runway with approximately 0.3 tsf. The simplified geometry of the problem is as outlined below, with the runway length being 1 mile.

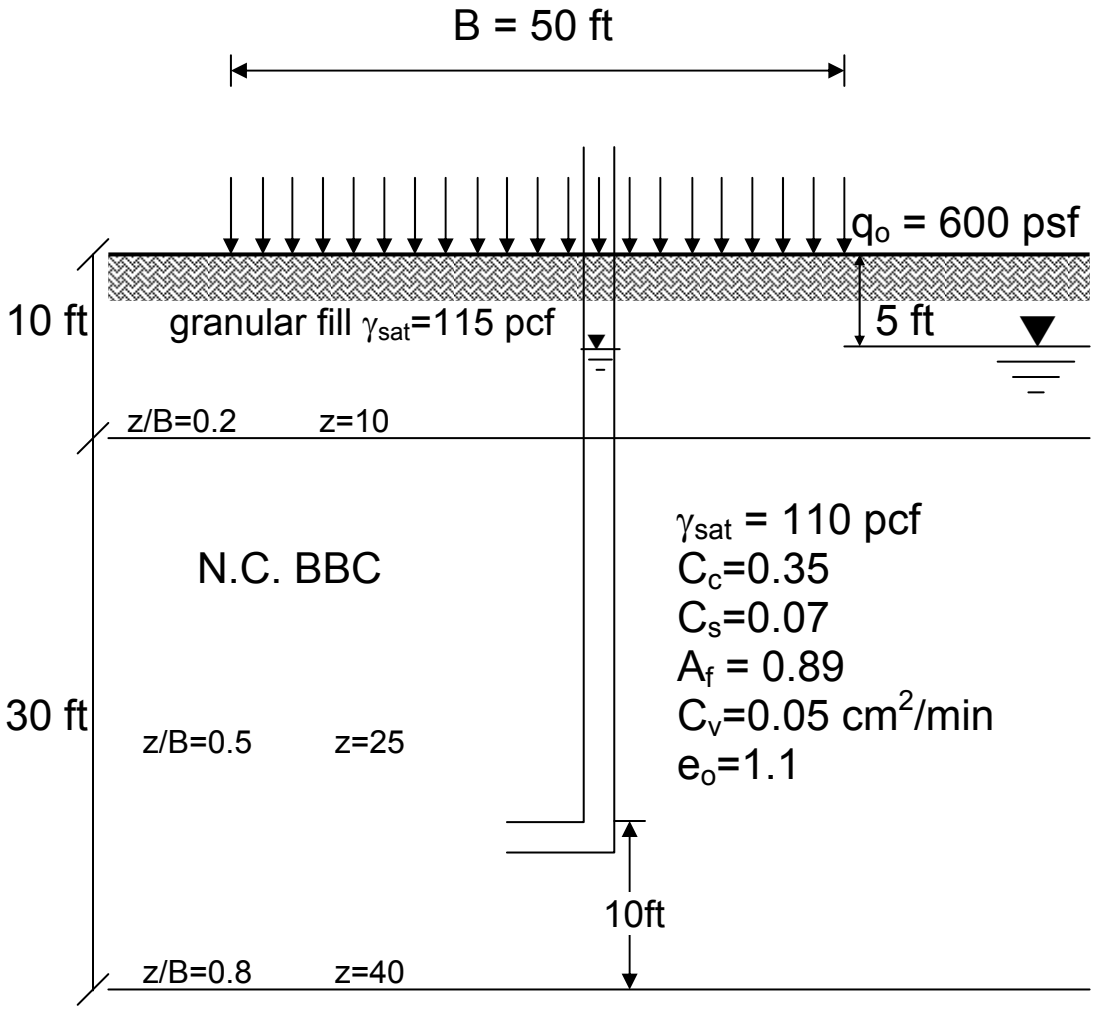

1) Calculate the final settlement.

Assuming a strip footing and checking the stress distribution under the center of the footing using Fig. 3.41 (p. 12 of the notes)

Location	z (ft)	z/B	$\Delta q / q_o$	Δq (psf)
Top of Clay	10	0.2	~0.98	588
Middle of Clay	25	0.5	~0.82	492
Bottom of Clay	40	0.8	~0.60	360

Using the average method

$\Delta\sigma'_{av} = \frac{1}{6}(\Delta\sigma'_t + 4\Delta\sigma'_m + \Delta\sigma'_b)$ = 1/6 (588 + 4x492 + 360) = <u>486 psf</u>

The average number agrees well with the additional stress found for the center of the layer, (492psf).

Assuming that the center of the layer represents the entire layer for a uniform stress distribution. At 25 ft:

$p_o' = \sigma_v'$ = 115 x 5 + (115 – 62.4) x 5 + (110 – 62.4) x 15

= 575 + 263 + 714 = 1552psf

$p_f' = p_o' + \Delta q$ = 1552 + 486 = 2038 psf

$\Delta e = C_c \log (p_f'/p_o')$ = 0.35 log (2038/1552) = 0.0414

$$s = \Delta H = H\left(\frac{\Delta e}{1+e_o}\right) = 30\ ft \times 12\ inch \times \left(\frac{0.0414}{1+1.1}\right) = 7.1\ inch$$

2) Assuming that the excess pore water pressure is uniform with depth and equal to the pressure at the representative point, find:

(a) The consolidation settlement after 1 year

- Find the time factor:

$$t_i = \frac{T_v \mathrm{H_{dr}}^2}{C_v} \qquad T_v = \frac{t_i C_v}{\mathrm{H_{dr}}^2}$$

C_v = 0.05 cm^2/min = 0.00775 in^2/min

H_{dr} = H/2 = 30 ft / 2 = 15 ft

T_v = 12 x 30 x 24 x 60 x 0.00775 / $(15 \times 12)^2$ = 0.124

- Find the average consolidation for the time factor.

For a uniform distribution you can use Das equation 1.74 (p.41) or the chart or tables provided in the notes.

Using the table in the class notes (p.53 & p.55)

T = 0.125 → Case I - uniform or linear initial excess pore pressure distribution.→ U = 39.89 % = 40%

$$U_{avg} = \frac{S_t}{S\infty} \qquad S_t = U_{avg} \times S_\infty$$

S_t = 0.40 x 7.1 = <u>2.84 inch</u>

(b) What is the pore pressure 10 ft. above the till 1 year after the loading?

From above; t = 12 months, T = 0.124

2 Hd_r = 30 ft

z / H_{dr} = 20/15 = 1.33 (z is measured from the top of the clay layer)

Using the isochrones with T = 0.124 and z/H = 1.33

We get u_e / $u_i \approx 0.8$

u_e = 0.8 x 486 = 389 psf

(c) What will be the height of a water column in a piezometer located 10 ft above the till: (i) immediately after loading and (ii) one year after the loading

(i) u_i = 486 psf $h_i = u/\gamma_w = 486/62.4 = 7.79$ft.

(ii) u_e = 389 psf $h = u/\gamma_w = 389 / 62.4 = 6.20$ ft

The water level will be 2.79 ft. above ground and 1.2 ft above the ground level immediately after loading and one year after the loading, respectively.

Journal of Geotechnical Engineering, ASCE, Vol.119, No.9
Sept. 1993

THE TWENTY-SEVENTH TERZAGHI LECTURE

Presented at the American Society of Civil Engineers

1991 Annual Convention

October 22, 1991

J. MICHAEL DUNCAN

Introduction to the Twenty-Seventh Terzaghi Lecture

By Clyde N. Baker Jr.

Dr. James Michael Duncan will feel right at home presenting the 27th Terzaghi lecture here today. He attended high school in Eustis, Florida, which is approximately 40 mi north of Orlando. One of the highlights of Mike's high school career was playing football, and he was team captain in his senior year. Unfortunately, that team had the worst record in the history of the school, and lost one game by a score of 67 to 6. Mike did a little better after high school. He attended Georgia Tech as a co-op student, graduating in 1959 with his B.S.C.E. His subsequent specialization in soil mechanics occurred accidentally. He resigned from his job as an engineer in Tampa when he was asked by a superior to falsify some time sheets. The next day, he received a phone call from a friend who said there was a research assistantship available in soil mechanics at Georgia Tech if he wanted to go back for his master's degree. Mike responded that he didn't really like soil mechanics, but since he had a wife and daughter to support, and it was better than starving to death, he'd take it. The rest is history.

Mike got his M.S.C.E. at Georgia Tech in 1962, and worked briefly in the Soils Division of the Waterways Experiment Station in Vicksburg on his way to the University of California at Berkeley, where he obtained his Ph.D. degree under Harry Seed in 1965. He taught at Berkeley until 1984 before moving to Virginia Polytechnic Institute and State University in Blacksburg, Virginia, where he now holds the title of University Distinguished Professor in the Department of Civil Engineering.

Throughout his 30 year career, Mike has been an outstanding researcher, teacher, and worldwide lecturer. He has received eight awards for teaching excellence, seven awards for professional achievement, and six awards for research and publications, including the Wellington Prize, the Walter H. Huber Research Prize, the Collingwood Prize, and the Thomas A. Middlebrooks award twice from ASCE. Tomorrow, he will be receiving the ASCE State-of-the-Art Civil Engineering Award for 1991.

Two themes appear consistently in his more than 180 publications and research reports: practical applications of numerical analyses, and investigation of soil properties and behavior. These two themes will be evident in Mike's Terzaghi lecture on the "Limitations of Conventional Analysis of Consolidation Settlement." The basis for the talk comes from his analysis of extensive settlement records at Bay Farm Island in San Francisco Bay, and at the Kansai International Airport project in Japan.

Mike's wife, Ann, their children Mary, Susan, and John, and his sister Sally are here with us today to enjoy the 27th Terzaghi lecture. It is with honor and great pleasure, that I present to you Dr. James Michael Duncan.

LIMITATIONS OF CONVENTIONAL ANALYSIS OF CONSOLIDATION SETTLEMENT

By J. Michael Duncan,[1] Fellow, ASCE

(The Twenty-Seventh Karl Terzaghi Lecture)

ABSTRACT: Consolidation settlements are often large and potentially damaging to structures. Estimating their magnitudes, and the rates at which they will occur, plays an important part in many civil engineering projects. At Bay Farm Island in San Francisco Bay, and Kansai International Airport in Japan, settlement magnitudes and settlement rates were of great importance for design. In these and similar cases it is important to understand what factors control the accuracy with which settlement magnitudes and settlement rates can be estimated. Accurate predictions of settlement magnitudes require accurate evaluations of clay compressibility and preconsolidation pressure. Accurate predictions of settlement rates require improved methods of anticipating whether embedded sand strata will or will not provide internal drainage; use of computer analyses to take into account important factors such as variations in c_v within clay layers, nonlinear stress-strain behavior, and nonuniform strain profile effects; and research to develop an improved model of clay compressibility that includes the effects of strain rate.

INTRODUCTION

The writer appreciates very much the invitation to present this lecture named in honor of Karl Terzaghi. Consolidation of clay was one of the principal topics of Terzaghi's pioneering book, *Erdbaumechanik*, published in 1925. It was the subject of some of the first laboratory tests Terzaghi performed at Robert's College in the early 1920s, and consolidation settlements were the focus of his first consulting job. Consolidation settlements of clay thus seem an appropriate subject for a lecture presented in his honor.

Other Terzaghi Lecturers have addressed aspects of this subject, notably Rutledge (1970), and Lowe (1974). As illustrated by the cases described here, consolidation settlements are still very important in many civil engineering projects, and there is still important progress to be made to improve our ability to anticipate accurately the magnitudes and rates of consolidation settlements.

PROBLEMS CAUSED BY SETTLEMENTS

Consolidation settlements can result in many different types of problems, as indicated in Table 1 (Skempton and MacDonald 1956; Bjerrum 1963; Wahls 1990).

Where settlements are large, the ground surface may subside below water, and be flooded. Flooding can be prevented if the initial ground surface is made high enough so that it remains safely above water after all settlement has taken place. To remediate flooding, it is necessary to construct dikes, and to use ditches to lower the water level below ground level.

[1]University Distinguished Prof., Dept. of Civ. Engrg., Virginia Tech., Blacksburg, VA 24061.

Note. Discussion open until February 1, 1994. To extend the closing date one month, a written request must be filed with the ASCE Manager of Journals. The manuscript for this paper was submitted for review and possible publication on March 8, 1993. This paper is part of the ***Journal of Geotechnical Engineering***, Vol. 119, No. 9, September, 1993. ©ASCE, ISSN 0733-9410/93/0009-1333/$1.00 + $.15 per page. Paper No. 5763.

TABLE 1. Settlement Problems

Problems (1)	Preventive measures (2)	Remedial measures (3)
Flooding	Raise ground elevation with extra fill	Keep ground-water levels below ground surface with dikes, ditches, and pumping
Loss of slope to drain	Allow all or part of settlement to occur before construction of drains Design original slopes with allowance for changes	Regrade surface drains Rebuild, replace, or supplement subsurface drains
Tilting of structures (tilt of 0.004 can be distinguished by unaided eye)	Allow all or part of settlement to occur before construction of structures Design foundations so they are concentrically loaded Use floating or deep foundations to reduce settlements	Relevel structures using jacks and shims, or mudjacking Possibly underpin foundations to minimize subsequent settlement
Architectural damage (cracks in walls or floors, jammed windows or doors, uneven floors)	Allow all or part of settlement to occur before construction of structures Use floating or deep foundations to reduce magnitudes of total and differential settlements Use stiff foundations so that differential settlement does not result in distortion of structure	Repair damage to restore value Possibly relevel structure Possibly underpin foundations to minimize subsequent settlement
Structural damage (cracks in column, floorbeams, or other structural elements)	Allow all or part of settlement to occur before construction of structures Use floating or deep foundations to reduce magnitudes of total and differential settlements	Repair damage to restore structural integrity Possibly underpin foundations to minimize subsequent settlement

Settlements are never uniform. Differential settlements can lead to many types of problems. One of these is the disruption of surface or subsurface drainage where differential settlements result in loss of slope to drain. This can be prevented, if the magnitude of differential settlement can be anticipated, by designing the initial slopes with allowances for the changes that will occur as settlement takes place. Impaired drainage can be restored by regrading existing drains or building new ones.

Uneven settlements cause a variety of problems for structures. When the structure or its foundation is stiff enough to prevent distortion of the structure, nonuniform settlements cause tilt. Tilt as small as 0.004 can be detected by the unaided eye, and gives the impression of instability, especially in tall structures. Designing foundations so they are centrally loaded eliminates one cause of tilting. Using floating or deep foundations can reduce the magnitude of settlement and tilt. Floating foundations reduce settlement by

reducing net load; excavation of 3 m (10 ft) of soil offsets the load of a building several stories high. Deep foundations (driven piles, drilled shafts, and caissons) reduce settlements by carrying loads to deeper, less compressible strata.

If structures and their foundations are distorted by differential settlements, they may be cracked and damaged. Architectural damage includes all those forms of distress that impair the looks or function of the structure, but do not reduce its structural load-carrying capacity. Architectural damage seldom occurs if the angular distortion resulting from the settlement is less than 1/500. Structural damage implies loss of structural capacity. Settlement damage rarely results in structural collapse, but a structure damaged by settlement is more likely to collapse under loads imposed by earthquake, wind, or live load.

Once a structure has been damaged by differential settlements, remediation can take two forms. One is repair of the architectural or structural damage to restore the structure to a useful state. Releveling the structure may be required to remove tilt or distortion. If settlement is continuing, it may be necessary to modify the foundations (underpin the structure) to reduce or eliminate future settlements.

It is not uncommon for settlements as large as several feet to occur as a result of consolidation of soft clays. It is therefore easy to understand the importance of being able to estimate the magnitudes and rates of consolidation settlements in advance, so that appropriate design features can be adopted to reduce settlements or to avoid settlement-induced damage. It is often desired to develop facilities, and to begin using them, while they are still settling, because time is money. To do this it is useful to be able to estimate accurately how much settlement will occur, and how fast it will occur.

The following sections of this paper discuss: (1) The effects of consolidation settlements on the design and construction of two modern projects constructed on fills over clays; (2) the difficulties involved in estimating the magnitudes and the rates of consolidation settlements; and (3) improvements that are needed in the current state of the art for estimating settlements and settlement rates.

The Bay Farm Island and Kansai Airport case histories that are described here have been treated in more detail by others (Duncan et al. 1991; Arai 1991; Arai et al. 1991; Endo et al. 1991; Maeda, et al. 1990; Oikawa and Endo 1990; Takeuchi 1990; Tohma and Yamamoto, 1990). The following sections use these cases to illustrate the importance of estimating settlement rates accurately, and the difficulties in doing so.

BAY FARM ISLAND

Bay Farm Island is located south of Alemeda, on the east side of San Francisco Bay. The area where large settlements occurred [about 260 ha (one square mile)] was originally a tidal flat underlain by 6–15 m (20–50 ft) of San Francisco Bay mud. The area was farmed beginning in about 1880, and was diked off and drained for more efficient farming in 1930. In 1945 the dikes failed. Episodes of draining and reflooding led to development of a rather complex crust on the top of the Bay mud. It was thick in some places, thin in others, and nonexistent where water-filled sloughs or ditches crossed the area. Detailed information regarding the conditions at the site and the consolidation properties of the San Francisco Bay mud can be found in Duncan et al. (1991).

Development of the site for commercial and residential use began in 1967 with placement of 2.5–6 m (8–20 ft) of hydraulic sand fill over the Bay mud. A cross section through the area is shown in Fig. 1. Thicker fill was placed where the underlying Bay mud was thicker. The fill was left in place for 12 years, so that most of the settlement due to consolidation of the Bay mud would occur before construction of streets and buildings. In 1979 final grading was done, and development of the infrastructure in the area began. Photographs of the area before and after development are shown in Fig. 2. Bay Farm Island today is an attractive area densely populated with residential and light commercial uses.

A total of 45 settlement plates were used to monitor the settlement at Bay Farm Island from 1967 to 1979 (Javete 1983). The settlements measured at the 10 locations where the Bay mud was thickest are shown in Fig. 3. Two things can be seen clearly in this figure: First, the settlements are large. As much as 2 m (7 ft) of settlement occurred by 1979. Second, the settlement is not uniform. In 1979 the measured settlements varied from a little more than 1 m (4 ft) to a little more than 2 m (7 ft).

The differences in the magnitudes of the settlements from point to point are not due to different thicknesses of Bay mud. For the 10 locations where the settlements shown in Fig. 3 were measured, the thickness of the Bay mud varied only from 14 m (45 ft) to 15 m (50 ft). The smallest settlements shown in Fig. 3 were measured at a location where the Bay mud was 14 m (46 ft) thick, the largest where it was 14.6 m (48 ft) thick.

The magnitudes of the settlements bear some relationship to effective fill depth. Javete (1983) defined effective fill depth as the thickness of fill weighing 17.3 kN/m^3 (110 lb/cu ft) that would produce the same load on the underlying Bay mud, considering moist unit weight above the observed average water level and buoyant unit weight below. Although there is some relationship between settlement and effective fill depth, it is not consistent. The point with an effective fill depth of 5.1 m (16.6 ft) settled less than the point with an effective fill depth of 3.3 m (10.9 ft). The point with an effective fill depth of 6.8 m (22.4 ft) settled less than a point with an effective fill depth of 6.2 m (20.3 ft). The scatter in the measured values is significant.

Studies done since 1980 (Javete 1983; Duncan et al. 1991) indicate that much of the erratic variation in settlement from place to place at Bay Farm

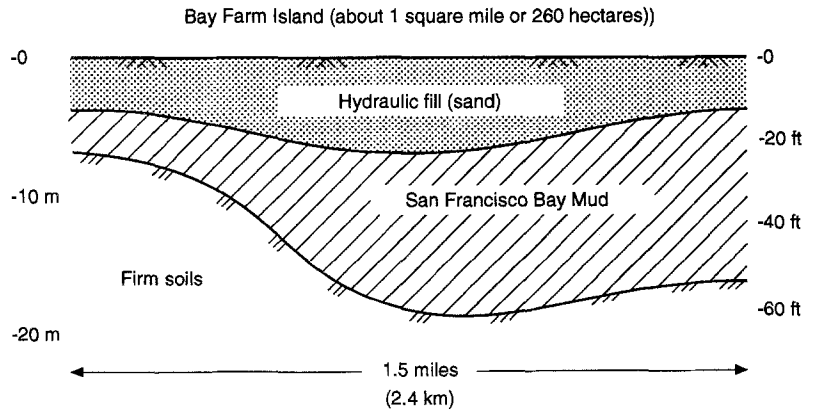

FIG. 1. Cross Section through Bay Farm Island

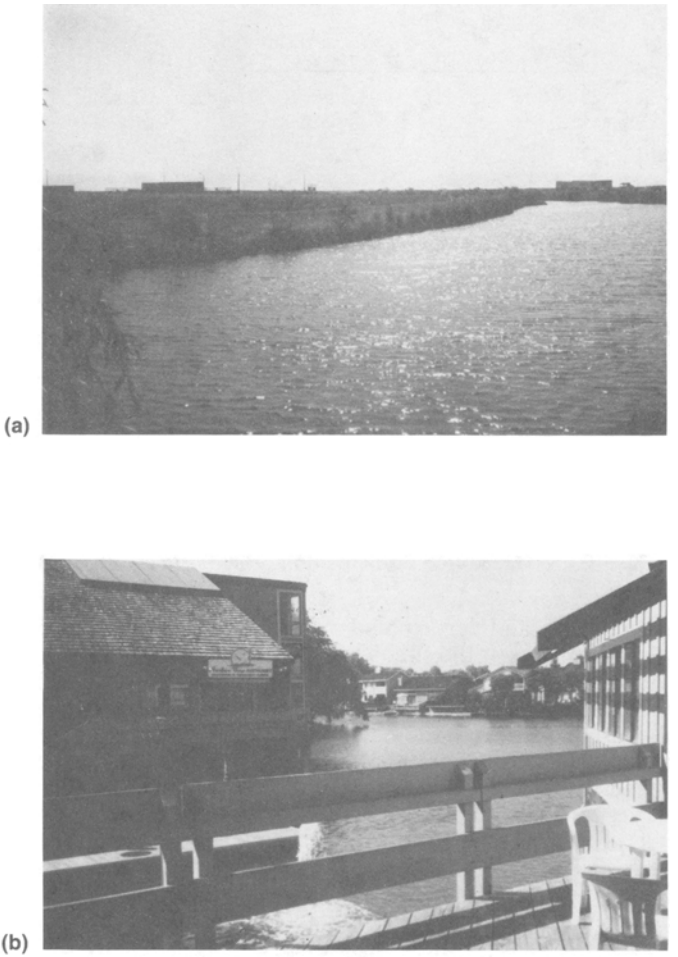

FIG. 2. Bay Farm Island: (*a*) after Filling, before Development of Infrastructure; and (*b*) after Development

Island was due to random variations in crust thickness from one location to another, as discussed later in this paper.

In 1979 the settlements were still continuing, at rates varying from 50 mm (2 in.) to 75 mm (3 in.) per year. Just before final grading and construction of streets and buildings was to begin in 1979, the developer asked a geotechnical engineering firm to make an estimate of the maximum amount of differential settlement that might be experienced by a building supported on shallow foundations at the site. This information was needed to obtain a permit for development of the site. For purposes of the estimate, a building was considered to cover an area of 23 m square (75 ft square).

The geotechnical firm (firm A) had done work at the site for many years. They had made borings, performed laboratory tests, estimated settlements

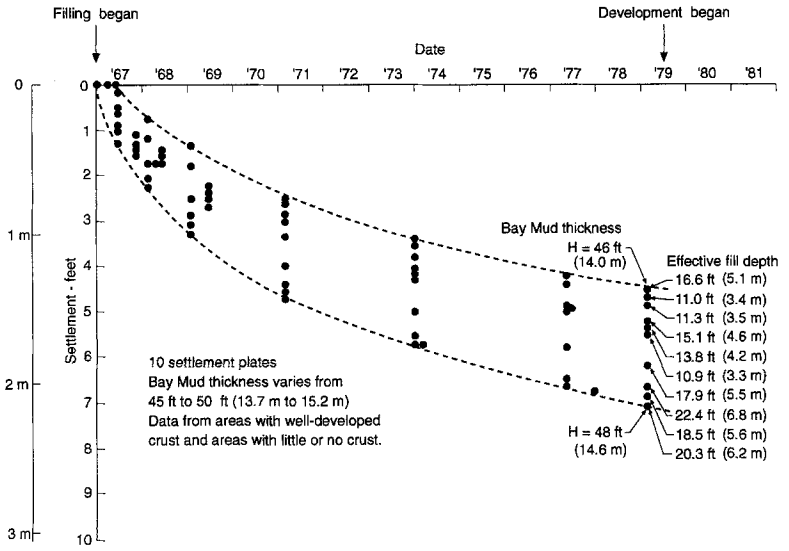

FIG. 3. Measured Settlements at Bay Farm Island

and settlement rates, and participated in evaluating the data obtained from the 45 settlement plates at the site. They thus had considerable information and experience on which to base their estimate of the maximum possible differential settlement in a building. They were also well aware of the possible legal consequences of underestimating the differential settlements. If differential settlements occurred that were larger than they estimated, they might be deemed liable for a share of the resulting damages.

Considering carefully all of the available information, and not wishing to incur exposure to undue liability, firm A estimated that differential settlements as large as 300 mm (1.0 ft) might be possible within a structure 23 m square (75 ft square) supported on shallow foundations at the site.

The developer was not pleased with this answer. Designing structures and foundations for such conditions would be exceptionally difficult and expensive. Obtaining the required development permit was probably out of the question if the developer had to base the development plan on such large values of estimated differential settlement.

Understandably, the developer (who already had made a very large investment in the site) wanted a second opinion. For this he turned to another geotechnical firm (firm B) that had also done considerable work at the site. Firm B considered the same information as firm A, but was more influenced by how their prospects of receiving further work from the developer might be influenced by their estimate.

Considering carefully all of the available information, and not wishing to jeopardize their chances for further work with the developer, firm B estimated that differential settlements larger than 30 mm (0.1 ft) were not likely to occur within a structure 23 m square (75 ft square) supported on shallow foundations at the site.

This answer was received more warmly by the developer. If differential settlements did not exceed 30 mm (0.1 ft) within any building, there should be little or no damage due to settlement. However, it was not possible

simply to accept the more favorable answer and to ignore the less favorable. Both had to be accommodated in the permit application.

At this stage the developer asked the writer if he could work with the two firms, to get them to agree on a common estimate. The writer, being optimistic and perhaps a little naive, replied that that certainly would be possible. He explained to the developer, as he had explained to students many times, that once the conditions to be analyzed had been decided, the answer was determined. Therefore all that would be necessary would be to get the two firms to agree on what conditions should be considered, and they would then arrive at the same answer.

It proved to be not so easy to get firm A and firm B to agree on the conditions for analysis. After a number of meetings, agreement was reached on many (but not all) of the points concerning what parameter values represented the conditions likely to result in the largest differential settlements within a 23 m square (75 ft square) area. However, there were still differences between the soil properties and analysis procedures that firms A and B chose to use. When it became evident that neither firm was willing to make any more adjustments in properties or analysis procedures, and that complete agreement was not possible, firms A and B then each prepared a new report to the developer, revising their earlier estimates of differential settlement. The revised estimates were: firm A = $\Delta_{diff} \leq 250$ mm (0.85 ft) and firm B = $\Delta_{diff} \leq 50$ mm (0.15 ft).

The developer was disappointed that the new estimates did not differ much from the earlier estimates. The writer was disappointed in his lack of success in resolving what he believed at the outset was a technical problem, amenable to fairly precise quantitative evaluation. It was clear from the outcome that: (1) Evaluating the parameters that defined the problem required the exercise of judgment, even though a considerable amount of detailed data was available; and (2) the intentions of the people performing the analyses had a very considerable bearing on their choices of properties and conditions for analysis, and therefore on the results of their analyses.

It was clear that further meetings and calculations would not close the gap between the estimates made by firms A and B. The developer therefore took a different tack, and asked the writer if he would prepare a report, discussing firm A and B's estimates, and making an independent estimate of the possible differential settlement. The writer agreed. By this stage of the proceedings so many trips had been made through the numbers that the range of possible answers was well known, and no further calculations were needed for the writer to arrive at his estimate of the maximum differential settlement in a 23 m square (75 ft square) area. Quite understandably, given the writer's involvement as a mediator, his estimate of differential settlement was less than firm A's and more than firm B's. The writer's estimate was 100 mm (0.35 ft), a little less than half firm A's revised estimate, and a little more than twice firm B's revised estimate. It seemed like a reasonable compromise.

The plan for development of Bay Farm Island was approved with a requirement that the design should allow for differential settlements. Allowances were made for grade changes in the streets and sewers, posttensioned foundation slabs were used beneath the structures, and an amount of money was accumulated in escrow for each structure built at the site, to be sure that repairs could be made, even if the developing company did not stay in business. As of 1992 the maximum differential settlement in any of the

houses is approximately 45–60 mm (0.15–0.2 ft) (Kasim 1992). Repairs of architectural damage have been made in a few houses.

KANSAI INTERNATIONAL AIRPORT

Kansai International Airport is being constructed on a man-made island in Osaka Bay. It will be Japan's first 24-hour airport, being far enough from populated areas so that noise restrictions will not require its closure at night. The artificial island 4.3 km (2.7 mi) long, 1.3 km (0.8 mi) wide, with fill 33 m (110 ft) thick, will contain 184,000,000 m^3 (240,000,000 cu yd) of fill. The cost of the fill alone is $3,600,000,000. The total cost of the project is estimated at $11,000,000,000. Construction began in 1987, and the airport is scheduled to begin operation in 1994 ("Kansai" 1986; Tohma and Yamamoto 1990; Oikawa and Endo 1990; Nakase 1991).

A cross section through the soils at the site is shown in Fig. 4 (Kanda et al. 1991). The water depth where the island was constructed is 18 m (60 ft) deep. Beneath the bottom of the Bay are about 20 m (65 ft) of soft alluvial clay, and beneath that is a thick layer [150 m (500 ft) or more] of diluvial clay with sand layers and lenses. The diluvial clays are of marine and nonmarine origin, of Pleistocene age. They are somewhat overconsolidated. Ordinarily these deep overconsolidated clays would not give rise to much settlement. Because the loads imposed by the 33-mm (110-ft)-thick fill are so large, however, and because the fill covers such a large area, compression of the clays will occur to depths as great as 150 m (500 ft).

The magnitudes of the settlements to be expected during the design life of the airport were an important factor in its design. It was important to know how much settlement would occur so that the fill could be constructed high enough initially to be sure that there would be adequate freeboard throughout the 50-year design life.

In 1986, when the airport was being designed, the settlements were estimated as shown in Table 2 ("Kansai" 1986; Oikawa and Endo 1990). It was estimated that, after 50 years, the fill would have settled 8 m (26 ft). Of this total, it was expected that 6.5 m (21 ft) of settlement would occur due to compression of the alluvial clay, and 1.5 m (5 ft) would be due to compression of the diluvial clay.

It was known that consolidation would occur very rapidly in the alluvial

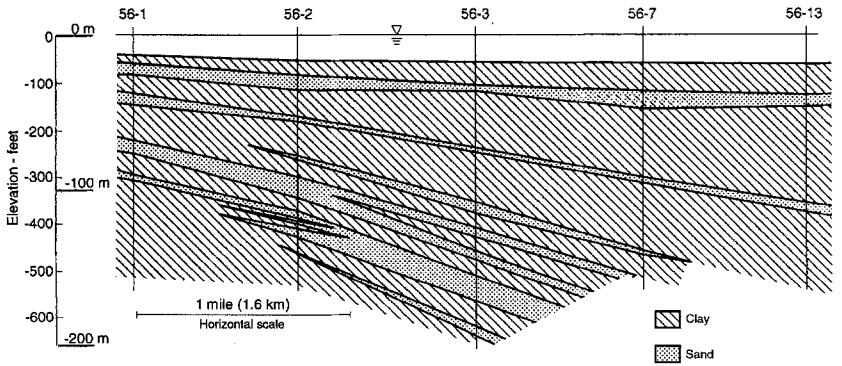

FIG. 4. Geologic Cross Section at Kansai International Airport Site, North End, Looking South [after Kanda et al. (1991)]

TABLE 2. 1986 Estimates of Settlement at Kansai International Airport after 50 Years

Layer (1)	Estimated Settlement	
	m (2)	ft (3)
Alluvial clay	6.5	21
Diluvial clay	1.5	5
Total	8	26

clay, because sand drains were used to accelerate its drainage (Maeda et al. 1990; Arai 1991; Arai et al. 1991). Consolidation of the alluvial clay was expected to be essentially complete by the time the airport opened. The ultimate consolidation settlement in the diluvial clay was estimated to be about 5.5 m (18 ft). However, because of the great thickness of this layer, it was expected that water would drain from it very slowly. Only 0.3 m (1 ft) of settlement was estimated by the time the airport opened, and only 1.5 m (5 ft) was expected within the 50-year design life.

These estimates were necessarily based on assumptions about the behavior of the clays at the site. The data defining the compressibilities of the clay, their preconsolidation pressures, and the rate at which they would drain contained significant scatter. The settlement estimates were therefore subject to considerable variation depending on how these data were interpreted.

To verify the accuracy of the estimated settlements, a monitoring area was constructed using the first fill placed in the island ("Kansai" 1986; Okawa and Endo 1990; Oikawa et al. 1990; Endo et al. 1991). As shown in Fig. 5, this area was constructed near the northwest corner of the artificial island. The monitoring area is about 335 m (1,100 ft) long by 170 m (550 ft) wide, and contains instruments for measuring settlements and pore pressures at many depths through the fill, and in the underlying natural soils.

A comparison of estimated and measured settlements is shown in Fig. 6 (Oikawa and Endo 1990; Endo et al. 1991). It can be seen that the settlements due to the alluvial clay were a little less, and the settlements due to the diluvial clay were considerably more than had been estimated in 1986. The rate of settlement in the diluvial clay was many times faster than had been estimated. It was concluded that the sand layers in the diluvial clay, which had been thought to be discontinuous and incapable of draining the clay, must in fact be continuous, and must be allowing the diluvial clay to drain more rapidly than had been anticipated. Accordingly, a new calculation model was developed, assuming that most of the sand layers in the diluvial clay are capable of draining the clay. The average length of drainage path in the new model was about one-sixth of the drainage path length used in the 1986 calculations. The rate of settlement in the diluvial clay calculated in 1990 was therefore about 36 times as fast as the rate calculated in 1986. The value of the compressibility used to calculate the alluvial clay settlements was also revised slightly, so that the calculated and observed settlements were in better agreement.

The results of the revised calculations are shown in Fig. 6. It can be seen that they agree more closely with the observed settlements than do the 1986 estimates. The estimated settlements after 50 years are shown in Table 3

TABLE 3. 1990 Estimates of Settlement at Kansai International Airport after 50 Years

Layer (1)	Estimated settlement	
	m (2)	ft (3)
Alluvial clay	5.5	18
Diluvial clay	5.5	18
Fill	0.6	2
Total	11.6	38

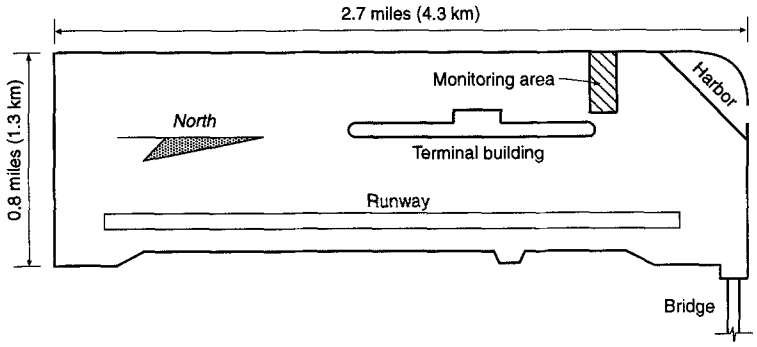

(a)

(b)

FIG. 5. Kansai International Airport [after Oikawa and Endo (1990), and *Skyfront Magazine*]: (a) Plan View of Man-Made Island [after Oikawa and Endo (1990)]; and (b) Photograph of Northwest Corner, Showing Monitoring Area Outlined by Dotted Lines (Courtesy *Skyfront Magazine*)

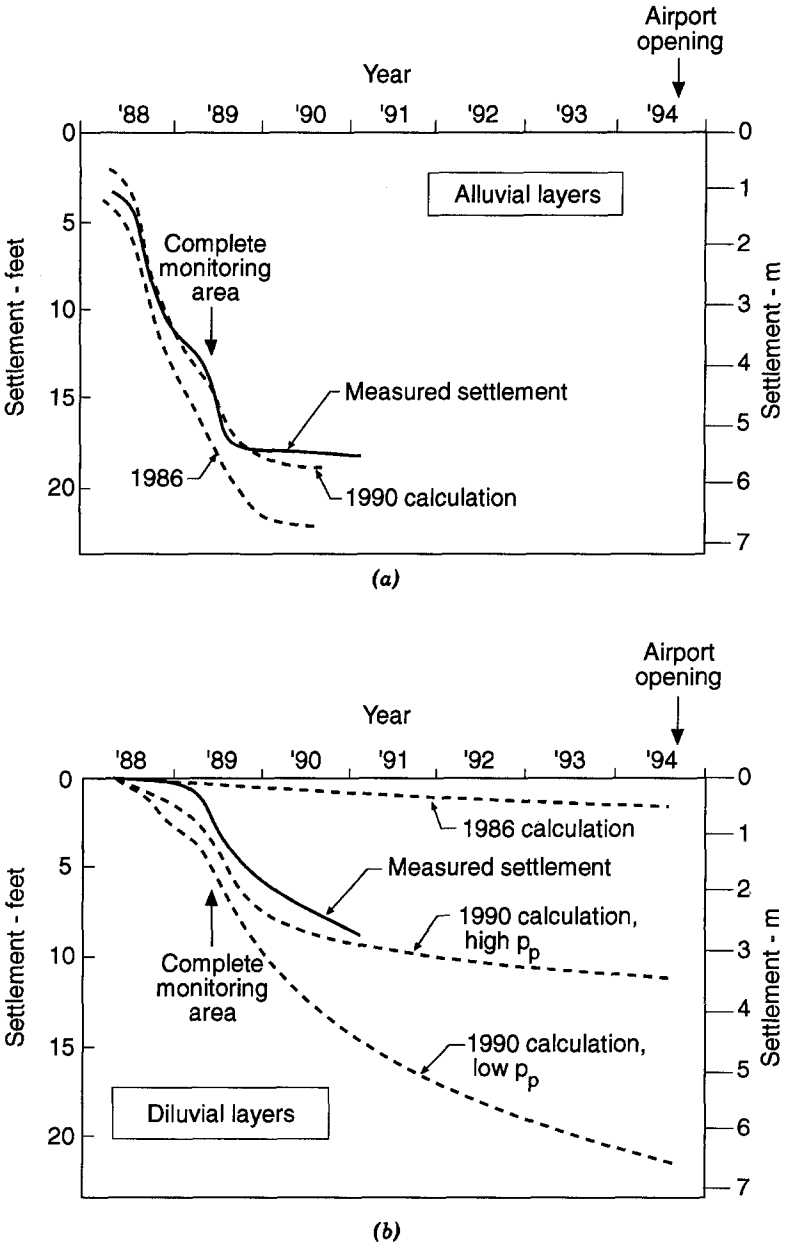

FIG. 6. Kansai International Airport Settlements [after Oikawa and Endo (1990) and Endo (1991)]; (*a*) Calculated and Measured Settlements in Alluvial Clay; and (*b*) Calculated and Measured Settlements in Diluvial Clay

(Oikawa and Endo 1990; Endo et al. 1991). These settlements are based on average values of p_p in the diluvial clay.

The settlements due to compression of the alluvial clay were estimated to be 5.5 m (18 ft), the settlements due to compression of the diluvial clay were estimated to be 5.5 m (18 ft), and 0.6 m (2 ft) of settlement was estimated to result from compression of the fill. The total settlement is expected to be 11.6 m (38 ft).

Most of the settlement at Kansai International Airport will occur before the airport opens in 1994. After the airport opens, 1.5 to 1.8 m (5 to 6 ft) of additional settlement is expected. The design of the terminal building incorporated two special features to prevent damage due to differential settlement: (1) Heavy fill (iron ore) was placed beneath the deepest parts of the basement under the terminal building, to compensate partially for the reduction in load due to the basement excavation; and (2) each column in the terminal building was fitted with an adjustable base so that it can be lengthened or shortened by 400 mm (16 in.) ("Kansai" 1991; Tekeuchi 1990; Kobayashi 1991; *Skyfront* 1992). The column lengths will be adjusted to keep the floors level as differential settlement occurs in the foundations. Sophisticated two-dimensional finite element analyses of the consolidation settlement were used to estimate the amount of travel needed in the column supports, which of the columns would need to be lengthened, and which would need to be shortened.

DIFFICULTIES IN ESTIMATING SETTLEMENTS AND SETTLEMENT RATES

The Bay Farm Island and Kansai International Airport experiences show the practical value of being able to estimate settlements accurately, and they also illustrate some of the problems involved in making accurate estimates of settlements and settlement rates. These and other experiences have shown that the most important shortcomings in the current state of the art for settlement prediction are due to:

- Difficulties in evaluating preconsolidation pressures.
- Difficulties in selecting values of c_v for consolidation rate calculations.
- Difficulties in determining whether embedded sand layers will or will not provide internal drainage to consolidating clay layers.
- Shortcomings in conventional consolidation theory.

These factors are discussed in the following pages.

Preconsolidation Pressures

The values of preconsolidation pressure estimated for a site have a very important effect on the magnitudes of the estimated settlements. This is because the compressibility of the clay is about 10 times as great at pressures above the preconsolidation pressure as it is at pressures below the preconsolidation pressure.

One of the difficulties in evaluating preconsolidation pressures for a site is illustrated by Fig. 7, which shows many values of p_p for the Kansai International Airport site (Onodera 1986; Kanda et al. 1991). These values were measured in conventional consolidation tests, where loads were applied at 24-hour intervals. It can be seen that there is considerable scatter in the

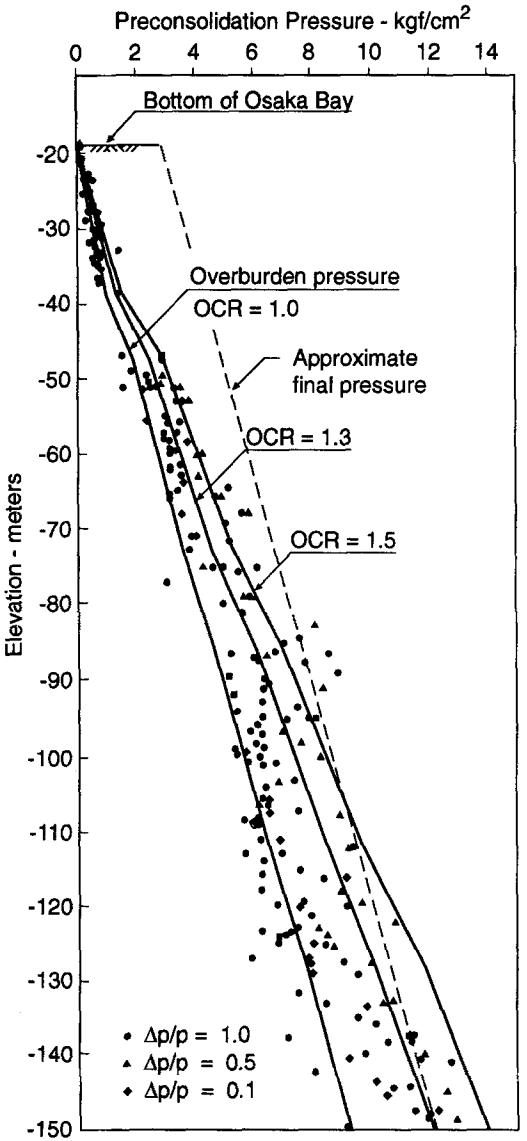

FIG. 7. Preconsolidation Pressures in Diluvial Clay at Kansai International Airport [after Kanda et al. (1991)]

data, even though great care was taken to minimize disturbance due to sampling, transporting, and testing the clay. Settlements calculated using variations of p_p with depth near the high end and near the low end of the range of measured values are shown in Fig. 6(*b*). Clearly the judgment regarding which values of p_p best represent the actual field conditions has a very important bearing on the magnitudes of the calculated settlements.

Another type of difficulty involved in estimating preconsolidation pressures is illustrated in Fig. 8, which shows the nature of the crust conditions

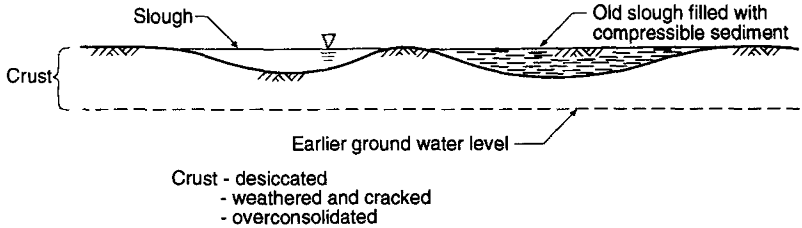

FIG. 8. Crust Conditions at Bay Farm Island

at the top of the Bay mud at Bay Farm Island. Due to the fact that the site had experienced recurrent episodes of drying, flooding, slough erosion, and slough filling, there were considerable variations from place to place in the preconsolidation pressures in the upper part of the Bay mud. In some places the crust was well developed and fairly highly preconsolidated due to desiccation. In other places, where sloughs had formed due to surface runoff and tidal flows, or where ditches had been dug, the preconsolidated crust had been removed, exposing the more compressible normally consolidated Bay mud beneath. In still other places older sloughs had been abandoned as new sloughs formed, and the old slough had become filled with soft new sediment. The resulting variations in preconsolidation pressure within the top 2 m (6 ft) or so are responsible for most of the variation in measured settlement shown in Fig. 3 (Duncan et al. 1991).

Values of c_v

The coefficient of consolidation (c_v) is the soil parameter that controls the rate of consolidation. The value of c_v depends on the permeability (k) and the compressibility of the soil (m_v) as shown by (1):

$$c_v = \frac{k}{m_v \gamma_w} \qquad (1)$$

in which c_v = coefficient of consolidation (length squared per unit of time), k = coefficient of permeability (length per unit of time), m_v = coefficient of volume compressibility (length squared per unit of force), and γ_w = unit weight of water (force per length cubed).

Both k and m_v decrease as consolidation pressure increases. Because both k and m_v decrease as the pressure increases, the value of c_v changes less with pressure than either k or m_v. For some clays under some conditions, c_v remains roughly constant as consolidation pressure increases.

Conventional consolidation theory assumes that c_v is constant, and it is necessary to select a single value of c_v when conventional theory is used to estimate settlement rates. Frequently, however, conditions are such that selecting a single value of c_v to represent an entire clay layer throughout a range of pressures is not a straightforward matter. Factors that complicate selection of a value of c_v for consolidation rate calculations include these:

1. The value of c_v for a given clay is about an order of magnitude larger at pressures below the preconsolidation pressure at it is at pressures above the preconsolidation pressure. Thus if the effective stress in part or all of the clay deposit is initially smaller than the preconsolidation pressure, and the effective stress subsequently becomes larger than the preconsolidation

pressure as the clay consolidates, the magnitude of c_v will change greatly during the process of consolidation.

2. In many cases in laboratory tests and field applications, the drainage path length (D) decreases significantly as the clay consolidates under higher pressures. Values of c_v are calculated by Casagrande's t_{50} method (Casagrande 1938) using (2*a*)

$$c_v = \frac{(0.197)D^2}{t_{50}} \quad \ldots\ldots (2a)$$

or by Taylor's t_{90} method (Taylor 1948) using (2*b*)

$$c_v = \frac{0.848D^2}{t_{90}} \quad \ldots\ldots (2b)$$

where D = drainage path length, t_{50} = time to reach a degree of consolidation equal to 50%, and t_{90} = time required to reach a degree of consolidation equal to 90%.

Where D decreases significantly as the pressure increases, values of c_v calculated using the initial value of D will be significantly different from values of c_v calculated using the smaller values of D after compression. In the case of San Francisco Bay mud, for example, application of a pressure of 8 kgf/cm^2 results in a reduction of specimen thickness and D from 25.4 mm (1.00 in.) to about 14.7 mm (0.58 in.). Because the value of D is squared in (2*a*) and (2*b*), there is a very significant difference in the value of c_v calculated using the initial value of D as opposed to the reduced value of D. In the case of San Francisco Bay mud at a pressure of 8 kgf/cm^2, the value of c_v calculated using the reduced value of D would be only about 34% of the value calculated using the original drainage path length.

Because the choice of D has a significant effect on the calculated value of c_v, the question arises as to which is more correct, the initial value of D, or the reduced value of D. The answer depends on how c_v will be used. If, as in many practical applications, the value of c_v is used to estimate rate of settlement, and the calculations are performed using the initial drainage path length in the field (as in most cases when the calculations are done manually), the initial drainage path length in the lab should be used to calculate c_v. If the settlement rate calculations are performed using reduced drainage path length in the field (as in the case with many computer programs for numerical analysis of consolidation) then reduced drainage path lengths in the lab should be used to calculate c_v.

3. The two methods commonly used to determine the value of c_v from laboratory test data—Casagrande's t_{50} method (Casagrande 1938) and Taylor's t_{90} method (Taylor 1948)—in general do not result in the same value of c_v. An example, for San Francisco Bay mud, is shown in Fig. 9. (These values were calculated using the initial value of drainage path length.) The values of c_v calculated using Casagrande's method vary from 0.6 to 3 m^2/yr (6 to 32 sq ft/yr), and those calculated using Taylor's method vary from 0.8 to 5.2 m^2/yr (9 to 56 sq ft/yr). Thus, for this particular highly plastic organic clayey silt, the value of c_v determined by Taylor's method is about 1.5 times the value determined by Casagrande's method.

If the shapes of laboratory time curves were exactly similar to the theoretical shape, Casagrande's and Taylor's methods would result in the same

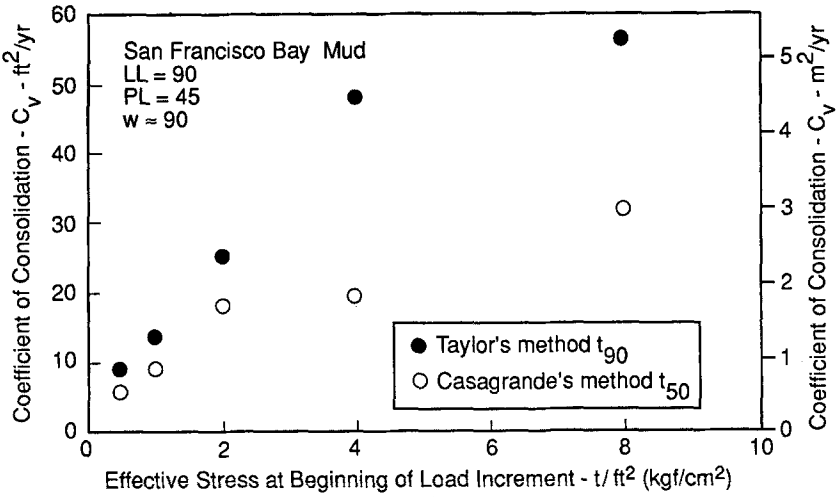

FIG. 9. Variation of c_v Values with Pressure for San Francisco Bay Mud

value of c_v. However, due to the fact that clay compressibility varies with effective stress and rate of strain, and due perhaps to other effects as well, the actual shapes differ from the theoretical shapes.

Data for seven undisturbed clays and two remolded clays are summarized in Table 4. (These values were calculated using the initial value of drainage path length.) It can be seen that Taylor's t_{90} method consistently gives higher values of c_v than Casagrande's t_{50} method. For the 33 individual tests listed in Table 1, in only one case is the value of c_{vt}/c_{vc} less than unity. For the other cases listed in Table 1, the values of c_{vt}/c_{vc} range from 1.01 to 3.43, with an average value of 1.66. An engineer using laboratory test data to estimate rate of settlement has to decide which of the methods to use. Both methods are equally rational, but they frequently give significantly different answers.

One rationale for deciding between Casagrande's and Taylor's methods is this: In most cases it is found that rates of settlement estimated using laboratory test data and conventional consolidation theory are slower than the actual rates of settlement observed in the field. Thus if Taylor's method is used to calculate c_v, the agreement between the estimated and observed rates of settlement will often be improved, because the calculated settlement rate will be faster.

4. The data in Fig. 9 and Table 4 show that the values of c_v for clays, calculated using initial drainage path length, in many cases increase as consolidation pressures increase. The effect is pronounced for San Francisco Bay mud, the Kansai Airport alluvial clay, the remolded Karita clay, and the remolded Kaolinite. Within the range of pressures for which data are summarized in Fig. 9 and Table 4, all of the soils are normally consolidated. Thus, even where a clay is not overconsolidated initially, the value of c_v may change significantly during consolidation.

5. The data in Table 4 also indicate that values of c_v increase with increasing initial drainage path length. The data for the Dramen clay, the

TABLE 4. Values of c_v Calculated by Casagrande's and Taylor's Methods

Reference (1)	Soil (2)	LL PL (3)	Initial drain path length (cm) (4)	Initial pressure (kg/cm²) (5)	Casagrande c_{vc} [m²/yr (sq ft/yr)] (6)	Taylor c_{vt} [m²/yr (sq ft/yr)] (7)	Ratio c_{vt}/c_{vc} (8)
This paper	SF Bay mud	90	1.27	0.5	0.54 (5.8)	0.85 (9.1)	1.58
		45	1.27	1.0	0.84 (9.0)	1.27 (13.7)	1.53
			1.27	2.0	1.67 (18.0)	2.37 (25.5)	1.42
			1.27	4.0	1.81 (19.5)	4.49 (48.3)	2.48
			1.27	8.0	2.97 (32.0)	5.24 (56.4)	1.76
Crawford (1964)	Leda clay	—	1.27	4.0	4.7 (51)	12.8 (138)	2.71
			1.27	8.0	10.3 (111)	23.3 (251)	2.26
			2.54	4.0	9.2 (100)	11.3 (122)	1.23
			2.54	8.0	10.4 (112)	11.3 (122)	1.09
Leonards and Altschaeffl (1964)	Mexico City clay	275–440 100–150	1.91	0.2	2.1 (23)	4.7 (51)	2.20
Berre and Iversen (1972)	Drammen clay	—	1.75	0.94	0.51 (5.5)	0.78 (8.4)	1.52
			7.50	0.95	1.97 (21.2)	1.99 (21.4)	1.01
			45.00	0.91	4.12 (44.3)	3.29 (35.4)	0.80
Felix et al. (1981)	Cubzac-les Ponts clay	—	0.5	8.0	0.39 (4.23)	1.25 (13.48)	3.19
			0.0	8.0	1.15 (12.38)	2.24 (24.16)	1.95
			2.0	8.0	1.09 (11.69)	3.72 (40.04)	3.43
			4.0	8.0	1.28 (13.76)	3.24 (34.89)	2.54
Leroueil et al. (1985)	Batiskan clay	—	0.95	0.7	0.10 (1.1)	0.21 (2.3)	2.04
			0.95	0.7	0.20 (2.1)	0.27 (2.9)	1.39
Kobayashi et al. (1988)	Kansai alluvial clay	70–95	1.00	1.6	1.10 (12)	1.5 (16)	1.36
		30–40	1.00	3.2	1.6 (17)	2.1 (23)	1.36
Takada et al. (1988)	Remolded Karita clay	105	1.00	0.4	0.48 (5.2)	0.78 (8.4)	1.62
		38	1.00	0.8	0.64 (6.9)	0.86 (9.3)	1.34
			1.00	1.6	0.98 (10.5)	1.3 (14)	1.33
			1.00	3.2	1.5 (16)	2.3 (25)	1.55
			1.00	6.4	2.0 (22)	3.1 (33)	1.51
Aboshi (1990)	Remolded Hiroshima clay	100	2	2.0	9.1 (98)	10.8 (116)	1.19
		58	4.8	2.0	10.5 (113)	10.7 (115)	1.02
			20	2.0	10.6 (115)	12.2 (131)	1.14
			40	2.0	17.6 (190)	20.3 (218)	1.15
			100	2.0	12.4 (134)	14.6 (157)	1.17
Mikasa and Takada (1984)	Remolded Kaolinite	—	1.00	1.0	3.2 (34)	3.4 (37)	1.07
			1.00	3.0	5.1 (55)	5.2 (56)	1.01

Note: Values of c_v calculated using initial drainage path length in all cases.

Cubzac-les-Ponts clay, and the remolded Hiroshima clay show this effect clearly. Possible explanations for this effect include these:

1. As layer thickness increases, the difference between the initial effective stress at the top and the bottom of the layer, due to the weight of clay, increases. Because compressibility decreases with increasing pressure ($m_v = C_c/(2.3p')$ for a normally consolidated clay) the strains are larger where the initial pressures are smaller. As discussed next, the resulting nonuniform strain profile can result in faster consolidation than would be indicated by conventional consolidation theory, which assumes that the strain profile is uniform. This factor is important for lab tests on very thick specimens and low initial pressures, and for field conditions where the initial pressure varies significantly from the bottom to the top of the layer.
2. Although conventional theory assumes that the compressibility of the clay skeleton is not time-dependent, lab tests and field observations show that there is a component in clay compressibility that depends on strain rate and load duration, as evidenced by the fact that clays undergo secondary compression. It may be possible that, at large strain rates, this strain rate-dependent resistance to compression is comparable in magnitude to the resistance that results from drainage of water from the clay. Being viscous in nature, the strain rate-dependent resistance of the clay skeleton would be higher when strain rates are high, and lower when strain rates are low. Following this logic, the portion of the resistance of the clay skeleton that depends on the rate of strain would inhibit compression by a greater amount for a thin clay test specimen in the laboratory (where the strain rate during consolidation is high) than it would for a thicker layer of clay in the field (where the strain rate during consolidation is low).

Considering these effects—change in the value of c_v as the preconsolidation pressure is exceeded, differences in the values of c_v calculated using Casagrande's and Taylor's methods, changes in the value of c_v as consolidation pressure increases, and changes in the value of c_v as layer thickness increases—it is clear that selecting a value of c_v for use in estimating rates of settlement is not a straightforward matter. Selecting a suitable value of c_v requires an understanding of the factors that can cause its value to change.

Further study of the fundamental causes of the effects discussed in the preceding paragraphs would provide useful guidance in how best to use laboratory time curves to estimate values of c_v for predicting rates of settlement in the field. A related improvement would be development of simple computer programs that could be used routinely for analysis of rates of consolidation wherein the values of c_v could be varied as the effective stress changed.

Mesri and Choi (1985) have developed a computer program that accounts for variations in c_v during consolidation through data that describe the variation of void ratio with effective stress and permeability with void ratio. They recommend that permeability values be measured at various stages during the consolidation test by performing falling head or constant head permeability tests. Use of their computer program (called ILLICON) avoids many of the problems involved in evaluating c_v, but does require inde-

pendent measurement of permeability during consolidation tests. The program operates on a mainframe computer.

Embedded Sand Layers and Lenses

Whether or not embedded sand strata are capable of providing internal drainage within a clay layer has a very important effect on the rate of consolidation and settlement. A single sand stratum in the middle of a clay layer can reduce the length of the drainage path by a factor of two, thereby increasing the rate of settlement by a factor of four. In the case of Kansai International Airport, the 1990 calculation model included many more internal drainage layers than the original calculation model used in 1986 (Oikawa and Endo 1990). The result was a reduction in average drainage path length by a factor of about 6, and an increase in the rate of settlement by a factor of about 36.

At the present time geotechnical engineers must rely on knowledge of geologic conditions, careful evaluation of boring logs, cone soundings, and judgment to guide them in developing a reasonable calculation model with respect to internal drainage in clay layers. Development of quantitative means of assessing the potential of embedded layers for providing internal drainage would be very helpful for improving the accuracy of settlement rate predictions.

Consolidation Theory

Conventional consolidation theory (Terzaghi 1925; Terzaghi and Frolich 1936) is one of the most widely applied theories in geotechnical engineering. Because it embodies the basic physical process of consolidation, uses properties that are measurable in fairly simple laboratory tests, and involves only calculations that can be done quickly by hand, conventional consolidation theory has found wide application in geotechnical engineering practice. More than 65 years after it was first developed, it is still taught to virtually every geotechnical engineering student, and is still used by virtually every practicing geotechnical engineer, even when more advanced methods are also taught or used from time to time. Even though more advanced types of analyses may eventually replace conventional consolidation theory in many applications, conventional theory is likely to continue to provide the most effective tool for teaching and learning the fundamental physics of consolidation, and the most useful means of establishing quickly the reasonableness of the results of more exotic and complex analyses.

The accuracy of conventional consolidation theory is limited by three simplifying assumptions on which it is based:

1. Conventional consolidation theory assumes that c_v is constant. However, as just noted, the value of c_v decreases greatly as the effective stress reaches the preconsolidation pressure, and its value may tend to increase with increasing pressure for normally consolidated clays. As a result of these effects, the value of c_v actually varies with depth in the layer, and with time during consolidation. These variations can result in rates of settlement different from the rate calculated using conventional consolidation theory.
2. Conventional consolidation theory assumes that the stress-strain behavior of the soil skeleton is linear and elastic. In fact the compressibility of real soils is neither linear nor elastic. Linear elastic behavior implies proportionality between change in stress and change in strain. For most

clays, however, strains increase in proportion (or approximately in proportion) to the log of effective stress. Also, the compressibility increases rapidly as effective stresses exceed the preconsolidation pressure. Further complexity arises due to the fact that, in the normally consolidated range of loading, clays are much stiffer for unloading (decreasing effective stress) than they are for loading (increasing effective stress). These differences between the behavior of real clays and the simple stress-strain relationship assumed in conventional consolidation theory have a significant effect on consolidation behavior under some circumstances.

3. Most of the time when conventional consolidation theory is applied to practical problems, the relationship between degree of consolidation (U) and time factor (T) shown in Fig. 10 as case A is used as the basis for the calculations. Case A corresponds to a condition where the strains that occur during consolidation are the same at every depth within the layer. Terzaghi and Frolich (1936) and Janbu (1965) have shown that the rate of consolidation is different when the strains are not uniform, as shown by curves B and C in Fig. 10. It can be seen that when the strains decrease with depth,

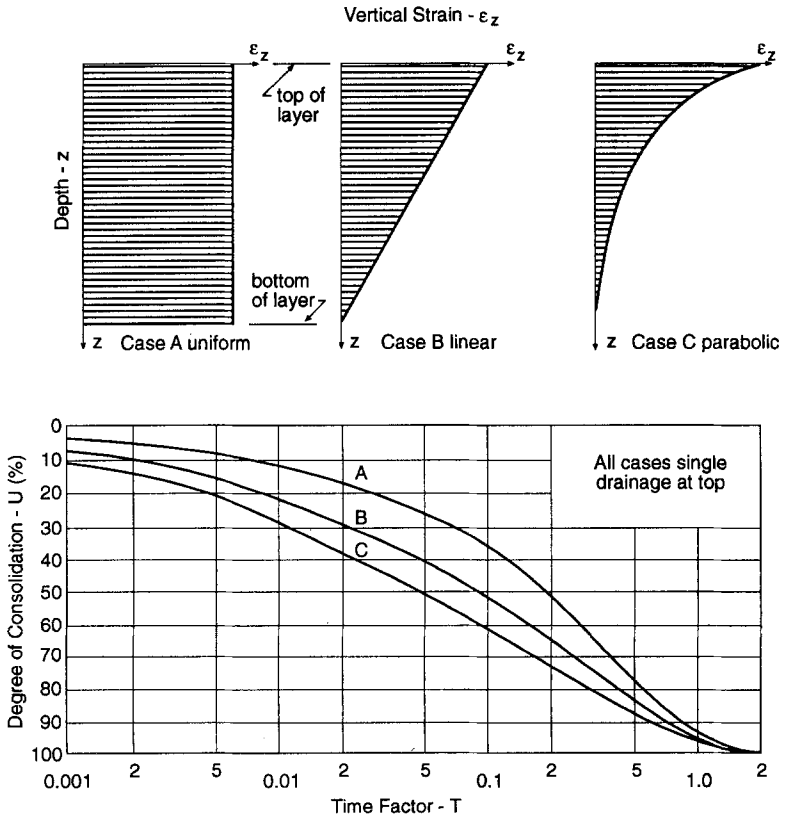

FIG. 10. Influence of Strain Profile on Rate of Consolidation [after Terzaghi and Frolich (1936) and Janbu (1965)]

as they often do, consolidation and settlement proceed more rapidly than when they are uniform, when drainage occurs only at the top of the layer.

In most practical circumstances, the strains that occur during consolidation are not uniform. Strains often decrease with depth because the stress increase caused by surface loads decreases with depth, or the clay compressibility decreases with depth, or both. Where an otherwise normally consolidated clay deposit has a dried surface crust, strains are usually relatively small in the crust, much larger immediately beneath the crust, and then decrease with depth further beneath the crust. Using time curve A to estimate settlement rates for cases where the strains are not uniform is inappropriate in principle, but it is common practice.

The assumption that strains are uniform with depth is not an inherent limitation of conventional consolidation theory, as shown by the work of Terzaghi and Frolich (1936) and Janbu (1965). When the theory is used in practice, however, curve A in Fig. 10 is almost always used to estimate settlements, even though curve B or C might be more appropriate. This simplification (using curve A) reduces the accuracy of estimated settlement rates.

The limitations of conventional consolidation theory, and particularly curve A, for estimating rates of settlement can be illustrated by a simple example. This example was first brought to the writer's attention by Mr. Albert Buchignani, a consulting engineer in the San Francisco area. It concerns the settlements to be expected four years after placement of a 3 m (10 ft)-thick layer of fill on San Francisco Bay mud, as shown in Fig. 11. The increase in pressure due to the fill is 60 kPa (1,250 psf). The thickness of the Bay mud varies across the site, from zero to 24 m (80 ft). Sections A, B, C, and D are located where the mud is 6 m (20 ft), 12 m (40 ft), 18 m (60 ft), and 24 m (80 ft) thick.

The settlements after four years are calculated as shown in Table 5. The calculations are made using the relationship between U and T given by curve A in Fig. 10, and assuming that the material beneath the Bay mud is impermeable (single drainage). The magnitudes of the final settlements shown in the fourth column were calculated using standard procedures. They vary from 1.4 m (4.5 ft) for a 6 m (20 ft) thickness to 2.8 m (9.3 ft) for a 24 m (80 ft) thickness of Bay mud.

The values of T vary inversely with the square of layer thickness, from

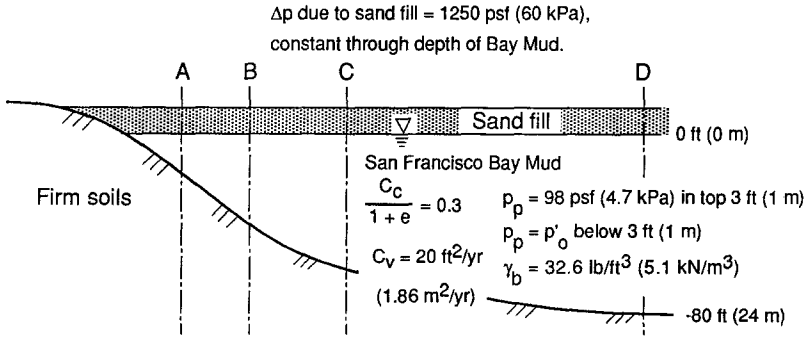

FIG. 11. Cross Section through Site Showing Fill over San Francisco Bay Mud

TABLE 5. Calculated Settlements for t = 4 Years

H [m(ft)] (1)	T for t = 4 years (2)	U for t = 4 years (3)	Δ_{final} [m(ft)] (4)	Δ_{4years} [m(ft)] (5)
6 (20)	0.2	50.4%	1.38 (4.52)	0.69 (2.28)
12 (40)	0.05	25.3	2.04 (6.70)	0.52 (1.69)
18 (60)	0.0222	16.8%	2.50 (8.20)	0.42 (1.38)
24 (80)	0.0125	12.6%	2.84 (9.33)	0.36 (1.18)

T = 0.2 for H = 6 m (20 ft) to T = 0.0125 for H = 24 m (80 ft). The corresponding values of U at t = 4 years vary from U = 50.4% for H = 6 m (20 ft), to U = 12.6% for H = 24 m (80 ft). Following conventional procedures, values of settlement at four years are calculated by multiplying these values of U by the corresponding final settlements, resulting in the values shown in the right-hand column in Table 5.

It can be seen that these results are not reasonable. The calculated settlements after four years are largest for a 6 m (20 ft) thickness of Bay mud, and smallest for a 24 m (80 ft) thickness of mud. The calculations indicate that, the greater the thickness of mud, the smaller the settlement after four years. Clearly this is not the way things would actually happen. As Taylor (1948) showed, rate of settlement should be independent of layer thickness for values of U less than about 60%.

Additional results calculated using conventional consolidation theory and curve A are shown in Fig. 12(*a*). It can be seen that the same unreasonable relationship (larger settlement for smaller Mud thickness) persists throughout a period of 20 years or so after the fill is placed. As full consolidation (U = 100%) is approached, the relationship is reversed, and the results are reasonable.

This example shows that using conventional consolidation theory to predict settlement rates can lead to clearly incorrect results. Why? The reason is that the settlements at four years were calculated using curve A, in effect assuming that the strain profile was uniform. It can be seen in Table 5 that the strain profile is not uniform. The final strain for the top 6 m (20 ft) is $\Delta H/H_0$ = 4.52/20 = 22.6%. The final strain for the bottom 20 ft [from 18 to 24 m (60 to 80 ft)] is $\Delta H/H_0$ = 1.13/20 = 5.5%. If the relationship between U and T corresponding to the actual strain profile had been available, and had been used in the calculations, the results would have been reasonable. They would have shown that the settlements for the greater thicknesses were as large or larger than the settlements for the smaller thicknesses.

The most effective means of estimating settlement rates for a problem of this type is through numerical analysis using a computer program. Using a computer program, it is possible to model nonlinear stress-strain behavior, and variation of the strain through the depth of the layer. The strain profile effects illustrated in Fig. 10 are automatically accounted for.

The rates of settlement at sections A, B, C and D have been calculated using a PC computer program called CONSOL (Duncan et al. 1988), which can model these effects. The variations of settlement with time resulting from these analyses are shown in Fig. 12(*b*). These results are more reasonable than those calculated using conventional consolidation theory with curve A. At early times (t < 5 years) the settlements are the same for all layer thicknesses, as Taylor (1948) showed they should be. At later times

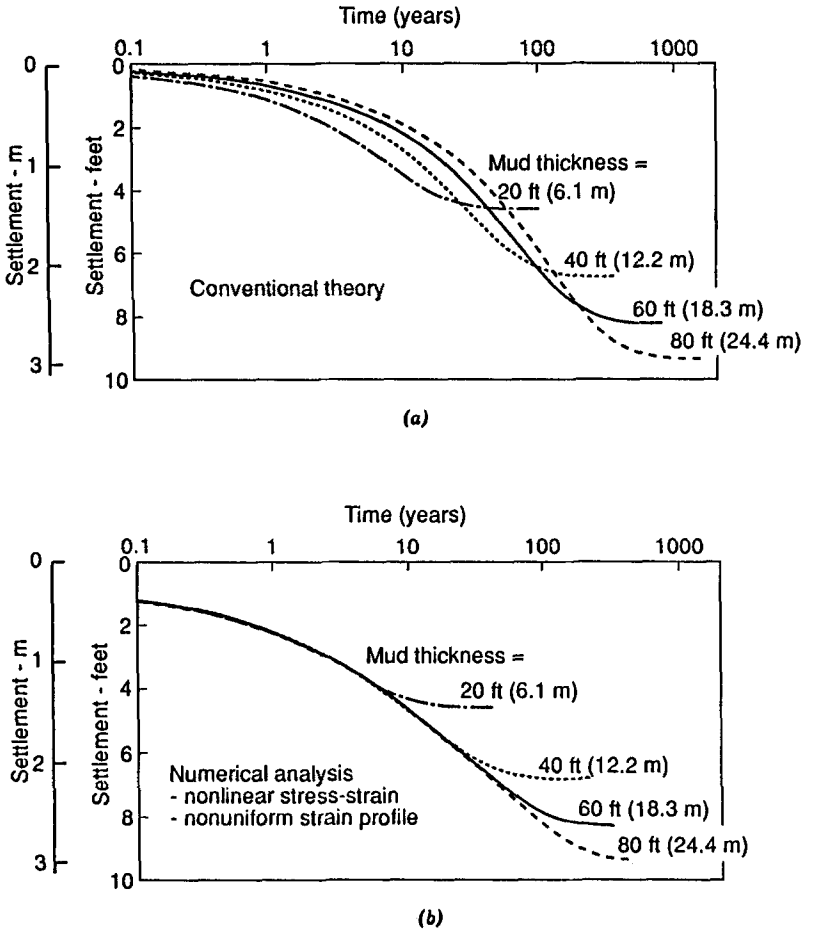

FIG. 12. Calculated Variations of Settlement with Time for Mud Thicknesses of 6.1 m (20 ft), 12.2 m (40 ft), 18.3 m (60 ft), and 24.4 m (80 ft): (*a*) Calculated Using Conventional Consolidation Theory; and (*b*) Calculated Using Numerical Analysis

the settlements become larger for the larger thicknesses of clay. These results are clearly more logical and realistic than those shown in Fig. 12(*a*).

In a case like the one shown in Fig. 11, where settlements are large, the loading on the clay decreases appreciably as the fill subsides below the water table and becomes buoyant. For simplicity this effect was not included in the results shown in Table 5 and Fig. 12. It can easily be included in computer analyses, and can be included in manual computations by trial and error.

REQUIREMENTS FOR BETTER SETTLEMENT ESTIMATES

The example shown in Figs. 11 and 12 illustrates the advantages of using computer analyses to estimate rates of consolidation settlement. Such analyses can model the actual field conditions more realistically than is possible with manual calculations and conventional consolidation theory. Although

the manual calculations are not complex or time-consuming, the simplifications they involve can lead to significant inaccuracy. By spending the same time and effort performing computer analyses, it is possible to model field conditions more realistically, and to achieve more reasonable results.

In some cases it may even be worthwhile to model two-dimensional conditions by performing 2-D finite element analyses of consolidation. The rates of settlement at Kansai International Airport were calculated by means of such analyses. The computer program used for these analyses employed the Sekeguchi-Ohta (1977) constitutive model, which includes viscoplastic behavior to model secondary compression effects. Such analyses are far from routine, are expensive, and require very careful examination to ensure that the results are reasonable.

More research is needed to develop an improved understanding of the effect of strain rate on clay compressibility, and how it influences the rate of consolidation. Logically, the model used to represent the soil skeleton in consolidation analyses would include a component of compressibility related to strain rate. To the writer's knowledge, however, no consistent theory for these effects has been developed that can be incorporated in a simple PC computer program, although this type of analysis technique has been developed for larger computers (Rajot 1992). Eventual availability of easy-to-use computer programs based upon such a model of clay compressibility will make possible fully rational interpretation of laboratory tests and fully rational analyses of consolidation settlements. The prime prerequisite for any analysis is good definition of soil properties that reflect the behavior of the undisturbed clay in situ.

To make better estimates of rates of consolidation, better methods are needed to determine which sand strata embedded in clay layers will provide internal drainage, and which will not. For clays like the diluvial clay at Kansai International Airport, which contain many embedded sand strata, the judgment of which sand layers will provide internal drainage is more important than any other factor in determining the rate of consolidation and settlement.

SUMMARY AND CONCLUSIONS

Consolidation of clay can result in large settlements. At Bay Farm Island the settlements exceeded 2 m (7 ft). At Kansai International Airport the settlements are expected to approach 12 m (40 ft) within the design life of the project. In order to design facilities at these sites that will not be damaged by these settlements, it is important to be able to anticipate both the amount of settlement and the rate at which it will occur. Accurate prediction of settlement rates requires improved methods of anticipating what embedded sand strata will provide internal drainage in clays; use of computer analyses to take into account important factors such as variations in c_v within clay layers, nonlinear stress-strain behavior and nonuniform strain profile effects; and research to develop an improved model of clay compressibility that includes the effects of strain rate.

ACKNOWLEDGMENTS

The writer is grateful to many people who made important contributions to this lecture. Don Javete provided much valuable information regarding Bay Farm Island. Yoshio Ozawa and Masaki Kobayashi arranged for the writer to visit the Kansai International Airport project, and provided very

extensive data regarding the project. Katsuji Ishihara, a Virginia Tech Ph.D. student, helped with translation, literature review, and computer analyses. Over many years Kai Wong, Al Buchignani, Jean-Pierre Rajot, Bob Schiffman, and Roy Olson have helped the writer understand the consolidation of clay, and how to analyze it better. This lecture and paper would not have been possible without their valuable assistance, so generously given. The writer also wishes to thank Charles Ladd, John Lowe III, Reza Mesri, and Tim Stark, who reviewed the paper and helped to improve it considerably through their many useful suggestions.

APPENDIX. REFERENCES

Aboshi, H. (1990). "Consolidation settlement and soil improvement of soft clay." *Soil Found.*, 38(10), 7–14.

Arai, Y. (1991). "Construction of an artificial offshore island for the Kansai International Airport." *Preprints of Special Lectures, Int. Conf. on Geotech. Engrg. for Coastal Development, Geo-Coast '91*, Port and Harbour Research Institute, Japan, S1,1–S1,17.

Arai, Y., Oikawa, K., and Yamagata, N. (1991). "Large scale sand drain works for the Kansai International Airport island." *Proc. Int. Conf. on Geotech. Engrg. for Coastal Development, Geo-Coast '91*, Port and Harbour Research Institute, Japan, 281–286.

Berre, T., and Iversen, K. (1972). "Oedometer test with different specimen heights on a clay exhibiting large secondary compression." *Geotechnique*, London, United Kingdom, 22(1), 53–70.

Bjerrum, L. (1963). "Alowable settlements of structures." *Proc. European Conf. on Soil Mech. and Foundation Engrg.*, Wiesbaden, 2, 13–137.

Crawford, C. B. (1938). "Interpretation of the consolidation test." *J. Soil Mech. and Found. Engrg. Div.*, ASCE, 90(5), 87–102.

Duncan, J. M., Javete, D. F., and Stark, T. D. (1991). "The importance of a desiccated crust on clay settlements." *Soil Found.*, 31(3), 77–90.

Duncan, J. M., Smith, R. W., Brandon, T. L., and Wong, K. S. (1988). "CONSOL version 2.0: A computer program for 1-D consolidation analysis of layered soil masses." *Geotech. Engrg. Report*, Virginia Polytechnic Institute and State University, Blacksburg, Va.

Endo, H., Oikawa, K., Komatsu, A., and Kobayashi, M. (1991). "Settlement of diluvial clay layers caused by a large scale man-made island." *Proc. Int. Conf. on Geotech. Engrg. for Coastal Development, Geo-Coast '91*, Port and Harbour Research Institute, 177–182.

Felix, B., Vuaillat, P., Darve, F., and Flavigny, E. (1981). "Viscous behaviour and consolidation of clays." *Proc., 10th ICSMFE*, 597–602.

Janbu, N. (1965). "Consolidation of clay layers based on non-linear stress-strain." *Proc., 6th Int. Conf. Soils Mech. and Foundation Engrg.*, International Society for Soil Mechanics and Foundation Engineering.

Jevete, D. F. (1983). "The importance of a desiccated crust on clay settlements," PhD thesis, University of California, Berkeley, Calif.

Kanda, K., Suzuki, S., and Yamagata, N. (1991). "Offshore soil investigation at the Kansai International Airport." *Proc. Int. Conf. on Geotech. Engrg. for Coastal Development, Geo-Coast '91*, Port and Harbour Research Institute, Japan, 33–38.

"Kansai International Airport—construction of airport island." (1986). Kansai International Airport Co., Ltd., Osaka, Japan.

"Kansai weighs that sinking feeling." (1991). *Engrg. News Record*, Jan. 7.

Kobayashi, M., Mizukami, J., and Tsuchida, T. (1988). "Horizontal coefficient of consolidation of clay." *Proc. Symp. on Special Consolidation Tests*, Japanese Society of Soil Mechanics and Foundation Engineering, 175–180.
Kogure, K., Yamaguchi, H., Ohira, Y., and Ono, H. (1986). "Experiments on consolidation characteristics of a fibrous peat." *Proc. Advances in Peatland Engrg., Carleton University Conf.*, National Research Council of Canada, 101–108.
Leonards, G. A., and Altschaeffl, A. G. (1964). "Compressibility of clay." *J. Soil Mech. and Found. Engrg. Div.*, ASCE, 90(5), 133–155.
Leroueil, S., Kabbaj, M., Tavenas, F., and Bouchard, R. (1985). "Stress-strain rate relation for the compressibility of sensitive natural clays." *Geotechnique*, London, United Kingdom, 35(2), 159–180.
Lowe, J. (1974). "New concepts in consolidation and settlement analysis (the eighth Terzaghi Lecture)." *J. Soil Mech. and Found. Engrg. Div.*, ASCE, 100(6), 571–612.
Maeda, S., Higuchi, Y., and Furuichi, M. (1990). "Large-scale sand drain works for the Kansai International Airport." *Proc. Airports into the 21st Century*, Hong Kong Institute of Engineers.
Mikasa, M., and Takada, N. (1984). "Determination of coefficient of consolidation (C_v) for large strain and variable C_v values." *Consolidation of Soils, ASTM, STP 892*, American Society for Testing and Materials, Philadelphia, Pa., 526–547.
Nakase, A. (1991). "The importance of geotechnical engineering in coastal development." *Preprints of the Keynote Lecture, Int. Conf. on Geotech. Engrg. for Coastal Development, Geo-Coast '91*, Port and Harbour Research Institute, Japan, K,1–K,10.
Oikawa, K., and Endo, H. (1990). "Construction of a large-scale man-made island for the Kansai international airport." *Soft Seabed Deposit, Kansai Int. Geotech. Forum '90 on Comparative Geotech. Engrg.*, Japanese Society of Soil Mechanics and Foundation Engineering, Kansai Branch.
Oikawa, K., Suzuki, A., and Yamagata, N. (1990). "Total field observation system for the settlement and stability control of large-scale reclamation work." *Proc. New Technologies in Field Observation*, Japanese Society of Soil Mechanics and Foundation Engineering, (in Japanese).
Onodera, S. (1986). "Study on the engineering properties of soils off Senshu in the Osaka Bay," PhD thesis, Tokyo Institute of Technology, Yokosuka, Japan.
Rajot, J. P. (1992). "A theory for the time dependent yielding and creep of clay," PhD thesis, Virginia Polytechnic Institute and State University, Blacksburg, Va.
Rutledge, P. C. (1970). "Utilization of marginal lands for urban development (the fifth Terzaghi Lecture)." *J. Soil Mech. and Found. Engrg. Div.*, ASCE, 96(1), 1–22.
Sekiguchi, H., and Ohta, H. (1977). "Induced anisotropy and time dependency in clays." *Proc. Specialty Session 9, 9th ICSMFE*, International Society for Soil Mechanics and Foundation Engineering, 229–238.
Skempton, A. W., and McDonald, D. H. (1956). "The allowable settlement of buildings." *Proc.*, Institute of Civil Engineers, 5, 724–784.
Skyfront Magazine. (1992). Skyfront Co., Osaka, Japan, vols. 14 and 15, 56–57.
Takada, N., Ohshima, A., Kusakabe, O., Hagiwara, T., Takahashi, M., and Yamada, S. (1988). "Oedometer tests with step loading." *Proc. Symposium on Special Consolidation Tests*, ASTM, 15–26.
Takeuchi, Y. (1990). "Coping with settlement due to landfill." *Skyfront Magazine*, Osaka, Japan, 2(Dec.), 67–71 (in Japanese).
Taylor, D. W. (1948). *Fundamentals of soil mechanics*. John Wiley and Sons, Inc., New York, N.Y.
Terzarghi, K. (1925). *Erdbaumechanik auf Bodenphysikalisher Grundlage*, Franz Deuticke, Leipzig, Germany.
Terzaghi, K., and Frolich, O. K. (1936). *Theory of settlement of clay layers*. Liepzig, Germany.

Tohma, T., and Yamamoto, S. (1990). "Construction of the Kansai International Airport." *Civil Engineering in Japan/'90*, ASCE, 28–44.
Wahls, H. E. (1990). "Design and construction of bridge approaches." *National Cooperative Highway Research Program Synthesis of Highway Practice 159*, Transportation Research Board, National Research Council, Washington, D.C.

5. Secondary Consolidation (Compression) Settlement (Bowles p.87)

Das Figure 5.33 (p.279)
(a) Variation of e with log t under a given load increment, and definition of secondary compression index.

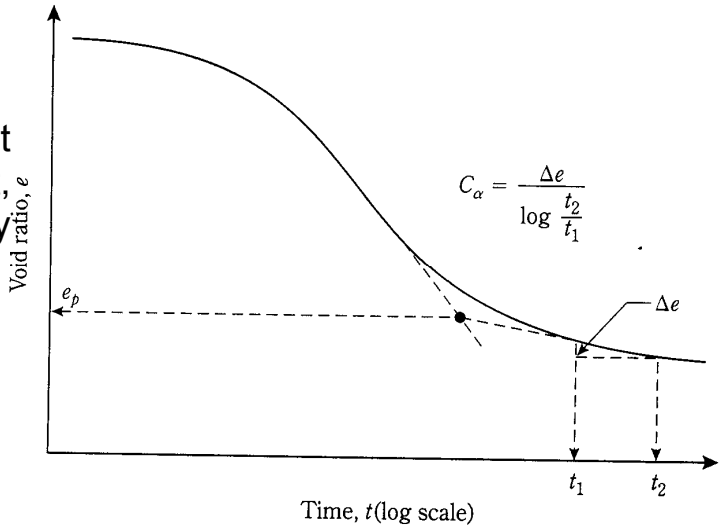

Following the full dissipation of the excess pore pressure, (primary consolidation) more settlement takes place, termed secondary compression or secondary consolidation. This settlement under constant effective stresses is analogous to creep in other materials. The secondary consolidation is relatively small in regular clays but can be dominant in organic soils, in particular peat.

$$C_\alpha = \Delta e / \log(t_2/t_1)$$

(relate to any 2 points on the secondary compression curve)

Magnitude of secondary consolidation:

$$S_{c(s)} = \frac{\Delta e}{1+e_0} H_c$$

where:

$$\Delta e = C_\alpha \log(t_2/t_1)$$

(relate to the time of interest)

clays $C\alpha/cc \approx 0.045 \pm 0.01$
peats $C\alpha/cc \approx 0.075 \pm 0.01$

see Bowles Table 2.5, p.89 for various correlations C_α = f(PI,ω,C_c)

Engineering Properties of Cranberry Bog Peat

Samuel G. Paikowsky, Assem A. Elsayed, and Pradeep U. Kurup

University of Massachusetts
Geotechnical Engineering Research Laboratory
Department of Civil and Environmental Engineering
1 University Avenue, Lowell, MA 01854 USA
Tel.: (978) 934-2277 Fax: (978) 934-3052
and
Geosciences Testing and Research Inc. (GTR)
55 Middlesex St. Suite 220
N. Chelmsford MA. 01863 USA
Tel.: (978) 251-9395 Fax: (978) 251-9396
Email: Samuel_Paikowsky@uml.edu
Assem_Elsayed@student.uml.edu
Pradeep_Kurup@uml.edu

ABSTRACT

Peat is an organic complex soil, well known for its high compressibility and low stability. Peat forms naturally by the incomplete decomposition of plant and animal constituents under anaerobic conditions at low temperatures.

A relocation of state highway No. 44 in Carver, Massachusetts requires the construction of sheet pile walls, fills and embankments through cranberry bogs and ponds containing deep peat deposits. The engineering properties of Carver peat in Southern Massachusetts (south of Boston) were investigated via laboratory testing including standard index tests, fiber content, engineering classification, consolidated undrained triaxial tests, and oedometer tests. The tests were carried out on vertically and horizontally oriented undisturbed samples.

Unlike inorganic clays, the secondary compression of peat is of great significance as it dominates its deformation and takes place over a long period of time. The presented test program examines the deformation properties of the peat and the ratio of the coefficient of secondary compression (C_α) to compression index (C_c). The data are compared to those reported in the literature.

The obtained engineering properties were found to be overall within the range reported for other peat types. The peat structure and fiber orientation seem to affect the properties. The time for primary consolidation for horizontally oriented samples decreases due to an increase in the horizontal permeability and the time of secondary compression increases due to compression mostly normal to the fibers' orientation.

1. INTRODUCTION

1.1 Background

US Route 44 spans east west across southeastern Massachusetts into Rhode Island. The Massachusetts Highway Department (MHD) is relocating Route 44 under project no. 113100. Parts of the new highway alignment spans across ponds and cranberry bogs in the town of Carver, located about 40 miles southeast of Boston. The proposed roadway is a four lane divided highway with a typical median width of 60 feet. Environmental concerns dictated that sheet piles need to be placed at the ponds and bogs roadway sections, in order to excavate and replace the underlaying organic soils and construct the embankments and roadway. The design of sheet piles supported by organic soils raises the difficulties of assigning engineering parameters to peat. These difficulties prevail whenever other engineering alternatives are considered. The objective of the presented work is to assess the engineering properties of the peat found along the proposed highway, and which is currently supporting the sheet piling. The investigated properties are to be utilized in the analysis of the supporting sheet piles and compared with the wall performance during construction as monitored by instrumentation.

1.2 Subsurface Conditions

Extensive subsurface investigation shows that the soil type and density is relatively consistent throughout the project and the wetland areas. The soil profile consists primarily of fibrous peat within a fine to coarse sand layer. The thickness of the Peat deposits range from 0 to 10.7m (35 feet) and the ground water table is near the ground surface. Figure 1 depicts a longitudinal section for a 427m (1,400ft.) long segment of the constructed route (a portion of the project) including the pond location from which the tested Peat samples were obtained (around station no. 150). The presented section in Figure 1 includes 10 borings and numerous probes outlining the contour of the Peat layer.

1.3 Peat/Bog - Overview

Peat is a material consisting of organic residues formed through the decomposition of plant and animal constituents under aerobic and anaerobic conditions associated with low temperatures and geological effects such as glacial ice. Common names for accumulation of organic soils include bog, fen, moor, muck, and muskeg. Cranberry is a Native American wetland fruit, which grows in places, called in Massachusetts, a Bog. Natural bogs evolved from organic deposits accumulation in kettle holes created by glaciers. Peat exhibits poor strength and undergoes large deformations over a long period of time. As a result, Peat and organic soils are characterized as being among the worst kinds of foundation material associated with low bearing capacity, high compressibility and long-term settlement. In most cases, the majority of the settlement in peat results from creep at a constant vertical effective stress (secondary compression) accounting for more than 60% of the total settlement. Among geotechnical materials, peat has the highest values of the ratio between coefficient of secondary compression-to-compression index; $C_\alpha / C_c = 0.06 \pm 0.1$ whereas for comparison, granular materials may display the lowest values of $C_\alpha / C_c = 0.02$ (Mesri et. al. 1997). Due to the high water content and the plant matter structure, Peat deposits accumulate at high initial void ratio (e) varying typically from 5 to 16 depending on the water content. Peat particles are light because of the lower specific gravity of the organic matter, resulting with a typical natural unit weight ranging from 9.1 to 11.6kN/m^3. When the organic matter decomposes, it turns into a sort of glue called humus, which is strong enough to bind several smaller particles together, making them into larger multi-particles, which can alter the behavior of the soil.

1.4 Design Consideration

Often a site is chosen for construction irrespectively of its geotechnical suitability but for its location; such is the case for route 44 relocation project. Due to unpredictable long-term settlement of organic soils, construction over such soils is usually impractical without a complete replacement or some sort of soil treatment. Many methods exist to improve sites with underlaying soft organic soils including, surcharging techniques to expedite the consolidation process, displacement method of placing fill directly on

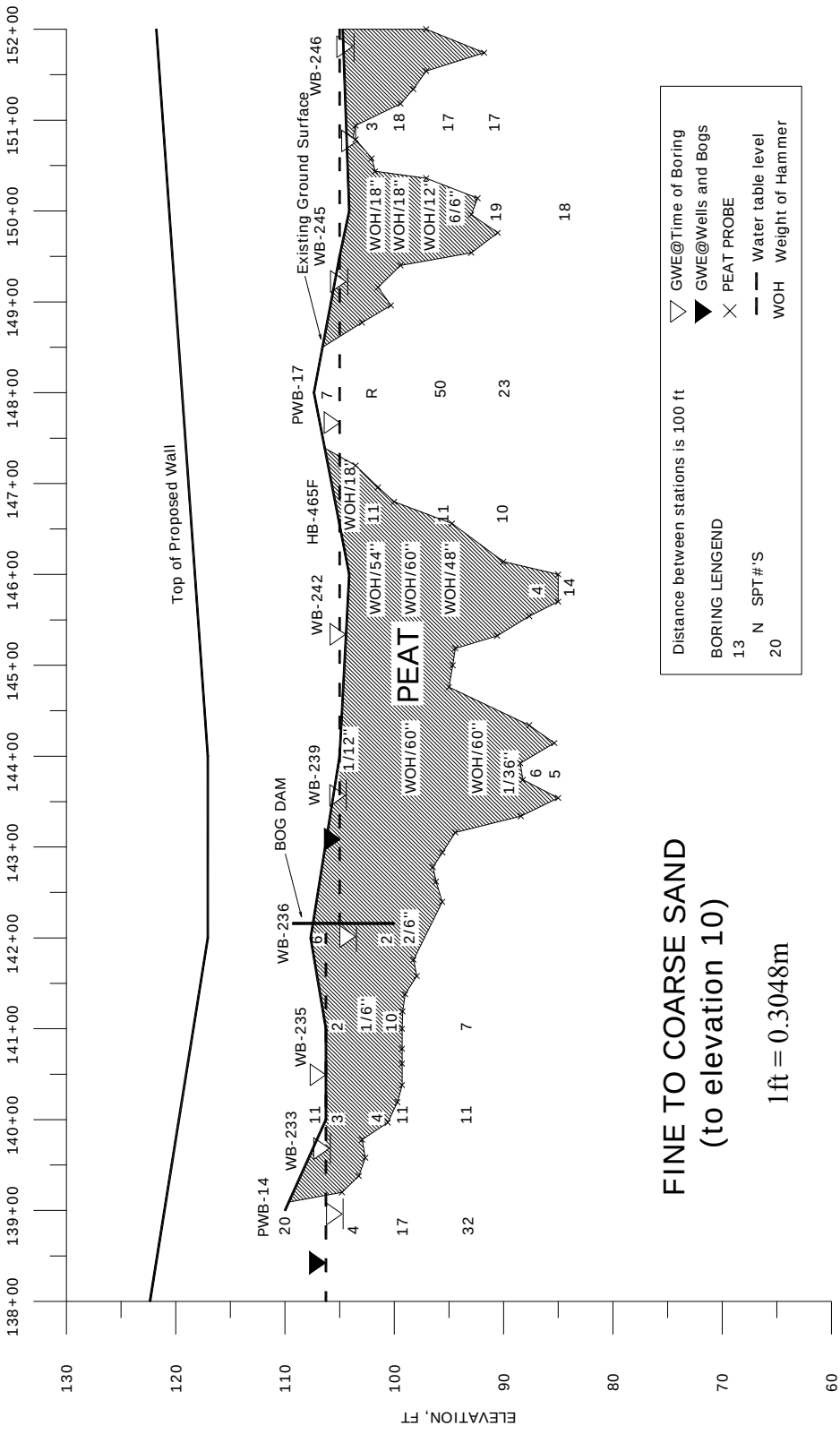

Fig.1 Typical subsurface conditions in the wetland area along a section of Route 44 between stations 138 and 152.

top of the deposit (which then by its weight, sinks and displaces the weak soil) or the use of geosynthetic products to either bridge over limited areas or to generate more evenly distributed settlement. For deep deposits, pile foundations may be employed to transfer loads through the organic soils to a firm lower layer or other methods of similar principles utilizing columns of gravel or cement and fill layers with or without synthetic material to bridge between them. Two challenges exist in the Route 44 project under the sheet pile construction requirement, one is the construction of the sheet pile itself having the peat as a reactive material, and the other is the treatment of the peat between the sheet piles. Embankments, walls, service roads and the highway are planned to be built in the area between the sheet piles. Due to long term maintenance concerns and the cost of alternative solutions, excavation and soil replacement were chosen for these areas. For the sheet piles themselves, no alternatives exist and hence their construction required the development of lateral loads in the peat. This study presents therefore experimental findings for the engineering qualities of the peat when loaded both; vertically and horizontally.

2. EXPERMENTAL PROGRAM AND BASIC PROPERTIES

2.1 Planned Testing and sampling

Table 1 presents a summary of the laboratory study detailing the type and number of tests planned and executed thus far. Issues considered included the knowledge of basic soil properties, index parameters, strength and deformation of vertically and horizontally oriented samples as well as the effect of the sample size on the obtained results. Due to the size of the fibers and roots in the tested peat the size of the common soil test samples relative to the fiber size became a concern. This factor along with the need for testing horizontally oriented samples and relatively shallow peat deposits in the bog, lead to a direct sampling from the surface utilizing large size samplers. Two square steel tubes dimensioned 15.24 x 15.24 cm (6x6 inch) and 25.4 x 25.4 cm (10x10 inch); both 6.35 mm (0.25 inch) thick and 1.83 m (6 feet) long, were used for sampling. The samplers were pushed into the peat from the surface at a location in which the water was at about the ground surface. A retainer (catcher) that was constructed for the sampler was found to be unnecessary as when pulled out, a full sample size was retained. The smaller and the larger size samples were designated as block (1) and block (2) respectively.

2.2 Carver Peat Characteristics

The obtained peat, termed Carver peat is classified by the different Peat classifications in the following way; Fibrous according to the plasticity chart for peat suggested by Casagrande (1966), Fibric according to Lynn et al. (1974) and Hemic, high ash, moderately acidic, and highly absorbent according to ASTM D-4427. The color of carver peat is dark brown to brownish-orange, it has strong odor and contains small woody elements. The Humification degree of Carver peat is H_3 to H_4 using Von Post's Humification Scale, (ASTM D5715). The principal characteristics of the Carver peat are summarized in Table 2.

3. CONSOLIDATION TESTS

3.1 General details

Three vertically oriented samples and four horizontally oriented samples were tested in oedometer cells with the details outlined in Table 3. The effective overburden pressure for the sampled peat (mid point) was approximately 1.2 kPa with effective preconsoildation pressure of approximately 9 kPa, and a resulting over consolidation ratio of about 7.5. Sample preparation of peat is more difficult than that of the typical inorganic soils due to the presence of fibers, the high initial water content and voids ratio. To minimize sample disturbance the samples were trimmed using a very sharp razor knife, and special care was taken in its placement. The porous stones were fully saturated before the test and filter papers were used to margin the biodegradation and decomposition of the samples. This is necessary considering the long period of time required for the consolidation tests in which each applied increment was sustained for about 10,000 minutes (1 week). A thin film of Silicone grease was applied to the cell wall in order to minimize the side friction. The consolidation tests were carried out at approximately constant temperature of 22 $\pm$ 4 ºC.

Table 1. Testing program of Carver peat

Test Type	No. Of Planned Tests	No. Of Performed Tests	Comments
(Bulk Unit Weight)	2	2	One test for each block
(Specific Gravity)	2	2	
(Organic Content)	2	2	
pH	1	1	
(Liquid Limit), (Plastic Limit)	2	2	

	Vertical Samples		Horizontal Samples		
	Planned	Performed	Planned	Performed	
Consolidation Test	4	3	4	4	Different aspect ratios
Consolidated Undrained Triaxial Test	4	1	4	0	
Direct Shear Test	4	0	4	0	

Table 2. Carver peat soil properties

Property	Unit	Block (1)	Block (2)	Reference
γ (Bulk Unit Weight)	kN/m^3	10.44	10.10	ASTM D4531
ω_0 (Water Content)	Percent	780.0 - 946.0	759.0 - 816.0	ASTM D2216
G_s (Specific Gravity)	-	1.48	1.52	ASTM D854
O_c (Organic Content)	Percent	60.0	77.0	ASTM D2974
pH	-	4.50	4.50	ASTM D2976
LL (Liquid Limit)	Percent	580.0	600.0	ASTM D4318
PL* (Plastic Limit)	Percent	375.0	400.0	ASTM D4318
Fibers Content	Percent	40.0	52.0	ASTM D1997

* Rolling the sample to 4.5mm instead of 3 mm due of the presence of fibers

3.2 The compression and rebound index

Figures 2 and 3 present the stress strain relations in the form of void ratio vs. consolidation pressure, (e-log σ) for samples oriented vertically and horizontally, respectively. Table 3 summarizes the compression index (C_c) and the rebound index (C_s) values for the different tests. The information presented in Table 3 show that for Block 1, the C_c values for samples oriented in the vertical and horizontal directions are 5.2 and 4.1, respectively resulting in a horizontal to vertical compression index ratio (C_{ch} / C_{cv}) of 0.78. For Block 2, the C_c values for the vertical and horizontal samples are 3.9 and 2.7 respectively, resulting in a ratio of 0.70. Subjected to the limited number of tests, these values indicate that the sample orientation and the block from which the samples were obtained, affected the obtained results while the oedometer size and it's aspect ratio had no effect. As both peat samples were retrieved at the same location, the obtained compression index values may reflect the large variation in the peat or alternatively suggest that the peat in the blocks were influenced by the sampler's size such that the peat in the small sampler was compressed more during sampling than the peat in the large sampler. The compression index values found for Carver peat is compared in Figure 4 with other values presented by Mesri (1973) and Terzaghi et al. (1996). The relationship in Figure 4 suggest that the compression index of Carver peat agrees well with the other values attributed to peat with the exception of the horizontally oriented samples having lower compression index as discusses above. The rebound index values agree with the range reported by Mesri et al. (1997) of C_s between 0.3 to 0.9.

Table 3 Oedometer test details and compression and rebound index results

Test No.	e_o	ω_0 (%)	C_c	C_s	Block No.	Sample Orientation[1]	Oedometer Diameter (cm) /Aspect Ratio[2]
1	12.41	837	3.40	0.47	2	V	11.28/2.89
2	12.00	800	4.30	0.43	2	V	11.28/2.89
4	14.00	935	5.18	0.90	1	V	11.28/2.89
5	11.54	760	2.67	0.34	2	H	11.28/2.89
6	11.54	770	4.03	0.34	1	H	11.28/2.89
7	11.54	772	2.72	0.36	2	H	7.00/4.40
8	11.54	775	4.07	---	1	H	7.00/4.40

[1] V,H–Vertically and Horizontally samples, respectively [2] Ratio of original sample height to diameter

3.3 Time – settlement relationship

The formulation of the consolidation process for fully saturated soils, (Terzaghi, 1923) assumes that the soil particles and water are incompressible and deformation takes place due to expulsion of water from the pores under the influence of hydrodynamic effects upon loading. This compression process, (termed primarily consolidation) assumes relationship between effective stresses to void ratio and should cease therefore when the dissipation of the excess pore-water pressure is completed. In fine-grained soils the compression continues after the dissipation of pore water pressure is completed and takes place under a constant effective stress in what is termed secondary compression or creep. Due to the high permeability of peat, the primary consolidation is relatively short but the secondary compression takes place over a lengthy period of time and hence is of great significance. The secondary compression has been attributed to the plastic deformation of the highly viscous adsorbed double layer and continuous adjustment and arrangement of soil constituents after they have been distributed during the primary consolidation, (Dhowian, 1978). Accordingly, the primary consolidation method of settlement analysis developed by Terzaghi seems to be inappropriate to address the secondary compression. Many investigators have assumed and used different relationships and models to describe the secondary compression. Gibson and Lo (1961) identified three types of secondary compression curves relating to the relationship between settlement and time on a logarithm scale; *type 1* shows a gradual decrease in the rate of secondary compression until ultimate settlement is finally reached; *type 2* exhibits a proportional relationship between secondary compression and logarithm of time for a

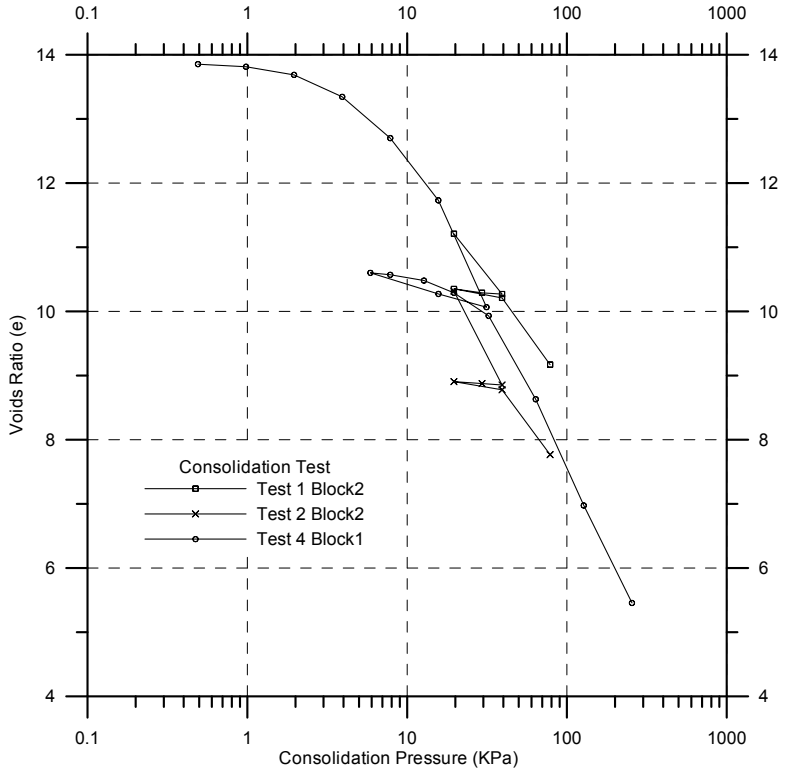

Fig.2 Void ratio versus consolidation pressure for samples oriented vertically

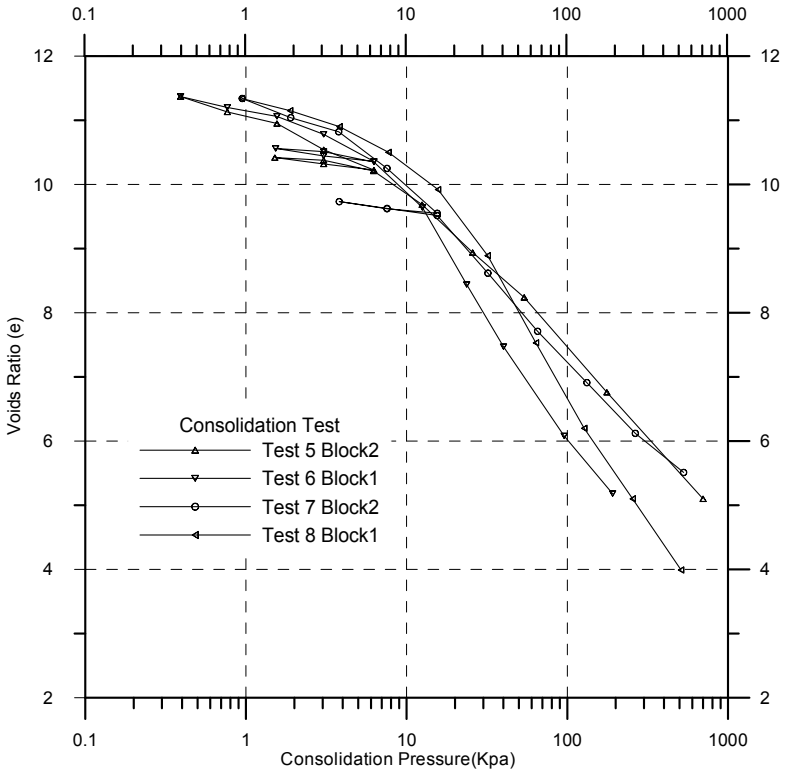

Fig.3 Void ratio versus consolidation pressure for samples oriented horizontally

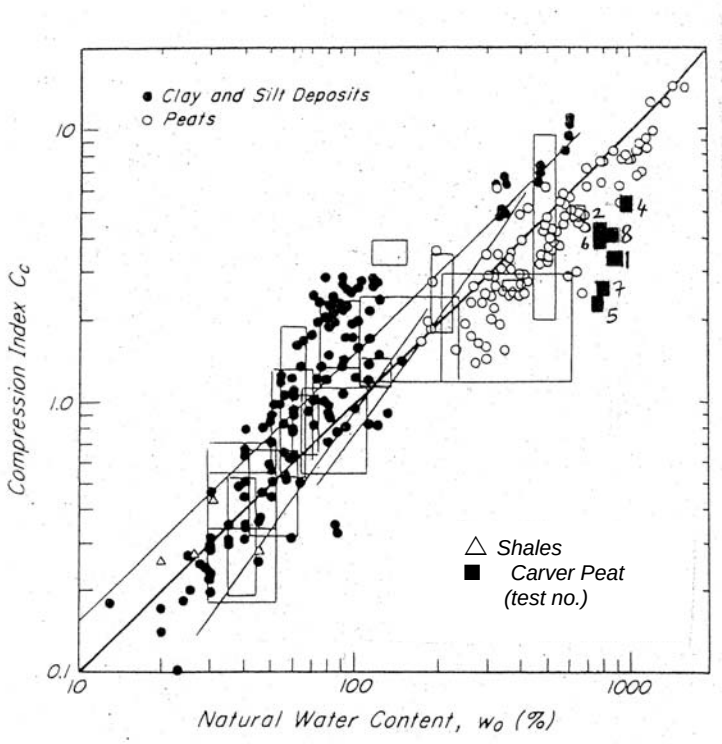

Fig. 4 Empirical correlation between compression index and in situ water content for clay, silt, shales and peats including the current study (based on Mesri, 1973 and Terzaghi et al. 1996).

significantly long period of time before reaching the final settlement, and *type 3* shows a proportional relationship to a certain point at which an acceleration of the rate of secondary compression takes place, believed to be the result of bond breakage of between particles. The compression-log time curve of type 3 materials consists of four components of strain; instantaneous strain which takes place immediately after load application, primary strain which lasts in most cases for several minutes, secondary strain which has a constant rate with log time and lasts for a considerable period of time and tertiary strain which is a higher rate secondary strain. This phenomenon is believed to be due to the breakage of bonds between particles and a curved transition zone usually exists from the secondary to the tertiary zones.

3.4 Secondary and tertiary compression

3.4.1 Obtained relations and the related parameters

Figures 5 and 6 describe some of the relationships between the void ratio and time for the vertically oriented samples under different loads. The obtained relations show that Carver peat behavior is in agreement with the aforementioned type 3 curves, exhibiting an accelerated rate of secondary compression. Dhowian and Edil (1980) and Mesri and Choi (1985) suggested that secondary compression begins after the primary compression ends; these hypothesis was adopted in this research study finding the related parameters in the following way:

(i) t_p - the time at the end of primary consolidation, (EOP) employing Taylor's square root method (Taylor, 1942).

(ii) C_α - the coefficient of secondary compression, defining the tangentional slope (δ_e / δ_t).

(iii) t_k – the designated time for the end of secondary compression and the beginning of the tertiary compression, defined by the interception of the tangents to the curves in the secondary and tertiary zones.

(iv) C_k -the coefficient of tertiary compression, defining the tangentional slope after the transitional zone between the secondary and the tertiary compression, (Edil and Dhowian 1979; Dhowian and Edil 1980).

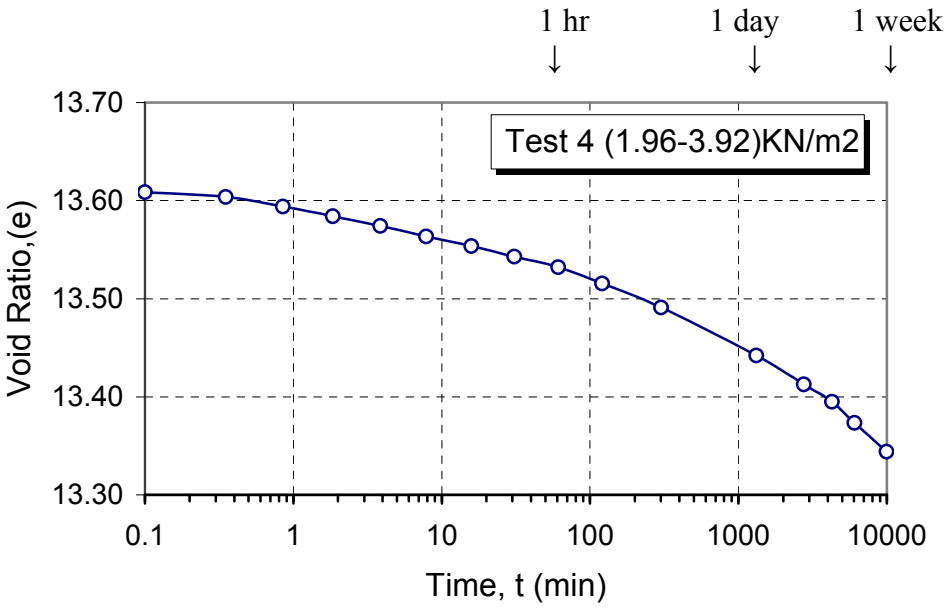

Fig. 5 Typical settlement vs. time relationship (e - log t) for test 4 under low stress level

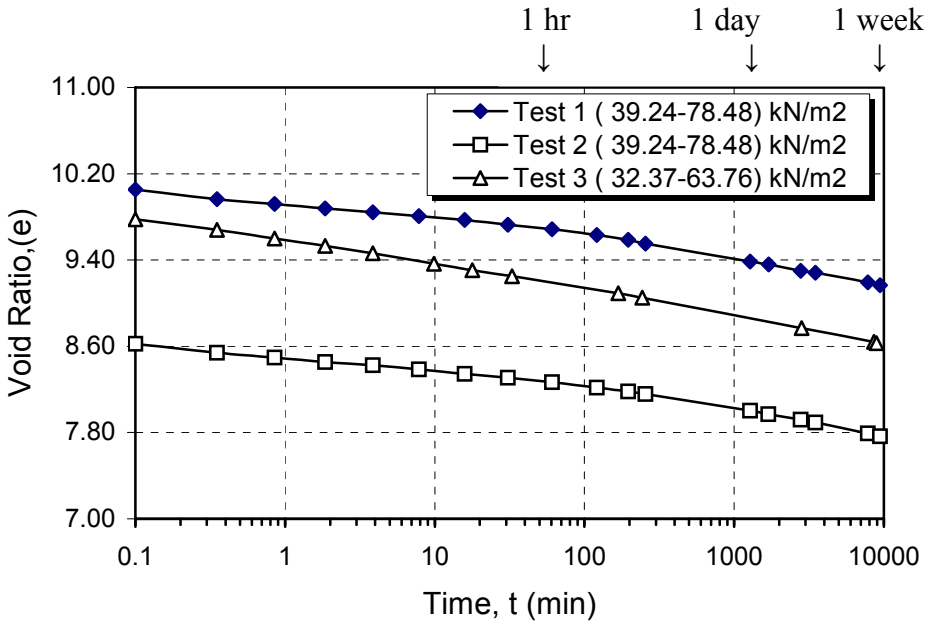

Fig. 6 Typical settlement vs. time relationship (e - log t) for the vertically oriented samples under similar stress levels

3.4.2 The time for secondary and tertiary compression

Figures 7a,b present the time in which the primary compression is completed and the secondary compression starts, (t_p) versus the consolidation pressure for vertically and horizontally oriented samples, respectively. In all cases, the primary consolidation takes place within 3 minutes, and for the horizontally oriented samples, the time is about one half of the time required to complete the primary consolidation in the vertically oriented samples. Figures 8a,b present the time in which the secondary compression is completed and the tertiary compression starts, (t_k) versus the consolidation pressure for vertically and horizontally oriented samples, respectively. The time of the secondary compression is measured in hundreds to thousands minutes with

distinctive peak(s) at particular stress levels. Overall, the time required for secondary compression is longer in the horizontally oriented samples compared with the time required for the vertically oriented samples under the same consolidation pressure.

It seems that the behavior observed in figures 7 and 8 is associated with the structure of the peat and it's deposition process, having the majority of the fibers oriented horizontally. Such structure results with a permeability in the horizontal direction being higher than in the vertical direction, and hence the time for the primary consolidation being shorter. In contrast, the structure in the vertical direction is more easily compressed (fibers in parallel) than in the horizontal direction, resulting with a shorter time for a secondary compression in the vertically oriented samples.

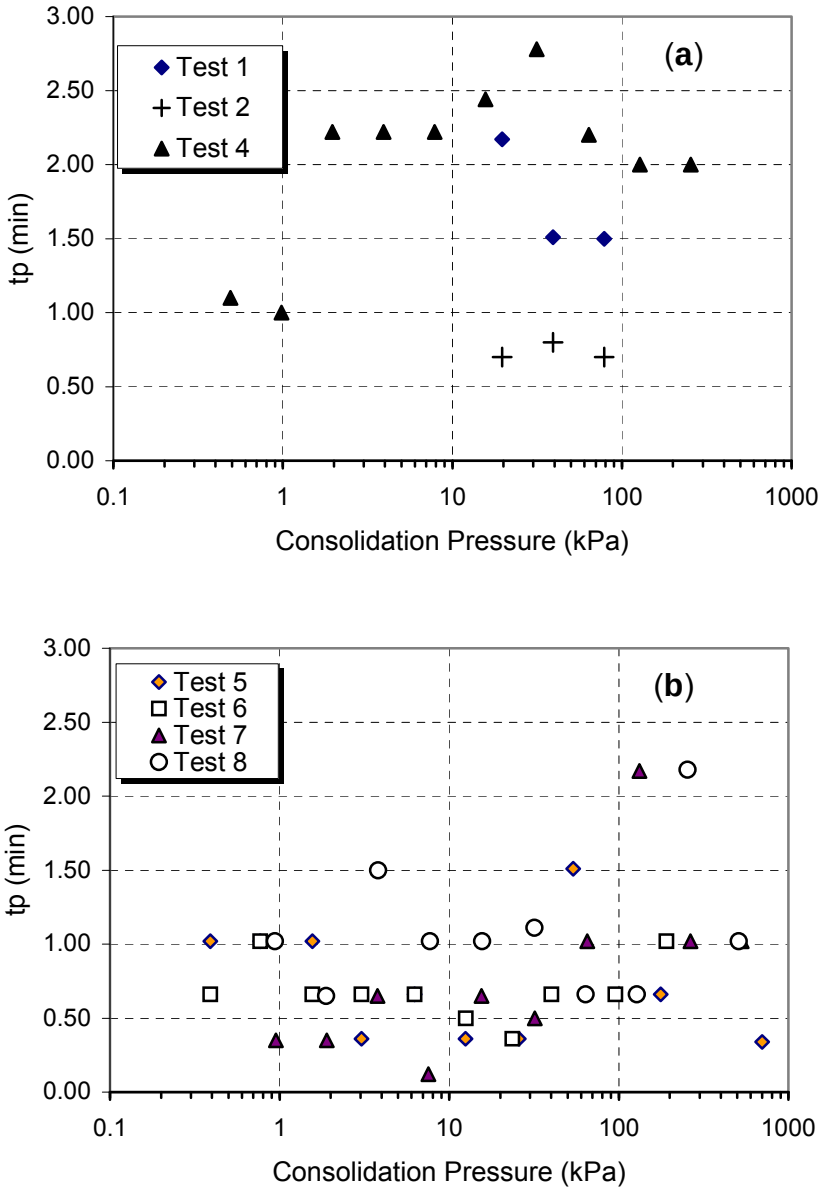

Fig. 7 The time to the end of primary consolidation and beginning of the secondary compression versus consolidation pressure for vertically (a) and horizontally (b) oriented samples.

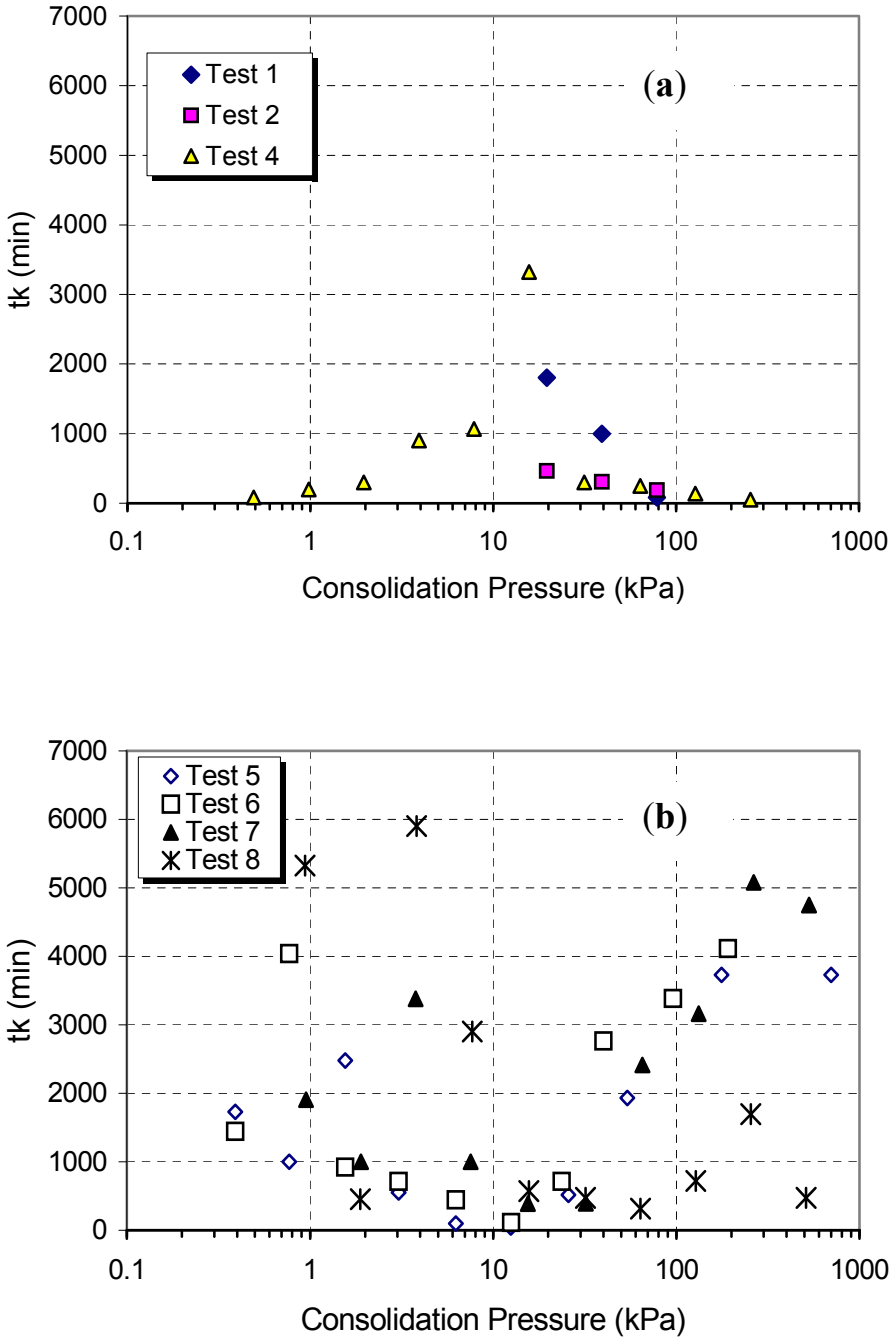

Fig. 8 The time to the end of secondary consolidation and beginning of the tertiary compression (tk) versus consolidation pressure for vertically (a) and horizontally (b) oriented samples.

3.4.3 Coefficients of secondary and tertiary compression of vertically oriented samples

Figures 9 and 10 present the values of the coefficient of the secondary compression (C_α) and tertiary compression (C_k) versus the consolidation pressure for test no.4, respectively. Beyond a pressure of about 1 kPa, approximately a linear increase exists between the stress and the value of the coefficient of secondary compression, (on a log stress axis). Variations of the values of the coefficient of tertiary compression exist with the increase of the consolidation stresses. Figures 11 and 12 present the values of the coefficient of the secondary compression (C_α) and tertiary compression (C_k) versus the consolidation pressure in the range of 10 to 100 kPa, respectively. The data in Figure 11 suggests that the values of C_α are about (0.15 ± 0.08). The data in figure 12 suggests a decrease in the coefficient of tertiary compression with the increase of the consolidation pressure. Dhowian (1978) describes similar trends for Portage peat. The secondary compression of six consolidation tests resulted with an average coefficient of secondary compression C_α = 0.15 (30 data points). The coefficient of tertiary compression reported by Dhowian decreased with the increase of the consolidation pressure from approximately 0.48 for 20 kPa to 0.38 for 60 kPa.

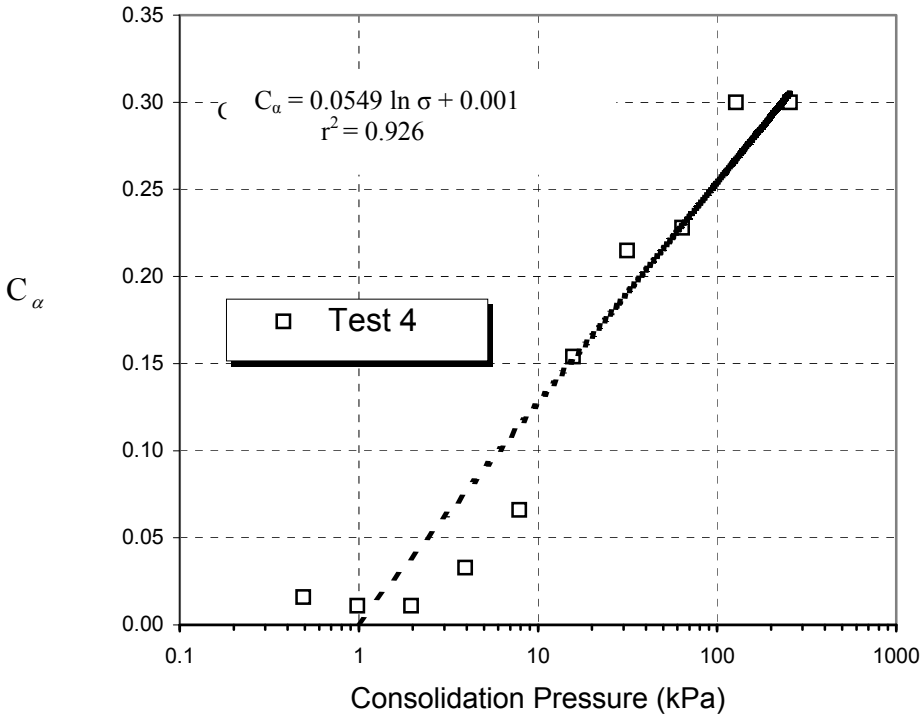

Fig. 9 C_α versus consolidation pressure for test 4

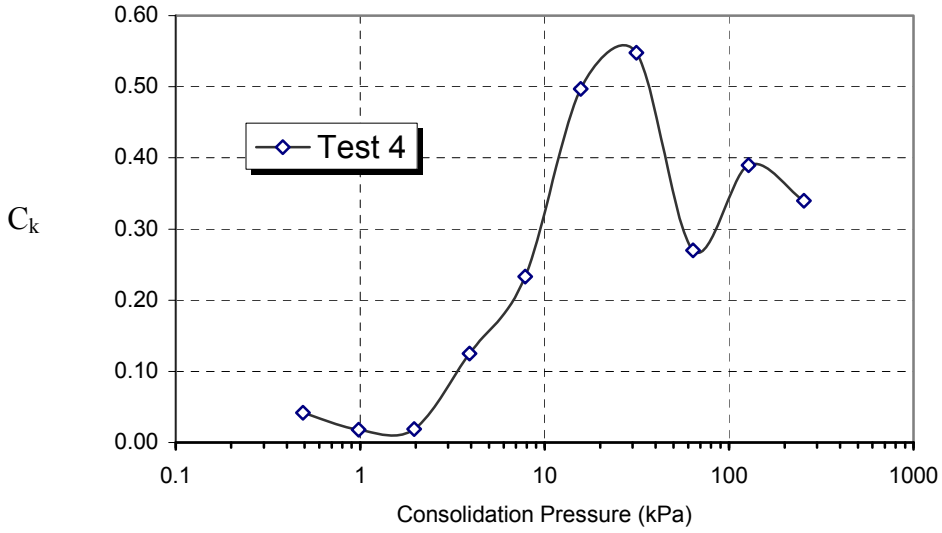

Fig.10 C_k versus consolidation pressure for test 4

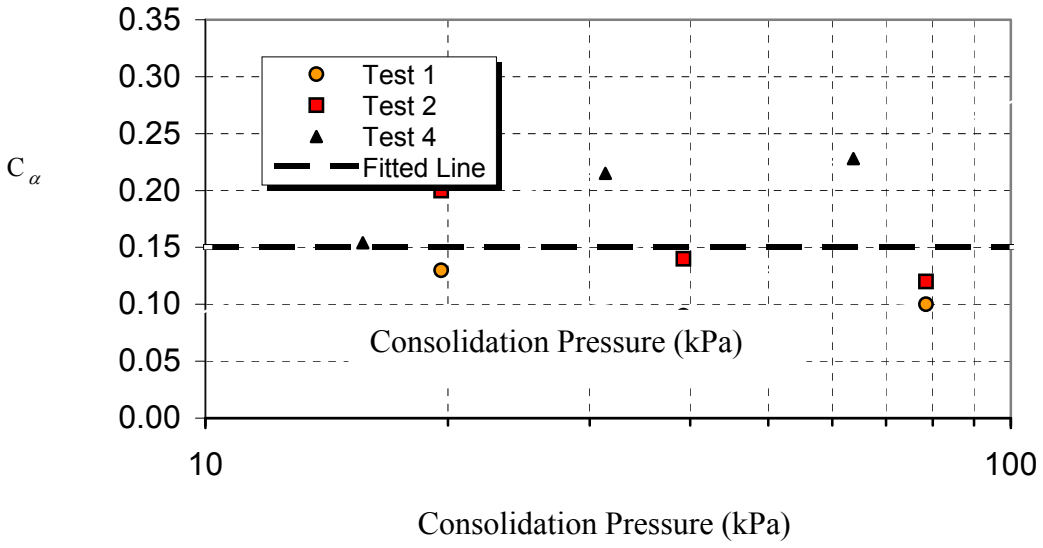

Fig.11 C_α for the consolidation pressure range of 10 -100 kN/m^2 for the vertically oriented samples

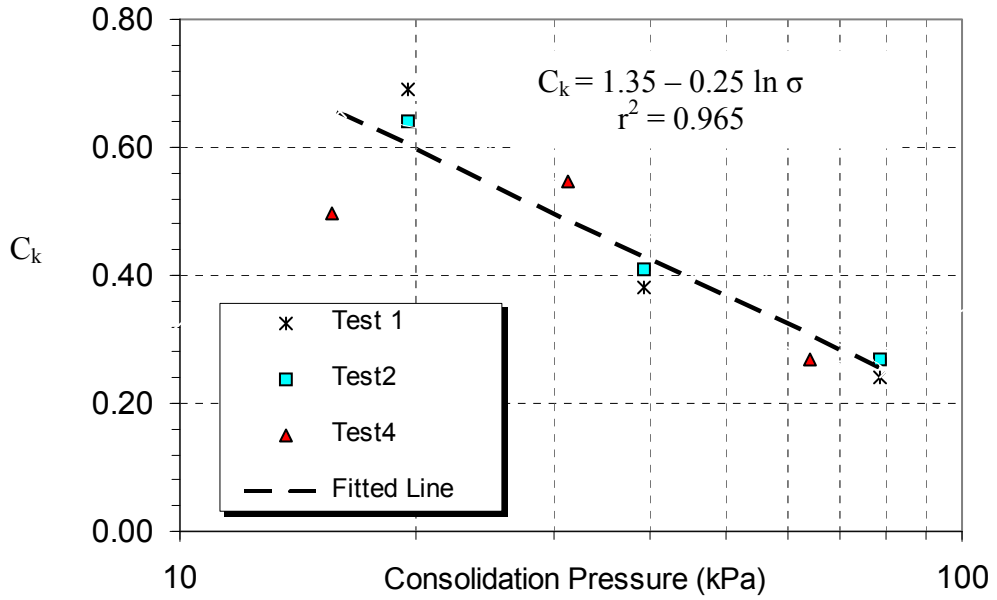

Fig.12 C_k versus consolidation pressure in the range of 10 -100 kN/m2 for vertically oriented samples

3.4.4 Coefficients of secondary and tertiary compression of horizontally oriented samples

Figures 13 and 14 present the values of the coefficient of secondary compression (C_α) and tertiary compression (C_k) versus the consolidation pressure for the consolidation tests of the horizontally oriented, samples, respectively. The coefficient of secondary compression show an approximate constant value of 0.02 to the pressure of 5.0 kN/m^2 from which a linear increase is observed up to a pressure of about 100 kPa beyond which the data is scattered. The coefficient of secondary compression C_α has the average value of (0.03) within the consolidation pressure range of 0.10 to 10.0 kPa and a range of values between 0.05 to 0.15 for the stress levels of 10 to 100 kPa. These values are about two third of the values observed for the vertically loaded samples under the same pressure range (Fig. 11). Mesri (1973) reported on conflicting relationships that have been proposed regarding the coefficient of secondary compression. Newland and Allely (1960) indicate C_α independent of consolidation pressure. Wahls, (1962) indicates C_α decreases with pressure. Ladd and Preston, (1965) indicate C_α increases slightly with consolidation pressure. In this paper, C_α may be assumed to be constant within some levels of stresses, but generally C_α increases with consolidation pressure for both horizontally and vertically oriented samples.
The data in figure 14 suggests a gradual consistent increase in the coefficient of tertiary compression with the increase of the consolidation pressure. This trend is opposite to that observed for the vertically loaded samples (Fig. 12).

As tertiary compression is an accelerated rate of the secondary compression, a ratio between the two may be both feasible and practical. Figure 15 presents this ratio (C_k/C_α) for all the tests. While the horizontally oriented samples show a larger scatter (open symbols) the ratio remains limited in magnitude for most consolidation pressures, resulting in $C_k/C_\alpha = 3.4 \pm 1.8$ (± 1SD, 22 points) for the consolidation pressures between 10 to 100 kPa.

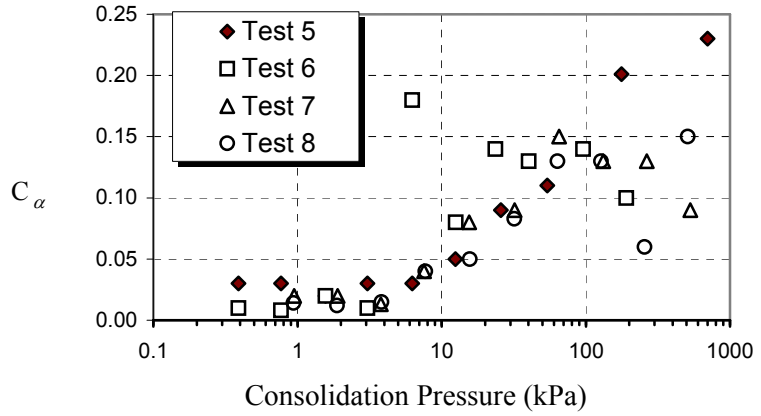

Fig. 13 C_α versus consolidation pressure for horizontally oriented samples

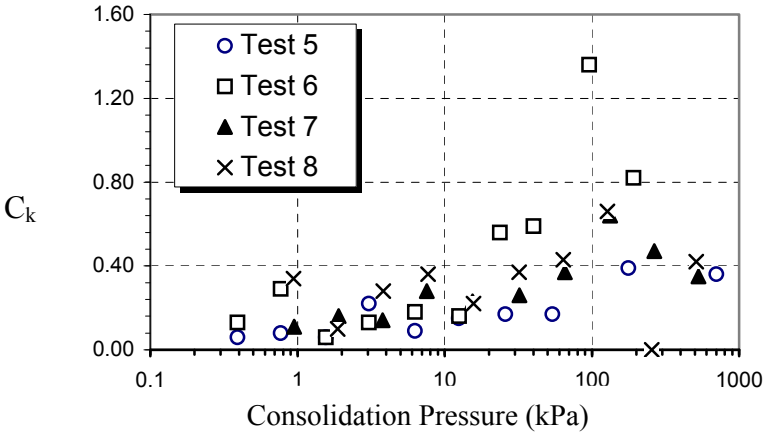

Fig. 14 C_k versus consolidation pressure for horizontally oriented samples

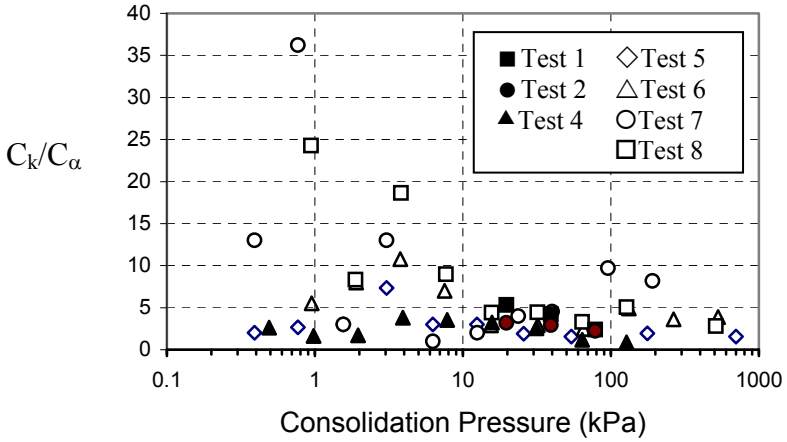

Fig. 15 The ratio between the tertiary and secondary compression indices (C_k/C_α) versus consolidation pressure for vertically and horizontally oriented samples.

3.5 The relationship between the primary and the secondary compression indices (C_α/ C_c)

Mesri and Godlewski, (1977) suggested that for natural soils, there seems to be a unique relationship between C_α and C_c that holds good at any effective pressure, void ratio, and time during secondary compression. Fox et.al. (1992), reported that the ratio C_α/ C_c is not constant because C_α increases with time under constant effective stress. Very often tertiary compression is also seen following secondary compression. Figure 16 shows the variation of the ratio C_α/ C_c with the consolidation pressure for test 4. It can be seen that the ratio C_α/ C_c ranges from 0.0026 to 0.058 and is not constant. Table 4 summarizes the range of values for the ratio C_α/ C_c found in the different tests, referring to all stresses tested and to a range between 10 to 100kPa. When referring to a limited range of stresses (mostly beyond 10 kPa) the ratio of C_α/ C_c seem to remain in a relatively small range for all practical proposes. This range did not defer much between the vertically and the horizontally oriented samples.

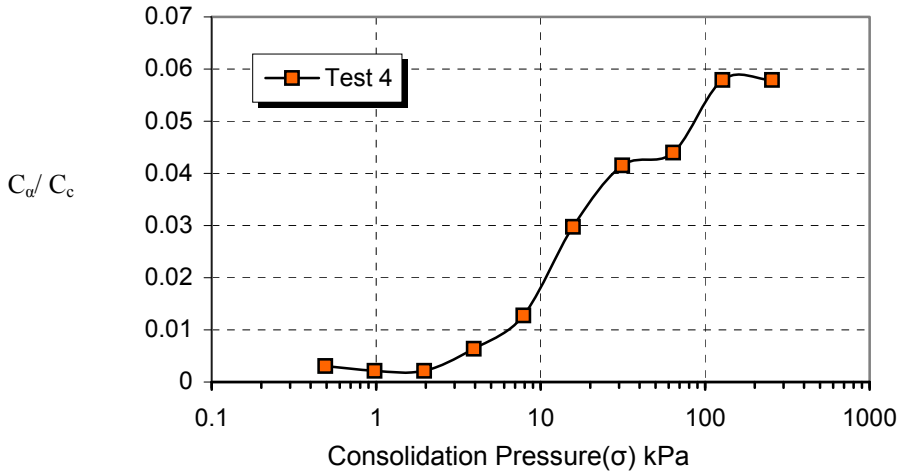

Fig .16 Values of C_α / C_c versus consolidation pressure

Table 4. Values of C_α/ C_c for the various tests

Test No.	C_α / C_c	C_α / C_c **10 < σ < 100kPa**
1	0.026-0.038	0.026-0.038
2	0.028-0.047	0.028-0.047
4	0.0026-0.058	0.030-0.044
5	0.0075-0.086	0.019-0.041
6	0.0020-0.035	0.020-0.035
7	0.0074-0.055	0.029-0.047
8	0.0034-0.037	0.012-0.032

4. CONSOLIDATED UNDRAINED TRIAXIAL TESTS

Isotropically consolidated undrained triaxial compression tests were performed on samples obtained from a depth of 1.80 m. The undisturbed triaxial specimens were approximately 7.0 cm in diameter, and 15.25 cm in height with an aspect ratio of 2.17. The specimens were taken from larger block samples and carefully trimmed to size using a razor knife. The porous stones were fully deaired and saturated with water. The drainage lines were flushed with water to eliminate air bubbles. Full saturation of the samples are essential in order obtain reliable pore pressure readings. The soft peat samples obtained from the field were essentially saturated. However the triaxial specimens enclosed in the membrane were flushed with deaired water under a low hydraulic gradient to remove any trapped air bubbles. The saturated samples yielded B values higher than 0.998.

Deviator stress versus axial strain for triaxial tests performed on vertically oriented peat samples are shown in Figure 17a. Results of excess pore-water pressure versus axial strain are shown in Figure 17b. The tests were performed at four different confining pressures (0.1 psi, 5 psi, 10 psi, and 20 psi). Apparently, the higher the consolidation stress the higher the strength. The following effective stress shear strength parameters were obtained from the Mohr Coulomb failure envelope presented in Figure 18: $\bar{\phi}$ = 12º, $\bar{c}$ = 12 kN/m^2. These preliminary triaxial test results differ from those reported by Edil and Wang (2000), that suggest higher friction angles and negligible cohesion for normally consolidated peats. Future testing of Carver peat will further address this issue.

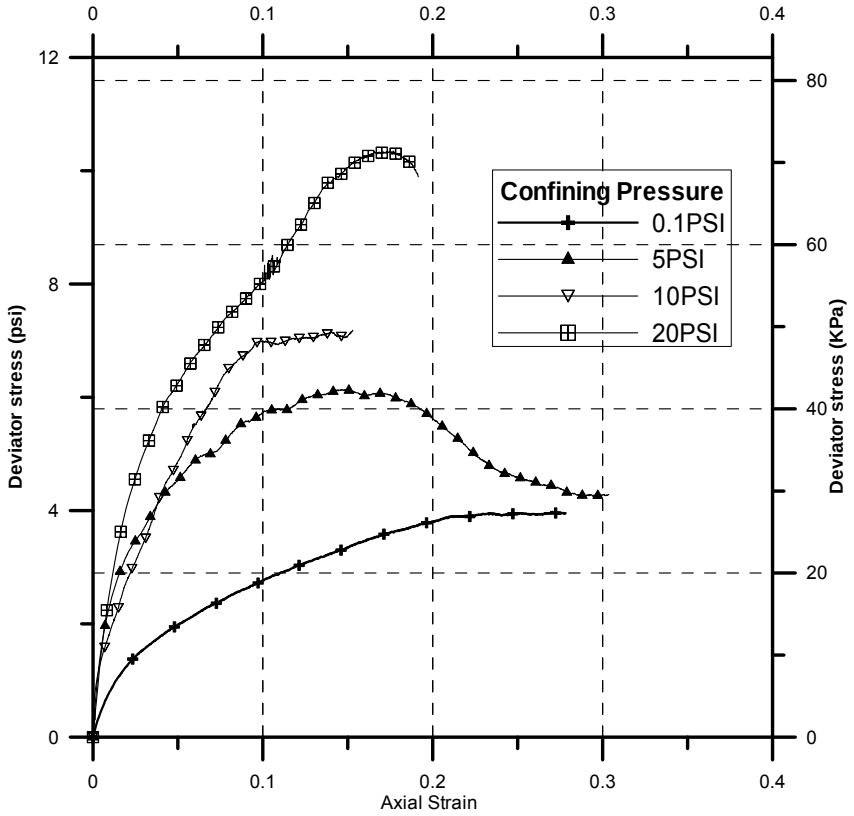

Fig. 17 (a) Axial strain versus deviator stress for the peat samples

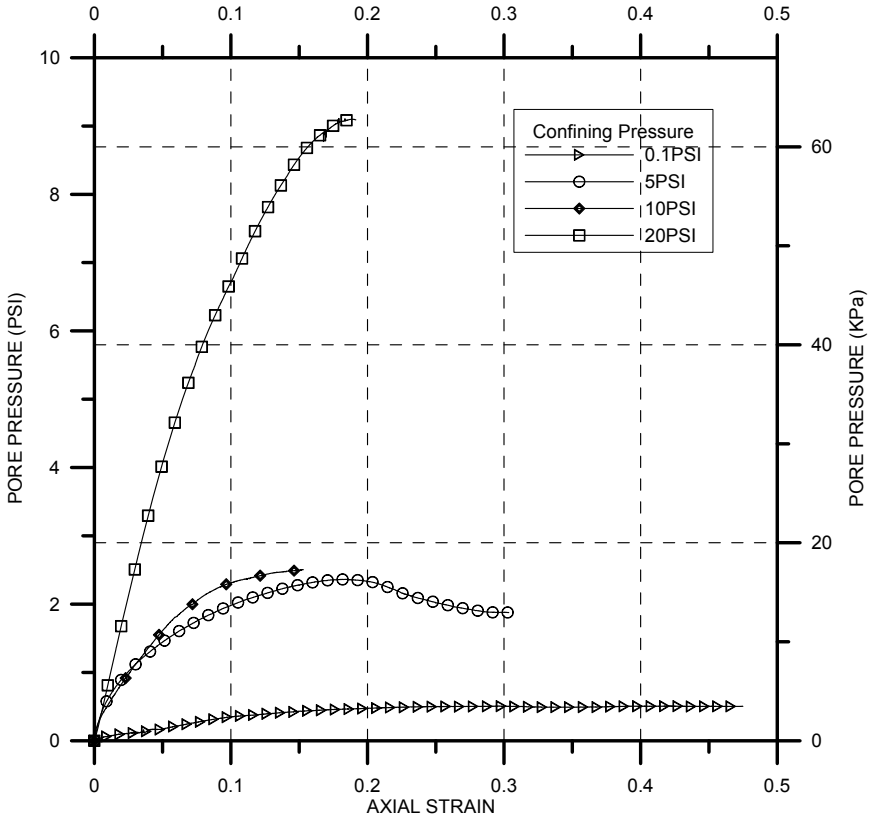

Fig. 17 (b) Excess pore pressure versus axial strain

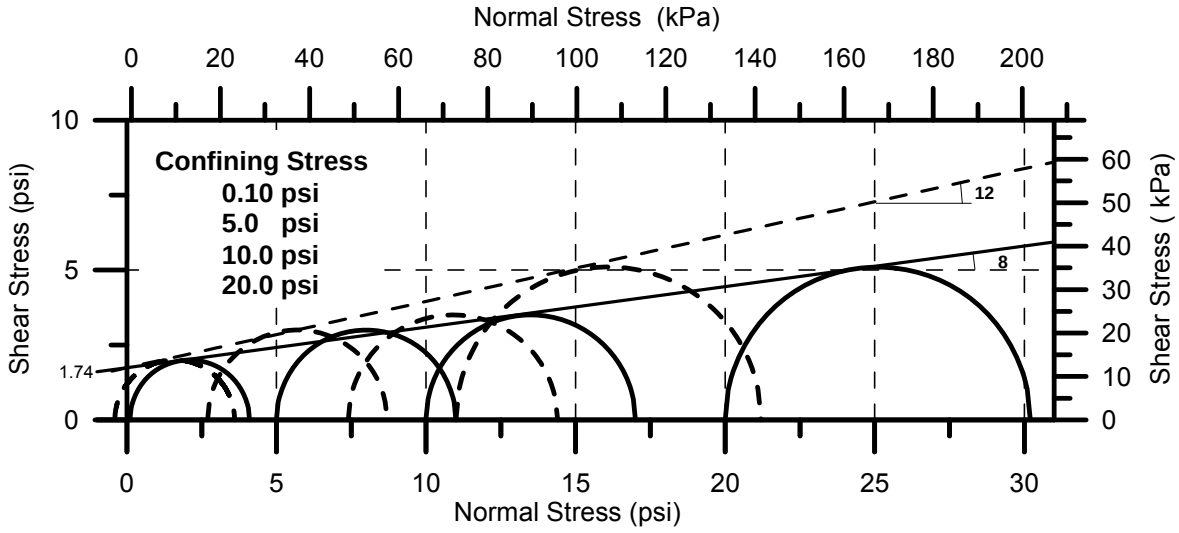

Fig. 18 Shear strength parameters from triaxial tests on vertically oriented peat specimens

SUMMARY AND CONCLUSIONS

Peat samples from Carver, Massachusetts, were tested to characterize their engineering properties. Carver peat is fibrous; over consolidated and was tested on vertically and horizontally oriented samples. Conventional long duration oedometer tests showed that primary consolidation was very rapid, (especially for the horizontally oriented samples) and creep effect counted for the majority of the compression. The different long-term behavior curve related to the heterogeneity of the peat, the different fibrous content and the orientation of the loading relative to the orientation of the peat deposition.

The compression index for the vertically oriented samples was between 3.4 to 5.2. These values are within the range observed for other vertically loaded peat types at similar natural water contents. The compression index for the horizontally oriented samples was lower, at the approximate ratio of $C_{ch}/ C_{cv} \approx 0.75$.

The time for primary consolidation for horizontally oriented samples is shorter compared to that in the vertically oriented samples. The time of secondary compression is longer in the horizontally oriented samples (while scattered was overall significantly longer) than that in the vertically oriented samples under the same consolidation stresses. These observations seem to be explained through the peat structure and fiber orientation such that the permeability increases along the fibers and the compressibility increases normal to the fibers' orientation. Further research is required and will be carried out to examine these observations.

The coefficient of secondary compression (C_α) increases with the consolidation pressure once exceeding a threshold stress level between the overburden pressure and the precompression pressure. A coefficient of secondary compression of $C_\alpha = 0.15$ was found for the consolidation pressure in the range of 10 to 100 kPa. The coefficient of tertiary compression (C_k) decreased with the increase of the consolidation pressure for the vertically oriented samples and increased for the horizontally oriented samples. The trends and absolute values of the vertically oriented samples matched those reported in the literature for other peat types.

The ratio between the primary and secondary compression indices C_α/ C_c is not constant as C_α varies with the consolidation pressure. This ratio seems to remain, however, within a relatively limited range of 0.03 ± 0.01 for stresses between 10 to 100 kPa, regardless of the orientation of the sample. The ratio between the tertiary to the secondary compression indices (C_k/C_α) was found to be within the range of 3.4 ± 1.8 for both; vertically and horizontally oriented samples within a limited zone of consolidation pressure between 10 to 100 kPa.

Isotropically consolidated undrained triaxial compression tests were performed on Carver peat, showing that the peat has apparent cohesion of 12.0 kN/m^2 at 45 % fibers content, undrained angle of friction of 8º, and a drained angle of friction of 12º. These initial tests were performed without backpressure; future planned tests will be performed using backpressure, and the results will be closely compared to those available for other peat types.

ACKNOWLEDGMENT

This project was carried out at the Geotechnical Engineering Research Laboratory of the University of Massachusetts at Lowell and sponsored by Geosciences Testing and Research Inc. (GTR) of N. Chelmsford MA. contracted through Northeast Pile and P.A Landers (Contractors) to the Massachusetts Highway Department, (MHD). The collaboration and support of Mssrs. Nabil Hourani, Peter Connors and Helmut Ernst of the Geotechnical and Construction sections of the MHD is appreciated. Mssrs. Todd Elliot and Terry Edwards of P.A Landers assisted in the sampling and other relevant field activities.

REFERENCES

CASAGRANDE, L. (1966). Construction of embankments across peaty soils. *J. Boston Soc. Civil Engrs*., Vol. 53, No. 3 pp. 272-317.

COLLESELLI F. and CORTELLAZO, G., (1998), Laboratoring Testing of an Italian Peaty Soil, *International Symposium on Problematic Soils*- IS- TOHOKU 98, Sendai.

DHOWIAN, A. W. (1978). Consolidation Effects on Properties of highly Compressible Soils- Peats, *Ph.D Thesis, Department of civil and Environmental Engineering*, University of Wisconsin- Madison.

DHOWIAN, A. W. and EDIL, T. B. (1980). Consolidation behavior of peats*, Geotech. Testing J., ASTM,* 3(3), 105-114

EDIL, T.B. and DHOWIAN, A. W. (1979). Analysis of long- term compression of peats. *Geotechnical Engineering, Southeast Asian Soc. Of Soil Engineering*, 10, 159-178.

EDIL, T. B. and FOX, P. J. (1994). Field testing of thermal precompression. Vertical and Horizontal Deformations of Foundations and embankments, *Geotechnical Special Publication* No. 40, ASCE, New york, New york.

EDIL, T.B. and WANG, X. (2000). Shear Strength and K_o of Peats and Organic Soils. *Geotechnics of High Water Content Materials, ASTM STP 1374,* T.B. Edil and P.J. Fox, Eds., American Society for Testing and Materials, West Conshohocken, PA.

FOX P.J. (1992). An Analysis of One – Dimensional Creep Behavior of Peat, *Ph.D. thesis, univ. of Wisconsin-Madison.*

FOX, P. J. and EDIL, T. B., and LAN, L. T. (1992). C_α / C_c Concept applied to compression of peat. J. *Geotech. Eng., ASCE,* 118(8), 1256-1263.

GIBSON, R. E. and LO, K. Y. (1961). A Theory of Consolidation of Soils Exhibiting Secondary Compression. *Acta Polytechnica Scandinavia, Ci.* 10296, 1-16.

KABBAJ, M., TAVENAS, F., and LEROUEILK, S., (1988), In Siyu and Laboratory Stress-Strain *Relationships, Geotechnique*, Vol. 100, No.1, pp. 38-83.

LADD, C. C., and PRESTON, W. E., On the Secondary Compression of Saturated Clays, Soils Publication 181, *Massachusetts Institute of Technology, Cambridge*, Mass., (1965).

LYNN, W. C., MCKINZIE, W. E., and R. B. GROSSMAN (1974), Field Laboratory Tests for Characterization of Histosols. Histosols: Their Characteristics, Classification, and Use, *Soil Science Society of America*, Special Publication Number 6.

MACFARLANE, I. C. (ed.) (1969). *Muskeg Engineering Handbook, University of Toronto Press*

MESRI, G. (1973). Coefficient of Secondary C ompression. J. *Soil Mech. and Found. Div., ASCE*, 99(1), 123-137

MESRI, G. and GODLEWSKI, P. M. (1977) Time- and stress- compressibility interrelationship. J. *Geotech. Eng.*Div. Proc. ASCE, 103(GT5), 417-430

MESRI G. and CHOI, Y. K. (1985). The Uniqueness of the end- of – primary (EOP) void ratio- Effective Stress Relationship, Proc. *11th ICSMFE*, Vol. 2, pp. 587-590

MESRI, G., STARK, T.D., AJLOUNI, M.A., and CHEN, C.S. (1997). Secondary Compression of Peat with or without Surcharging, *Jnl. Of Geotechnical Engineering*, Vol. 123, No. 5, pp.411-421.

NEWLAND, P. L., and ALLELY, B. H., A study of the Consolidation Characteristics of a clay, *Geotechnique, London, England*, Vol. 10, 1960, pp. 62-74

TAYLOR ,D. W. (1942).Research on Consolidation of clays, Serial No.82, Department of Civil and Sanitary Engineering, Massachusetts Institute of Technology, Cambridge, Mass.

TERZAGHI, K. (1923). Die Berechnung Der Durchlassigkeitsziffer des Tones aus dem Verlauf der Hydrodyn TERZAGHI, K. amischen Spannungserscheinungen Sber. Wien. Akad. Wiss.

TERZAGHI, K, Peck. R.B, and Mesri.G.1996 Soil Mechanics in Engineering Practice Third Edition John Wily & Sons, Inc.NY

WAHLS, H. E., Analysis of Primary and Secondary Consolidation*, Journal of the Soil Mechanics and Foundation Division, ASCE*, Vol. 88, No. SM6, Proc. Paper 3373, Dec., 1962, pp. 207-231.

BIOGRAPHY

Samuel G. Paikowsky holds a B.S. and a MSc. from the Technion, Israel and a Sc.D. in Geotechnical Engineering from MIT. He is a Professor in the Department of Civil and Environmental Engineering at the University of Massachusetts at Lowell and a Principal in Geosciences Testing and Research (GTR) of N. Chelmsford MA. His basic research relevant to granular material behavior includes original mechanical models, dedicated laboratory and field experimental apparatuses and ideal testing systems utilizing photoelasticity, image analysis, and tactile sensor technology. His applicative research and consulting relates to foundations design and construction addressing various issues like time dependent pile capacity, dynamic analyses, static-cyclic testing, multiple deployment model piles, Load and Resistance Factor Design (LRFD) and innovative load-testing systems

.

Dr. Pradeep U. Kurup is an Associate Professor in the Department of Civil and Environmental Engineering at the University of Massachusetts Lowell. He has vast expertise in advanced experimental techniques and in analytical modeling. He has done extensive research in the areas of site characterization and monitoring, application of novel sensing technologies to geotechnical and geo-environmental engineering, calibration chamber testing, soil-structure interaction, "seeing-ahead techniques" for trenchless technologies, and artificial neural network modeling. He has published his research contributions in several journals and conferences proceedings. Dr. Kurup is an active member in several professional societies, and is also a registered Professional Engineer.

Assem Elsayed holds a BSc. in Civil Engineering from Alexandria University, Egypt in 1992. His engineering experience started in Alexandria and Cairo, Egypt, when he was working for several consultant offices in the field of structural and geotechnical engineering. After 4 years of working in Egypt, he joined Arab Construction Inc. in Saudi Arabia, where he supervised the foundation and structural work of power plants in Dhahran. In fall 2001 he has become a graduate research assistant at the University of Massachusetts Lowell during pursuing his master degree. Assem is the 1992 recipient of excellence award by Alexandria University for the best senior project in Highways and Airports design. He presented "The Engineering Properties of Peat" at the Northeast Geo-technical Graduate Research Symposium, Amherst Massachusetts 2002.

Example

Excavation and replacement of the organic soils was carried out between the sheet piles in Rt. 44 relocation project. Due to various reasons, a monitoring program has detected a remnant peat layer, 4ft thick as shown in the figure. Using the expected loads due to the fill and the MSE (Mechanically Stabilized Earth) Walls, estimate the settlement of the peat:

(a) During primary consolidation, and
(b) During secondary consolidation over a 30 year period.

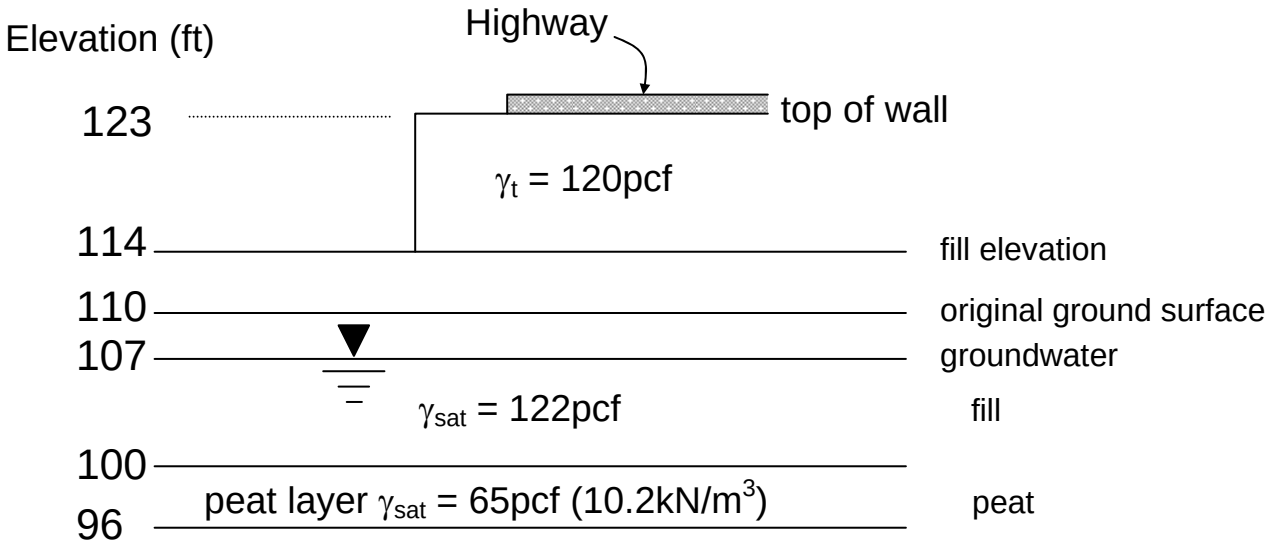

Peat Parameters:

Based on Table 2 of the paper, γ_{sat} = 10.2kN/m^3 = 65pcf

Based on Tables 3 and 4 for vertically loaded samples,

$e_0 \approx 13$ $C_c \approx 4.3$ $C_s \approx 0.68$ $C_\alpha/C_c \approx 0.036 \rightarrow C_\alpha \approx 0.15$ (see Figure 11)

Assuming a 2-D problem and a peat cross-section before the excavation,

σ'_{vo} = (110-107) x 65 + (107-98)(65-62.4) = 218.4psf

$\Delta\sigma'_v$ = (123-114) x 120 + (114-107) x 120 + (107-100)(122-62.4) + (100-98) x (65-62.4) = 2342.4psf

$$S_c = \frac{C_c}{1+e_0}\log\frac{\sigma'_f}{\sigma'_0}H_0 = \frac{4.3}{1+13}\log\frac{2342.4+218.4}{218.4}4 = (0.307)(1.07)4 = 1.31\,ft = 15.75 inch$$

$$S_{c(s)} = \frac{C_\alpha}{1+e_0}\log\frac{t}{t_p}H_0$$

Evaluation of t_p – end of primary consolidation

From the consolidation test result,

$t_p \approx$ 2min (Figure 7a, and section 3.4.2 of the paper)

$$t = \frac{T_v H_{dr}^2}{C_v}$$

As C_v and T_v are the same for the sample and the field material:

$$\frac{t_{p\ field}}{t_{p\ lab}} = \frac{H_{dr\ field}^2}{H_{dr\ lab}^2} = \left(\frac{H_{dr\ field}}{H_{dr\ lab}}\right)^2$$

$H_{dr\ lab}$ = 2.89/2 = 1.45inch (see table 3)

$H_{dr\ field}$ = 2ft = 24 inch

$t_{p\ field} \cong$ 2min x $(24/1.45)^2$ = 548min $\cong$ 9.1hours

$$S_{c(s)} = \frac{0.15}{1+13}\log\frac{(30)(365)(24)}{9.1}4 = (0.011)(4.46)(4) = 0.20\,ft = 2.3 inches$$

Conclusions:

1. A relatively thin layer of peat, 4ft thick, will undergo a settlement of 18 inches, 38%, of its thickness.

2. Most of the settlement will occur within a very short period of time, theoretically within 9 hours, practically within a few weeks.

3. The secondary settlement, which is significant, will continue over a 30-year period and may become a continuous source of problem for the road maintenance.

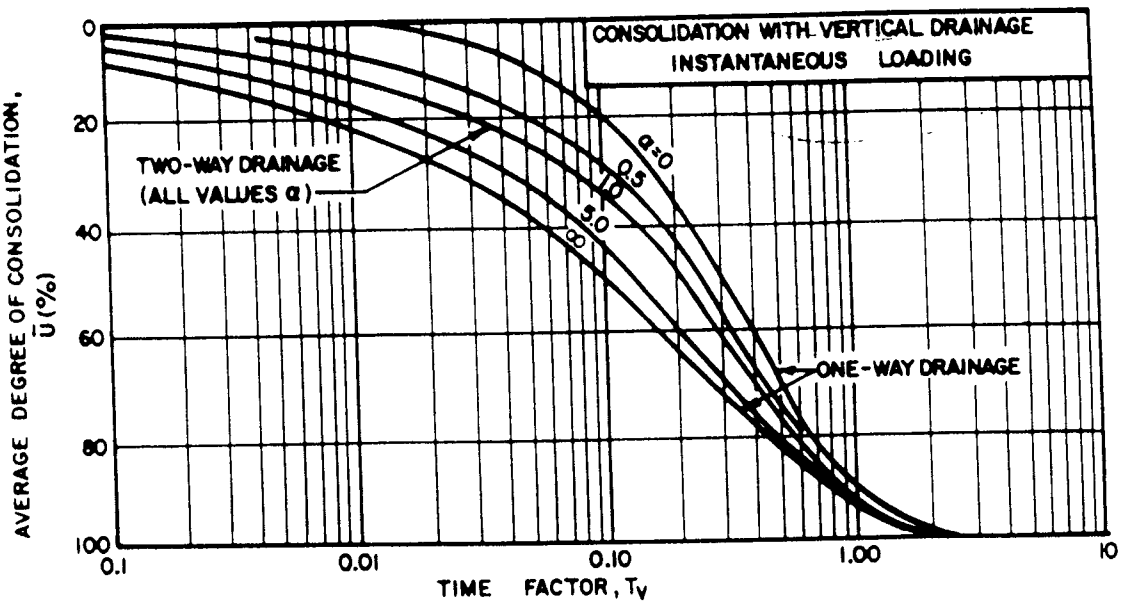

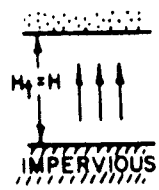

ONE WAY DRAINAGE

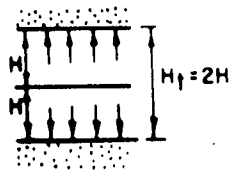

TWO WAY DRAINAGE

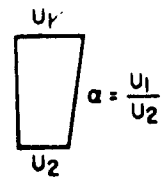

DISTRIBUTION OF INITIAL PORE PRESSURE

① INSTANTANEOUS LOADING, VERTICAL DRAINAGE ONLY

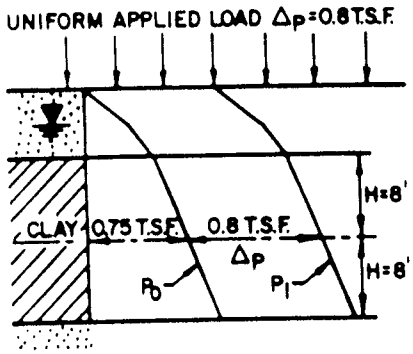

FROM LABORATORY TESTS ON THE CLAY STRATUM:

$e_0 = 1.00$ $C_c = 0.21$ $C_v = 0.03$ FT.^{2}/DAY $C_\alpha = 0.010$

LOAD INCREMENT, Δp = 0.8 TSF (VIRGIN COMPRESSION)

(1) FOR 100% PRIMARY CONSOLIDATION:

$$\Delta H = \frac{H_f C_c}{1+e_0} \log\left(\frac{P_0+\Delta P}{P_0}\right) = \frac{12\,(16)(0.21)}{2.00}\,(0.315) = \underline{6.35\ \text{IN.}}$$

(2) SECONDARY COMPRESSION FOR 1 CYCLE OF TIME:

$$\Delta H_{SEC} = C_\alpha H_f \log\left(\frac{t_{SEC}}{t_p}\right) = 0.01\,(12)(16)\log(10) = \underline{1.92\ \text{IN.}}$$

(3) TIME - CONSOLIDATION RELATIONSHIP: $T_V = \frac{t C_v}{H^2}$ { T_V = TIME FACTOR FOR VERTICAL DRAINAGE. t = TIME FOLLOWING LOADING.

$T_V = t\frac{(0.03)}{8^2}$ $\underline{t = 2130\ T_V\ \text{DAYS}}$

USE UPPER PANEL FOR T_V vs $\bar{U}$. PLOT SETTLEMENT vs TIME - SEE CURVE ① IN FIGURE 10 (LOWER PANEL)

FIGURE 9
Time Rate of Consolidation for Vertical Drainage
Due to Instantaneous Loading

NAVFAC Manual

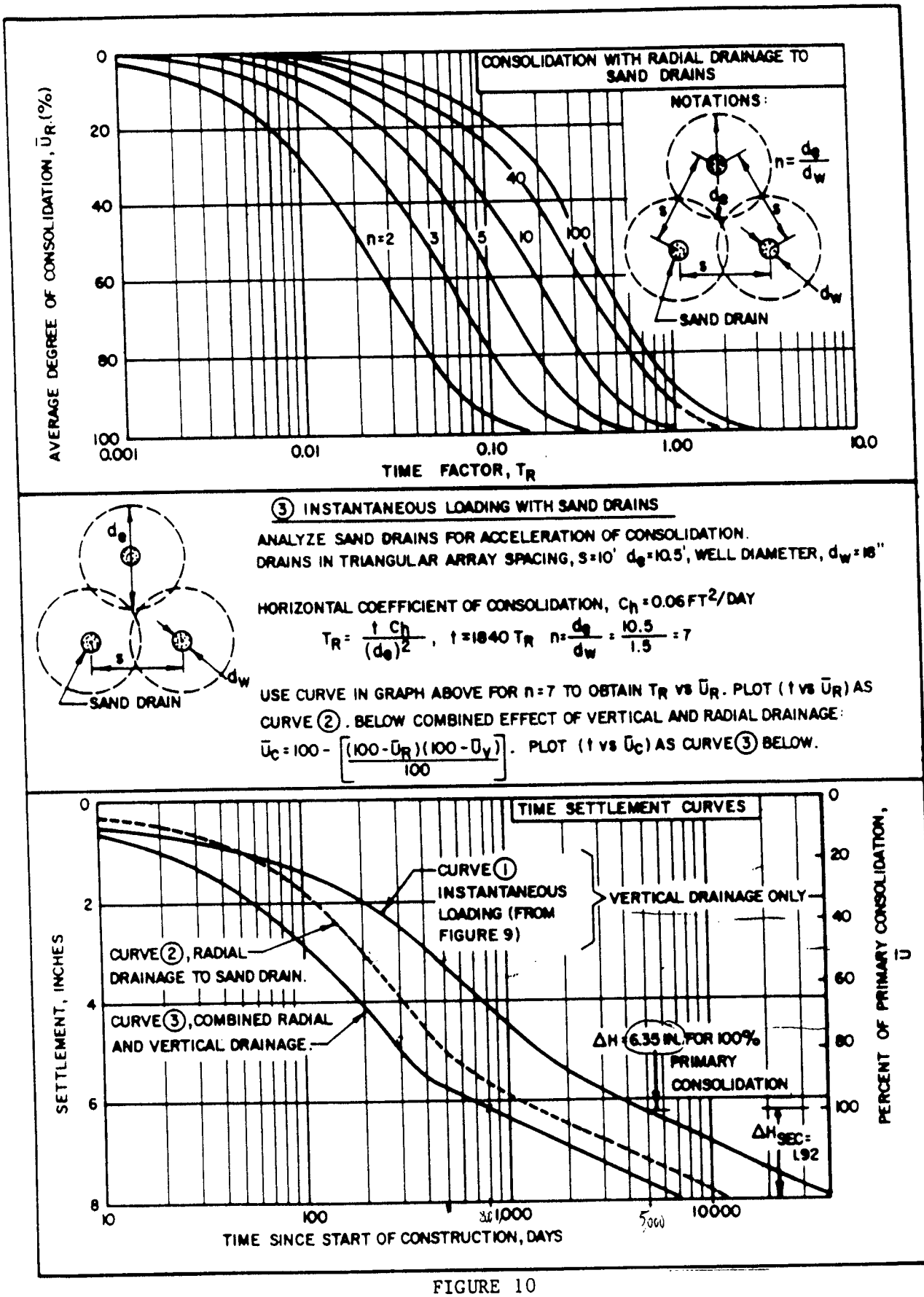

FIGURE 10
Vertical Sand Drains and Settlement Time Rate

7.1-228

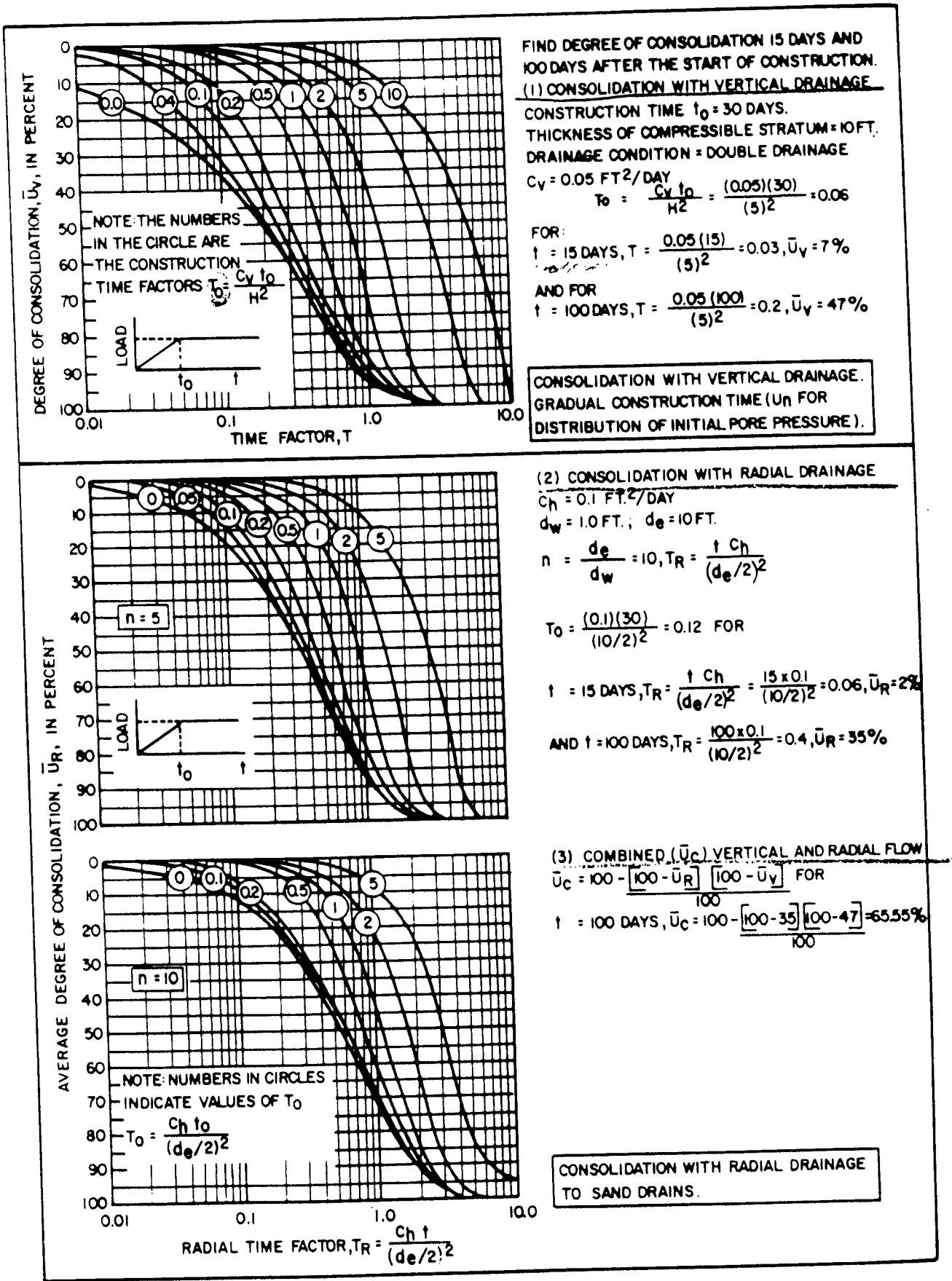

FIGURE 13
Time Rate of Consolidation for Gradual Load Application

7.1-232

ADDITIONAL TOPICS

1. Allowable Bearing Pressure In Sand Based On Settlement Consideration (Das sect. 5.13, pp.263-267)

- Using an empirical correlation between N SPT and allowable bearing pressure which is associated with a standard maximum settlement of 1 inch and a maximum differential settlement of ¾ inch.
- Relevant Equations (modified based on the above)

$q_{net} = 19.16 \times N \times F_d \times \left(\frac{S_e}{25.4}\right)$ $B \leq 1.22m$ (Das eq. 5.63)

[kPa]

$q_{net} = 11.98 \times N \times F_d \times \left(\frac{S_e}{25.4}\right) \times \left(\frac{3.28B+1}{3.28B}\right)^2$ $B > 1.22m$ (Das eq. 5.64)

q_{net} (q_{all}-γD_f) is the allowable stress, N = N corrected

depth factor

$F_d = 1 + \frac{1}{3}$ $\frac{Df}{B} \leq 1.33$

S_e = tolerable settlement in mm

English Units

- The same equations in English units:

$q_{net} = \frac{N}{2.5} \times F_d \times S_e$ $B \leq 4$ ft. (Das eq. 5.59)

q_{net} [kips/ft^2] S_e [inches]

$q_{net} = \frac{N}{4}\left(\frac{B+1}{B}\right)^2 \times F_d \times S_e$ B > 4ft (Das eq. 5.60)

The following figure is based on Das equations 5.59 and 5.60: q_{net} over the depth factor vs. foundation width for different $N_{corrected}$ SPT.

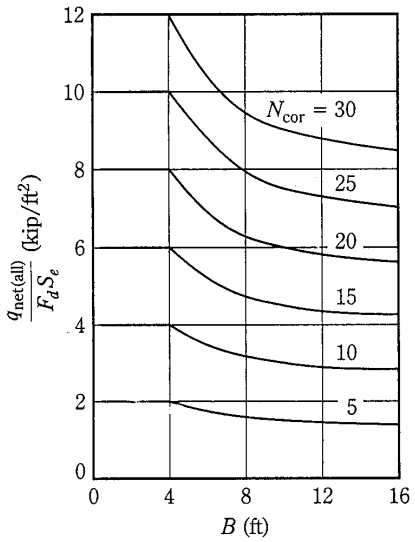

Find B to satisfy a given Q_{load} following the procedure below:

1. Correct NSPT with depth for approximately 2-3B below the base of the foundation (use approximated B).
2. Choose a representative $N_{corrected}$ value
3. Assume B → Calculate F_d → Calculate q_{net} using B&N or find from the above figure $q_{net}/(F_d \times S_e)$
4. Use iterations: